การตรวจวัดโดยการวัดสีของสารกำจัดศัตรูพืชกลุ่มออร์แกโนฟอสเฟตโดยใช้พอลิไดแอเซทิลีนเวสิ
เคิลร่วมกับแอเซทิลโคลีนเอสเทอเรสและสารลดแรงตึงผิว

นางรุ่งนภา พิมเสน

วิทยานิพนธ์นี้เป็นส่วนหนึ่งของการศึกษาตามหลักสูตรปริญญาวิทยาศาสตรดุษฎีบัณฑิต
สาขาวิชาปิโตรเคมี
คณะวิทยาศาสตร์ จุฬาลงกรณ์มหาวิทยาลัย
ปีการศึกษา 2556
ลิขสิทธิ์ของจุฬาลงกรณ์มหาวิทยาลัย

COLORIMETRIC DETECTION OF ORGANOPHOSPHATE PESTICIDES USING

POLYDIACETYLENE VESICLES WITH ACETYLCHOLINESTERASE AND SURFACTANTS

Mrs. Rungnapha Pimsen

A Dissertation Submitted in Partial Fulfillment of the Requirements

for the Degree of Doctor of Philosophy Program in Petrochemistry

Faculty of Science

Chulalongkorn University

Academic Year 2013

Thesis Title	COLORIMETRIC DETECTION OF ORGANOPHOSPHATE PESTICIDES USING POLYDIACETYLENE VESICLES WITH ACETYLCHOLINESTERASE AND SURFACTANTS
By	Mrs. Rungnapha Pimsen
Field of Study	Petrochemistry
Thesis Advisor	Associate Professor Mongkol Sukwattanasinitt, Ph.D.
Thesis Co-Advisor	Assistant Professor Sumrit Wacharasindhu, Ph.D.

Accepted by the Faculty of Science, Chulalongkorn University in Partial Fulfillment of the Requirements for the Doctoral Degree

....Dean of the Faculty of Science

(Professor Supot Hannongbua, Ph.D.)

THESIS COMMITTEE

....Chairman

(Professor Pattarapan Prasassarakich, Ph.D.)

....Thesis Advisor

(Associate Professor Mongkol Sukwattanasinitt, Ph.D.)

....Thesis Co-Advisor

(Assistant Professor Sumrit Wacharasindhu, Ph.D.)

....Examiner

(Associate Professor Nuanphun Chantarasiri, Ph.D.)

....Examiner

(Associate Professor Voravee P. Hoven)

....External Examiner

(Gamolwan Tumcharern, Ph.D.)

รุ่งนภา พิมเสน : การตรวจวัดโดยการวัดสีของสารกำจัดศัตรูพืชกลุ่มออร์แกโนฟอสเฟต โดยใช้พอลิไดแอเซทิลีนเวสิเคิลร่วมกับแอเซทิลโคลีนเอสเทอเรสและสารลดแรงตึงผิว. (COLORIMETRIC DETECTION OF ORGANOPHOSPHATE PESTICIDES USING POLYDIACETYLENE VESICLES WITH ACETYLCHOLINESTERASE AND SURFACTANTS) อ.ที่ปรึกษาวิทยานิพนธ์หลัก: รศ. ดร.มงคล สุขวัฒนาสินิทธิ์, อ.ที่ปรึกษาวิทยานิพนธ์ร่วม: ผศ. ดร.สัมฤทธิ์ วัชรสินธุ์, 103 หน้า.

สารกำจัดศัตรูพืชกลุ่มออร์กาโนฟอสเฟตมีการใช้กันอย่างกว้างขวางในการเกษตร มีการสะสมตัวในอาหารและน้ำ สารกลุ่มนี้จำนวนมากโดยเฉพาะอย่างยิ่งไดคลอวอส พบว่ามีความเป็นพิษทั้งแบบเฉียบพลันและแบบเรื้อรัง มีความเสี่ยงสูงที่จะเป็นอันตรายต่อทั้งมนุษย์และสิ่งแวดล้อม จึงได้มีการพัฒนาวิธีการสำหรับตรวจวัดสารกลุ่มดังกล่าว โดยอาศัยหลักการของพอลิไดแอเซทิลีนร่วมกับการยับยั้งเอนไซม์แอเซทิลโคลีนเอสเทอเรสด้วยสารกลุ่มออร์กาโนฟอสเฟต ไมริสโทอิลโคลีนเหนี่ยวนำพอลิไดแอเซทิลีนเวสิเคิล ทำให้เกิดการเปลี่ยนแปลงสีจากสีน้ำเงินเป็นสีแดง เอนไซม์แอเซทิลโคลีนเอสเทอเรสทำปฏิกิริยาไฮโดรไลซิสกับไมริสโทอิลโคลีนได้กรดไมริสติกและโคลีน ซึ่งไม่ทำให้เกิดการเปลี่ยนสีของพอลิไดแอเซทิลีนเวสิเคิล เมื่อมีไดคลอวอสในระบบ การทำงานของเอนไซม์แอเซทิลโคลีนเอสเทอเรสจะถูกยับยั้ง ส่งผลให้ไมริสโทอิลโคลีนสามารถเหนี่ยวนำให้เกิดการเปลี่ยนสีของพอลิไดแอเซทิลีนเวสิเคิลจากสีน้ำเงินเป็นสีแดงอีกครั้ง โดยมีความสัมพันธ์เป็นเส้นตรงต่อความเข้มข้นของไดคลอวอสและมีความจำเพาะเจาะจงในการตรวจวัดเมื่อเปรียบเทียบกับสารกำจัดศัตรูพืชกลุ่มออร์กาโนฟอสเฟตอื่นๆ มีความสามารถในการตรวจวัดไดคลอวอสโดยเครื่องยูวีวิสสเปกโทรมิเตอร์ และโดยการสังเกตด้วยตาเปล่า ที่ระดับความเข้มข้นเป็น 6.7 พีพีบี และ 150 พีพีบี ตามลำดับ ซึ่งความสามารถในการตรวจวัดด้วยตาเปล่าได้รับการปรับปรุงให้เป็น 50 พีพีบี โดยการผสมกับไดไมริสโทอิลฟอสฟาทิดิลโคลีนกับไดแอเซทิลีนลิปิดในการเตรียมพอลิไดแอเซทิลีนเวสิเคิล การพัฒนาตัวตรวจวัดแบบอินดิเคเตอร์กระดาษให้ความสามารถในการตรวจวิเคราะห์ที่ต่ำ โดยตรวจวัดได้ในระดับการตรวจวัดด้วยตาเปล่าที่ความเข้มข้นของไดคลอวอสสูงถึง 500 พีพีบี

สาขาวิชา ปิโตรเคมี	ลายมือชื่อนิสิต ....
ปีการศึกษา 2556	ลายมือชื่อ อ.ที่ปรึกษาวิทยานิพนธ์หลัก ....
	ลายมือชื่อ อ.ที่ปรึกษาวิทยานิพนธ์ร่วม ....

5273842723 : MAJOR PETROCHEMISTRY

KEYWORDS: PESTICIDE / ORGANOPHOSPHATE / POLYDIACETYLINE / ENZYME ACETYLCHOLINESTERASE / INHIBITOR / CHOLINE ESTER / SURFACTANT

RUNGNAPHA PIMSEN: COLORIMETRIC DETECTION OF ORGANOPHOSPHATE PESTICIDES USING POLYDIACETYLENE VESICLES WITH ACETYLCHOLINESTERASE AND SURFACTANTS. ADVISOR: ASSOC. PROF. MONGKOL SUKWATTANASINITT, Ph.D., CO-ADVISOR: ASST. PROF. SUMRIT WACHARASINDHU, Ph.D., 103 pp.

Organophosphate pesticides have been widely used in agriculture and in domestic purposes. It has posed serious concern for food and water contamination. Numerous of these pesticides, especially for dichlorvos, possess both acute and chronic toxicity posing hazardous risks to humans and environment. A new colorimetric method for the detection of dichlorvos based on polydiacethylene and acetylcholinesterase inhibition is developed. The blue-to-red color transition of poly(10,12-pentacosadynoic acid) vesicles can be induced by myristoylcholine which is enzymatically hydrolyzed by acetylcholinesterase to myristic acid and choline that prevents the color transition. In the presence of dichlorvos, the hydrolytic activity of the enzyme is inhibited that the blue-to-red color transition is restored with a linear correlation to the dichlorvos concentration with good selectivity over other organophosphate pesticides. Using UV-vis absorption spectrometer, the limit of detection is 6.7 ppb dichlorvos and the detection of 150 ppb by naked eye observation is possible. Sensitivity improvement of the naked eye detection to 50 ppb is achieved by mixing dimiristoylphosphatidylcholine to the diacetylene lipid in the preparation of the polydiacetylene vesicles. Development of paper-based poly(PCDA) indicator was attempted but it gave less sensitivity with the detection of 500 ppb for naked eye detection.

Field of Study: Petrochemistry   Student's Signature ....

Academic Year: 2013   Advisor's Signature ....

                                            Co-Advisor's Signature ....

ACKNOWLEDGEMENTS

CONTENTS

LIST OF TABLES

LIST OF FIGURES

LIST OF ABBREVIATIONS

AChE	Acetylcholinesterase
PDA	Polydiacetylene
PCDA	10,12-pentacosadiynoic acid
PBS	Phosphate buffered saline
UV	Ultraviolet
CR	Colorimetric response
OP	organophosphate
DMPC	Dimyristoylphosphatidycholine
CTAB	Cetyltrimethylammonium bromide
CTAC	Cetyltrimethylammonium chloride
AIE	Aggregation-induced emission

TPE	Tetraphenylethylene
-SO_3^-	Sulfonate
AuNP	Gold nanoparticles
ATCh	Acetylthiocholine
AgNP	Silver nanoparticles
Hcy	Homocysteine
DTT	Dithiothreitol
VOC	Volatile organic compound
$CHCl_3$	Chloroform
CH_2Cl_2	Dichloromethane
KCl	Potassium chloride
Na_2HPO_4	Sodium hydrogen phosphate
KH_2PO_4	Potassium dihydrogen phosphate
NaOH	Sodium hydroxide
HCl	Hydrochloric acid
$MgSO_4$	Magnesium sulfate
NMR	Nuclear magnetic resonance spectroscopy
CLSM	Confocal Laser Scanning Microscope
DSC	Differential scanning calorimetry
MC	Myristoylcholine
LC	Lauroylcholine
PC	Palmitoylcholine
SC	Sterylcholine
LA	Lauric acid
MA	Myristic acid

PA	Palmitic acid
SA	Stearic acid
MRL	Maximum residue limit
MHz	Megahertz
pH	Potential of hydrogen ion
°C	Degree celsius
g	Gram
mol	Mole
mL	Millilitre
mM	Millimolar
μW	Microwatt
μL	Microlitre
μM	Micromolar
μm	micrometer
nm	Nanometre
ppm	Part per million
ppb	Part per billion
min	Minute
%	Percent

CHAPTER I

INTRODUCTION

1.1 Background and statements of problems

Organophosphate compounds are a group of chemicals that are wildly used as pesticide for crop protection in agriculture and residential settings show low environmental constancy, however they display extreme toxicity [1]. The result of organophosphates at the high level concentration possess both acute neurotoxicity and carcinogenicity which effect on human health and environment [2]. In general, organophosphates are extremely effective inhibitors of the enzyme acetylcholinesterase (AChE) participating in nerve-impulse transmission. Therefore, if AChE activity is inhibited, acetylcholine accumulates in the nerves, results in the nerves overstimulation. Moreover, long term exposure to low levels of organophosphates can lead to persistent and additive inhibition of AChE resulting in a delayed neuropathy [3]. Because of their high toxicological behavior, Maximum residue limits (MRL) and acceptable daily intake (ADI) values for parent pesticides have been set by several organizations, such as the Food and Agriculture Organization of the World Health Organization (FAO/WHO) and the European Union (EU). The EU has set a very low limit for pesticides in baby food. According to this regulation, infant formulae must not contain residues of individual pesticides at levels exceeding 10 µg kg^{-1} [4], In order to monitor the level of organophosphates and prevent the over contamination in water resources and agriculture products, a convenient and sensitive method for determination of organophosphates is indispensable.

In well equip laboratories, chromatographic methods such as GC and HPLC [5–8] are the method of choice for highly sensitive and accurate determination of organophosphates. However, these methods are expensive, time-consuming, and require skillful operators that are not suitable for on-site analysis [1, 9–11]. To achieve the on-site application, recent development of organophosphate sensors based on nanosensors [12], chemiluminescence [13], fluorescence [14, 15] and colorimetry [16] have been reported. The colorimetric method provides particularly desirable features for on-site screening of the interested analysts, simply by naked eye observation.

Polydiacetylene (PDA), a conjugated ene-yne polymer of diacetylene, has been successfully used as colorimetric sensors for various types of external stimulants such as temperature [17–24], mechanical stresses [25, 26], pH [27–29], and chemicals [20, 30–34]. Recently, oxime functionalized 10,12 pentacosadiynoic acid (PCDA), a diacetylene lipid, was developed for organophosphate detection. However, this sensing system required a head group modification of PCDA and gave rather low sensitivity with the detection limit around 160 ppb of diisopropylfluorophosphate [16]. In this research, the development of organophosphate sensor based on colorimetric transition of polydiacetylene (PDAs) and the AChE enzyme inhibition effect by organophosphate. In our view, the utilization of enzymatic method will provide not only a high selectivity but also a sensitivity enhancement due to its catalytic nature.

The strategy in this work was inspired by the report that the color transition of PDAs can be induced by certain cationic surfactants [18, 32]. In this work, we hypothesized that the cationic choline ester derivative of a fatty acid can induce the blue-to-red transition of poly (PCDA) vesicle. In the presence of AChE, the ester derivative is enzymatically hydrolyzed back to the corresponding fatty acid and

choline [15]. These products lack of the cationic surfactant properties that should not induce the color transition of poly(PCDA). The AChE hydrolytic activity should be inhibited if there is dichlorvos in the system and the blue-to-red color transition of poly(PCDA) vesicle is restored. Therefore, the concentration of organophosphates can be determined from the color transition level of poly(PCDA) (Scheme 1.1).
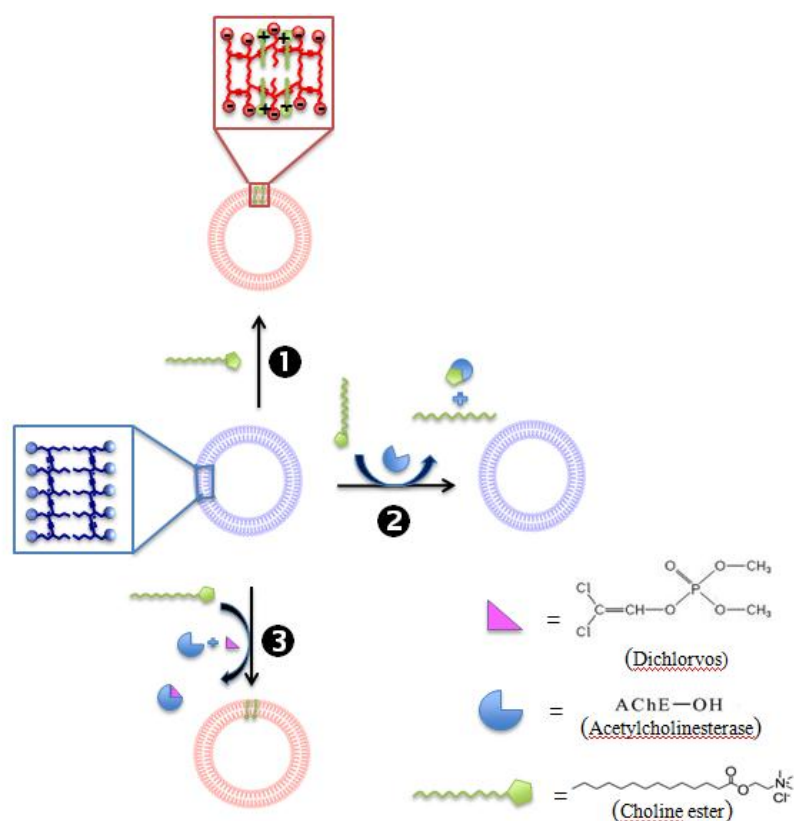
Scheme 1.1 Schematic illustration of dichlorvos detection based on poly(PCDA) vesicles/AChE/choline ester system. ❶ colorimetric response of poly(PCDA) to choline ester; ❷ colorimetric response of poly(PCDA) to mixture of choline ester and AChE; ❸ colorimetric response of poly(PCDA) to mixture of choline ester, dichlorvos and AChE.

1.2 Theory

1.2.1 Polydiacetylene vesicles

Polydiacetylene (PDA) is ene-yne conjugated polymer which exhibits unique chromatic properties. PDA is formed through topological 1,4 addition polymerization of diacetylene monomer, initiated by ultraviolet (UV) light or γ-rays irradiation as shown in Figure 1.1.
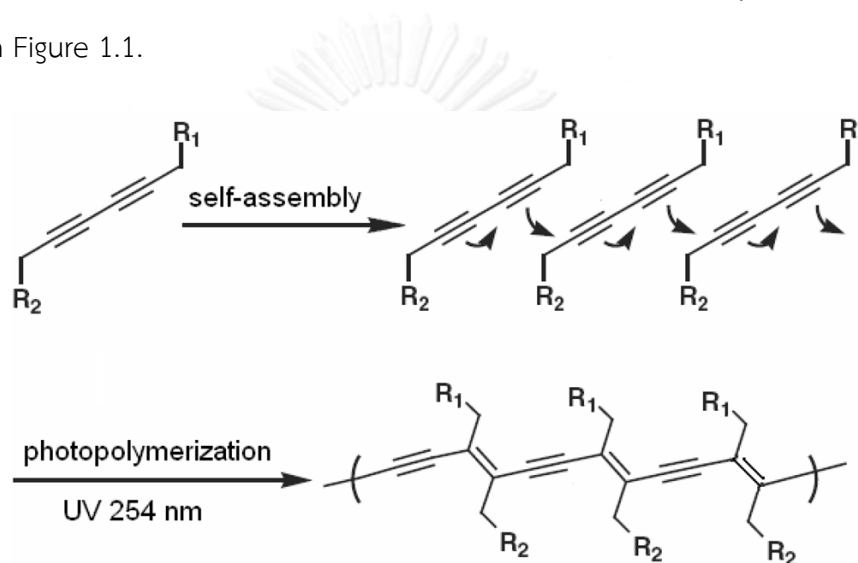
Figure 1.1 Phototopolymerization of diacetylene monomers upon irradiation with UV light [35].

The topopolymerized diacetylene crystals are nearly perfectly ordered crystals which cannot be occurred by solution polymerization or recrystallization of a preformed polymer from solution or melt. The resulting PDA, if generated under optimized conditions appears as an intense blue-colored PDA. PDA can change color from blue to red, having the maximum absorption peak at 630 nm and 540 nm in the blue and red form, respectively, under external perturbation such as temperature, pH, solvent, mechanical stress and ligand-receptor interactions due to reduction of the effective conjugation length resulted from strain and torsion imposed onto the backbone induced by order-disorder transitions in the side chains. Owing to these color changing properties, PDA-based sensors have been prepared in

a wide range of organized structures such as single crystals, thin films on solid supports using Langmuir-Blodgett or Langmuir-Schaefer techniques, PDA-embedded polymer matrix films, self-assembled monolayers, liposomes or vesicles in water.

Diacetylene lipid acids are known to spontaneously organize into vesicle structure in aqueous media which can be further photopolymerized by UV light to provide spherical nanostructure of polydiacetylene vesicles. One of the most commonly used lipid monomer for preparation of vesicles is 10,12-pentacosadiynoic acid (PCDA). PCDA monomers have carboxylic group that can dissociate in water and make these monomers hydrophilic but long hydrocarbon chain make these monomers hydrophobic. PCDA monomer can thus assemble in the form of lipid bilayer vesicles in water and can be polymerized by irradiation with UV light (Figure 1.2).
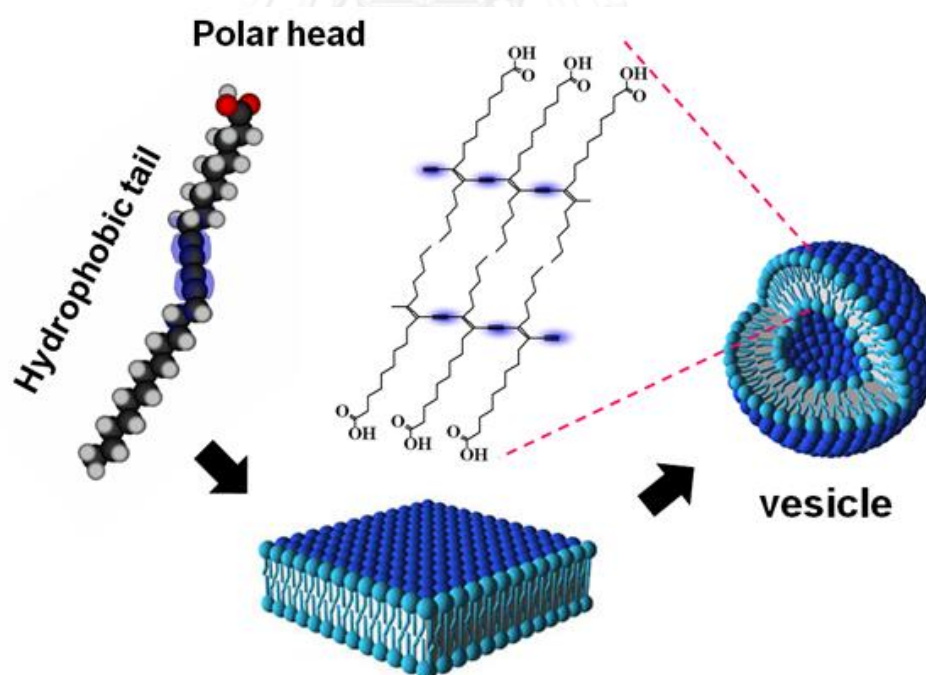
Figure 1.2 Structure and formation of a PDA lipid vesicle [36].

1.2.2 Electronic transition of polydiacetylene

Optical absorption in polydiacetylene occurs via $\pi \longrightarrow \pi^*$ absorption within the linear π-conjugated polymer backbone. Upon polymerization, frequently the first chromogenically interesting state of PDA appears blue in color. The exposure of PDA to environmental perturbations involve a significant shift in absorption from low to high energy bands of the visible spectrum, so the polydiacetylene transforms from blue to red color that resulted from molecular conformational changes such as side chain packing, ordering, and orientation, impart stresses to the polymer backbone that alter its conformation, thus changing the electronic states and the corresponding optical absorption.

1.2.3 Colorimetric properties of polydiacetylene

PDAs usually appear as deep colored materials that exhibit interesting colorimetric properties. Optical absorption in polydiacetylene occurs via an electronic $\pi \longrightarrow \pi^*$ transition within the linear π-conjugated polymer backbone. Upon polymerization, frequently the first chromogenically interesting state of PDA appears blue in color. The exposure of PDA to environmental perturbations, such as temperature, UV light, pH, solvent, mechanical stress and ligand-receptor interactions, induce a significant shift in absorption from low to high energy bands of the visible spectrum, so the polydiacetylene transforms from blue ($\lambda_{max} \sim 630$ nm) to red ($\lambda_{max} \sim 540$ nm). These perturbations alter the polymer side chain orientation that inturn change the backbone strain and torsion, thus changing the electronic states and the corresponding optical absorption.

The most investigated PDAs are those having blue color, which can change their color to red corresponding to the shift of the maximum absorption peak from

as a result of reduction of the effective conjugation length. The color transition can be induced by several external stimuli.

1.2.4 Chromisms of polydiacetylene

One of the most intriguing properties of PDA is its ability to change the color upon its exposure to external stimuli such as heat (thermochromism), organic solvent (solvatochromism), mechanical stress (mechanocromism) and ligand-receptor interaction (affinochromism). The color change induced by an external stimulus which may release backbone strain or disturb the backbone conformation by the change of packing, ordering, and orientation of the side chain of PDA can cause the electronic absorption of PDA shifted to shorter wavelength resulting in the blue-to-red color transition [37, 38].

A general inclusive concept, the conformation change of PDA by external stimuli can lead to the twisting of the structure and the decreasing in the length of conjugated system which concerns the interaction between side chains of PDA. In addition, the C-C bond rotation in the polymer backbone may influence the overlap of the PDA-molecular orbitals and consequently the change of the energy level. The red PDA may consist of a non-planar backbone configuration in combination with the alkyl side-chains rotation and distortion (Figure 1.3) [39]. Both of released backbone strain and conformational change concept are thus changing the electronic states and the corresponding optical absorption [36, 40]. Generally, visible absorption in PDA occurs via $\pi \rightarrow \pi^*$ absorption within the linear π-conjugated polymer backbone. A significant shift in the visible absorption spectrum from low to high energy band is a result of the change of light absorbed by π electron of conjugate system in a polymer main chain.
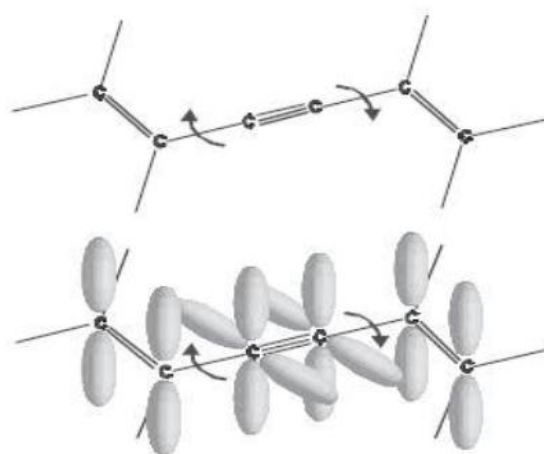
Figure 1.3 Molecular orbitals in the **π**-conjugated PDA backbone in the planar configuration [40] .

Solvatochromism

      Solvatochromism is one of the chromic properties of polydiacetylene. It is believed that solvation of polymer side chain by organic solvent can cause the side chain disorder that effect on the conjugation of PDA backbone resulting in the color change of the PDA from blue to red or yellow. In 2006, Kim and coworkers reported the PDA embedded electrospun fiber by using electrospining technique to fabricate a high surface area microfiber to make a colorimetric sensor array for volatile common organic solvents detection [41]. The electrospun fiber that produce from four different types of diacetylene monomer showed characteristic color response pattern to common organic solvents such as chloroform, tetrahydrofuran, ethylacetate and hexane (Figure 1.4).
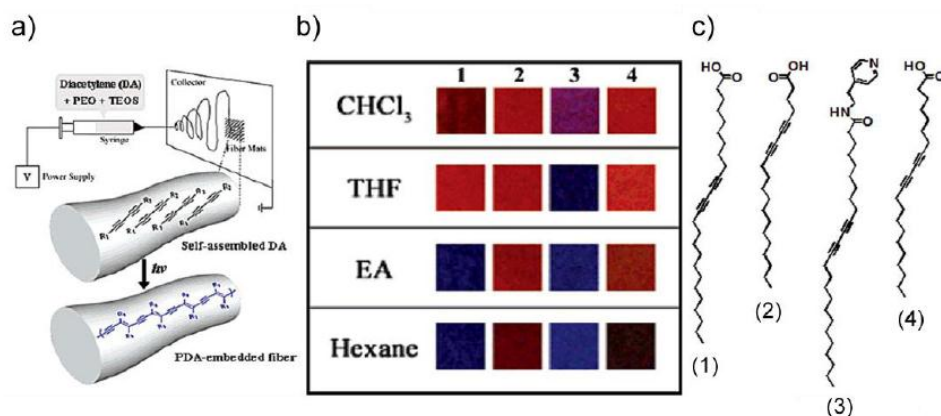
Figure 1.4 PDA embedded electrospun fiber. a) preparation of electrospun fiber, b) PDA embedded electrospun mat sensor array after exposure to volatile organic solvents, c) four types of diacetylene monomers [41].

In 2009, Kim and co-workers continued to report the investigation of PDA embedded electrospun fiber prepared from mixture of two PCDA derivatives, PCDA-ABA and PCDA-AN, in response to nine organic solvents [42]. The color pattern showed the unique color character of each organic solvent (Figure 1.5). This work has developed from their previous work that mentioned above but reduced the type of diacetylene monomers that necessary to use from four types to two types.
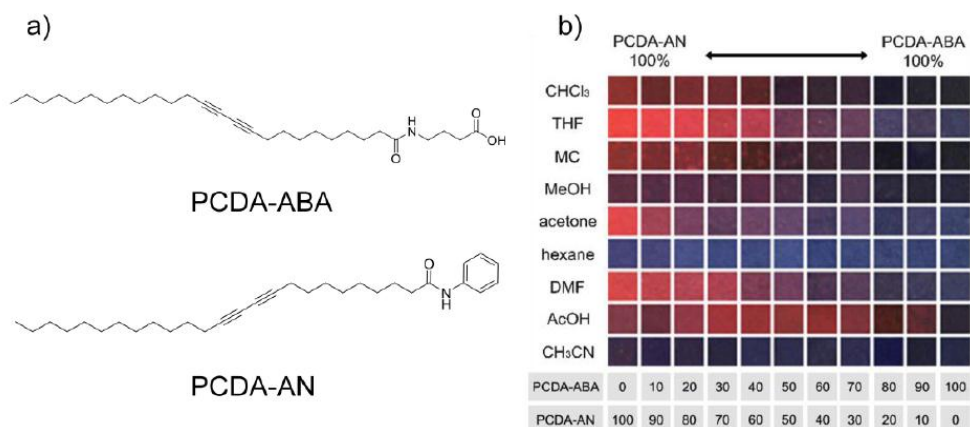
Figure 1.5 a) two types of diacetylene monomers and b) PDA embedded electrospun mat sensor array after exposure to volatile organic solvents [42].

Alkalinochromism and acidochromism

Alkalinochromism and acidochromism were chromic properties that the color change of material is caused by deprotonation and protonation, respectively. Poly(10,12-tricosadiynoic acid) (poly(TCDA)) was reported to exhibit the alkalinochromism by changing its color from blue to red during the addition of basic solution [43]. The titration of poly(TCDA) vesicles by NaOH solution produced a red vesicle. The pKa of PDA was in the range of 9.5-9.9 depending on a kind of metal hydroxide (Figure 1.6). The author proposed the color transition mechanism which started by 1) deprotonation of carboxylic proton, 2) metal ion binding with the carboxylate anion and 3) the conformational change of the alkyl chain.
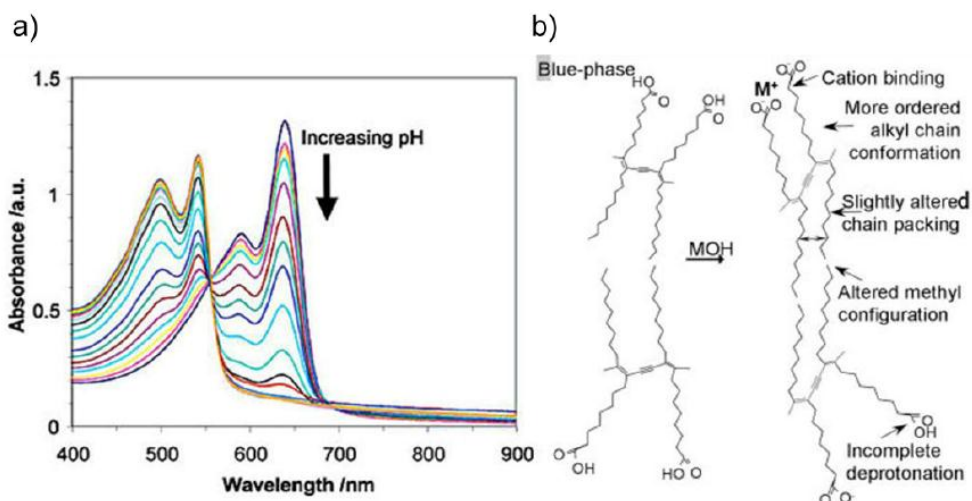
Figure 1.6 a) Absorption of the titration of 0.5 mM poly(TCDA)vesicle with 0.1 N NaOH solution, b) propose of color transition mechanism by alkalinochromism [43].

Mechanochromism

Mechanochromism is a property of which a material changes its color in response to an applied strain. The blue-to-red transition of PDA can be activated by some mechanical force. Muller and Eckhardt observed an irreversible transition in a PDA single crystal induced by compressive stress, which resulted in coexisting of blue and red phases [44]. Nallicheri and Rubner also observed reversible mechanochromism of conjugated PDA embedded in a host elastomer that was subjected to tensile strain [45].

Thermochromism

Thermochromism is probably the earliest chromism property found for PDA. The most notable thermochromism involves the color change from blue to red that have been developed for various colorimetric and fluorescence sensing applications. The thermochromic PDA can be either reversible or irreversible depending on the

interaction between the side chain substituents and side chain head groups. There are many dedicated effort research to elucidate the mechanisms of color change in PDA materials which is still not fully understood. It is likely that more than one mechanism causing thermochromic change depending on the nature of polymer. The report has shown that both side chain order and head group hydrogen bonding affect the chromic state [46].

Affinochromism

The most attractive feature of polydiacetylene to be discovered in recent investigation concerns the new chromic changes promoted by interaction with biologically, environmentally or chemically interesting target molecules. Generally, PDAs sensor derived from modification of head group of 10,12-pentacosadiynoic acid (PCDA) are able to underwent blue to red color change upon exposure to the target molecules. The DA monomers were modified to carry a receptor in the head group, matching with the target molecules. After addition of target molecule, showed the colorimetric transition induced by interaction of a PDAs with target molecules. For example, Kim and co-worker (ref) prepared two types of cyanuric acid-carrying PDA monomers; PCDA-CA and PCDA-EG-CA for melamine detection (Figure 1.7). The vesicle solution of poly PCDA-EG-CA/PCDA (9/1 mole ratio) displayed the color transition from blue-to-red upon addition of various concentration of melamine from 1 to 40 ppm. Such an excellent sensitivity is suitable to detect melamine at the world regulation level.
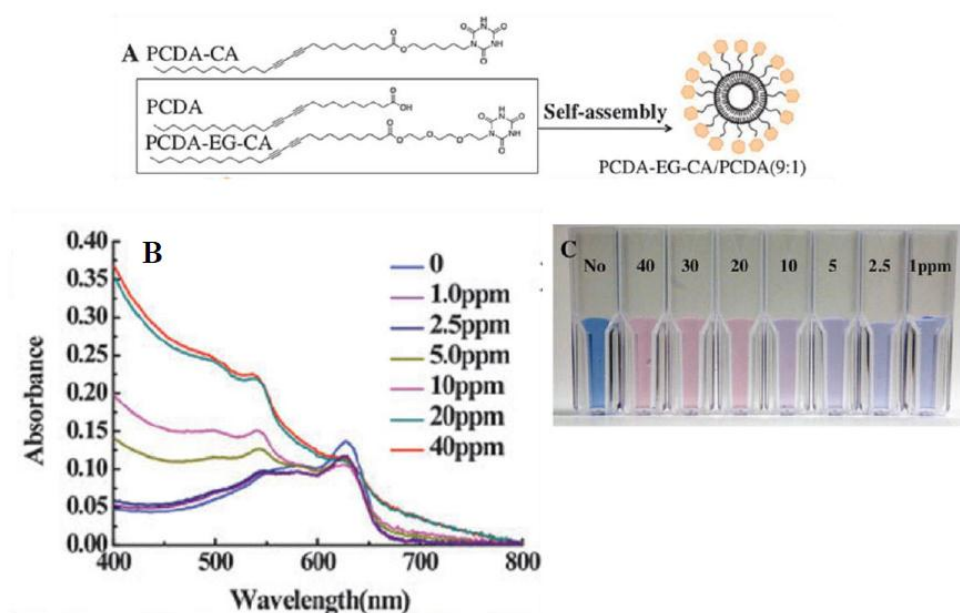
Figure 1.7 a) Structure of diacetylente monomers, b) UV-visible spectra and C) colorimetric transition of PDA detection with melamine [47].

1.2.4.1 Colorimetric Response (CR)

The color transition of the polymerized vesicles was monitored by measuring the absorbance differences between the vesicles before and after stimulation by an interesting parameter. This information is often converted to a percentage, termed the Colorimetric Response (CR) [48].

A quantitative value for the extent of blue-to-red color transition is given by the colorimetric response (%CR) which is defined as

$$\%CR = (PB_0 - PB)/PB_0 \times 100$$

Where $PB = A_{blue}/(A_{blue} + A_{red})$, A_{blue} and A_{red} are the absorbance of the blue and the red phase at 630 and 540 nm, respectively. The visible absorbance was measured by a temperature controlled UV-vis spectrometer. PB_0 is the initial percent blue of the

vesicle solution and film before heated. All blue-colored PDA vesicle solution and film samples were heated from 10 to 90 $^\circ$C.

1.2.5 RGB color model

According to development of paper based colorimetric respond of polydiacetylene is a simple method and suitable to use as a sensors application, since evaluate the results into a quantitative analysis can be collected by using the RGB color model. The RGB color model is an additive color model in which red, green, blue color are added together in various component ratio to reproduce a broad array of colors as shown in Figure 1.8. The name of the model comes from the initials of the three additive primary colors, red, green, and blue. The main purpose of the RGB color model is for the sensing, representation, and display of images. The RGB color model was used to descript how much of each red, green, and blue color is included in the photographic images [49].

For the basic of the RGB value(R, G, B), the color is black when the intensity of each component is zero (0, 0, 0) and the color is white when the intensity of each component is full (255, 255, 255). When the intensities are the same, the result is a shade of gray, darker or lighter depending on the intensity.
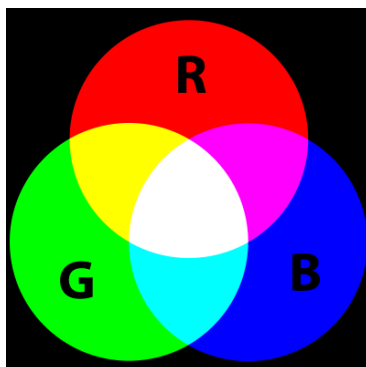
Figure 1.8 The RGB color model [49].

1.3 Organophosphate pesticides and dichlovos

The utilization of organophosphate (OP) compounds have played an important role to enhance productivity and crop yields in agricultural industry since 1940s [50]. OPs are broadly used for crop protection and pest control and there are a wide variety of chemical structures (Figure 1.9) being commercially available [51]. Up to 2000s, numerous of these pesticides, especially for dichlovos, have become popular for both agriculture and home uses [52]. OPs are potent nerve agents since they can irreversibly block acetylcholinesterase (AChE), an enzyme that is critical to nerve function. Due to their acute toxicity, the United States Environmental Protection Agency (US EPA) has banned most domestic uses of OPs, but they are still widely sprayed for crop protection and pest control, like mosquitos, in public spaces such as parks. For dichlovos, it was first considered for a ban by the US EPA in 1981. Since then it has been close to being banned on several occasions, but continues to be available. It also remains widely used in developing countries.
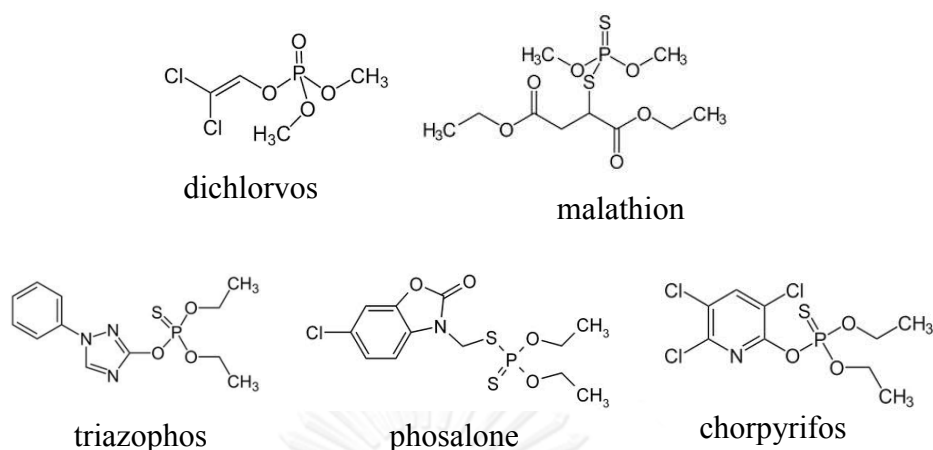
Figure 1.9 General chemical structure of OPs and their examples.

In general, AChE catalyzes the hydrolysis of neurotransmitter acetylcholine to choline and acetic acid after the completion of neurochemical transmission (Figure 1.10). Therefore, when AChE activity is inhibited, acetylcholine accumulates in the nerve cells resulting in overstimulation of the nerveous system. Organophosphate pesticides are particularly effective irreversible AChE inhibitors that form covalent phosphate bond to the serine active site of AChE, transforming it into inactive form of phosphorylated AChE (Figure 1.11) [52].

Acetylcholine

Acetylcholinesterase-Acetylcholine complex

+ H_2O

Acetic acid   **Choline**

Acetylcholinesterase
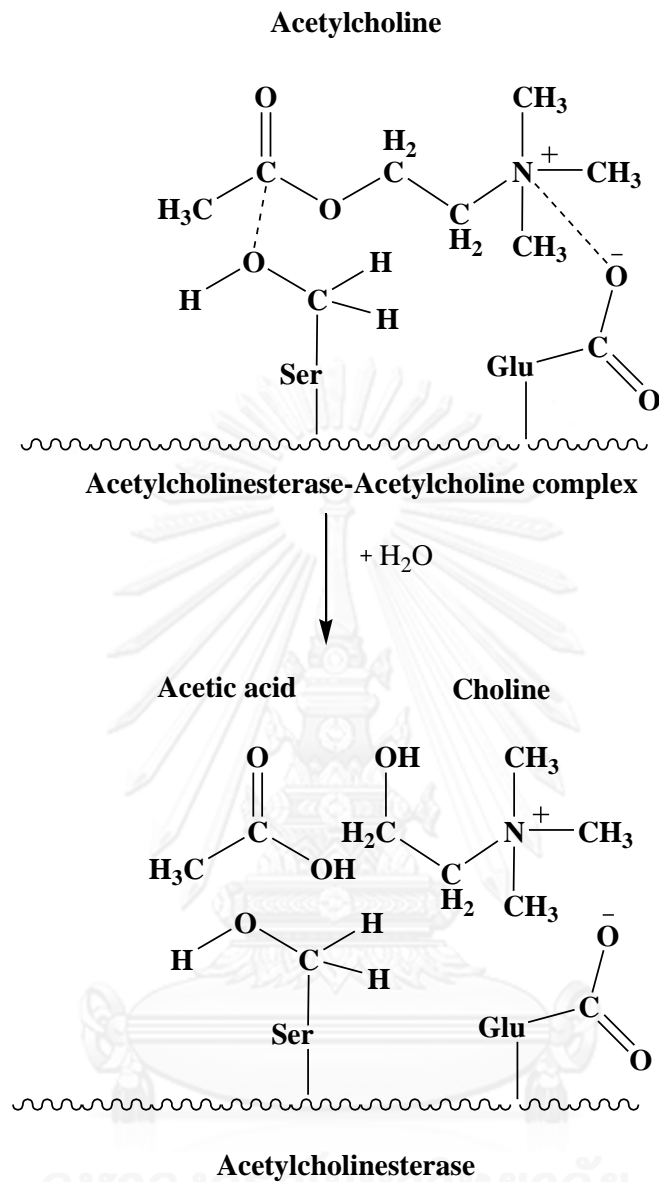
Figure 1.10 Schematic illustration of acetylcholine hydrolysis catalyzed by AChE [52]

.
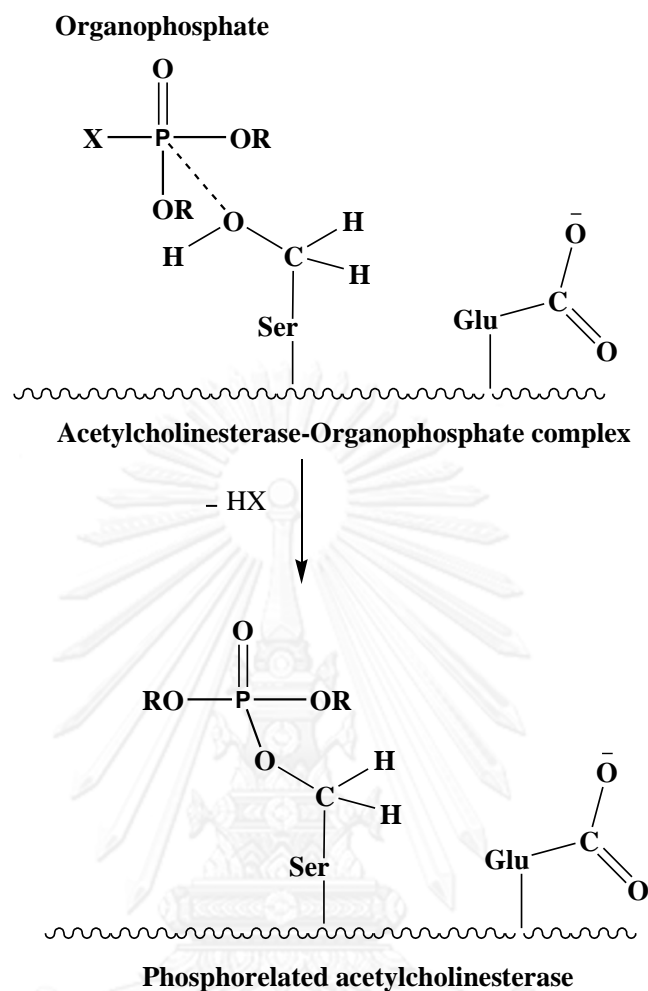
Organophosphate

Figure 1.11 Schematic inhibition of AChE by organophosphate pesticide [52].

OPs can be absorbed through all paths of exposure, including inhalation, ingestion, and dermal absorption. Human being are inevitably exposed to residues of these pesticides and their degradation products in air, water and food. These pesticides employment in agriculture and residential schedules has caused critical environmental pollution and potential health risks including acute and chronic cases of human and animal poisonings. The effect of persistent exposure to OPs are impaired memory and concentration, disorientation, severe depressions, irritability, confusion, headache, speech difficulties, delayed reaction times, nightmares, sleepwalking and drowsiness or insomnia. An influenza-like condition has been

reported. In the case of overdose symptoms are weakness, headache, blurred vision, nausea, vomiting, diarrhea, and abdominal cramps [53]. Jurewicz J. and Hanke W. found that the brain development of the fetuses and young children depends on a strict arrangement of biological actions that their contacts with OPs closely related to Attention Deficit Hyperactivity Disorder [54]. Hayden KM, et al. has found that OPs exposure is related with an increased risk of Alzheimer's disease [55]. In 2010, the US EPA classified parathion as possible human carcinogen [56].

There are two main types of OPs i.e. (a) phosphates and (b) phosphorothioates (Figure 1.12). The compounds with P=O functionality is sometimes referred to as an oxon while that with P=S is called a thion. The R^1 and R^2 side chain are usually alkyl or aryl groups which may be bonded directly or through oxygen or sulphur atoms. The group X represents one of a variety of substituted aliphatic, aromatic or heterocyclic groups linked to the phosphorus atom through a labile bond. X is thus often referred to as the 'leaving group', during AChE inhibition process, the phosphorus atom binds to an amino acid on the enzyme with X being eliminated [57].
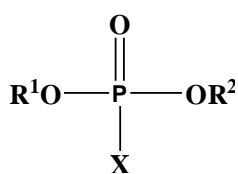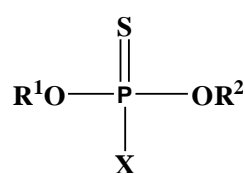
a) Phosphate   b) Phosphorothioate

Figure 1.12 Chemical structures of two types of organophosphate pesticides.

1.4 Literature reviews

1.4.1 Utilization of cationic surfactants in sensing applications

In 2005, Su *et al*. [32] studied the effects of cationic surfactant cetyltrimethylammonium bromide (CTAB) on the color transition of the polydiacetylene prepared from mixed lipid vesicles of dimyristoylphosphatidycholine (DMPC)/10,12-pentacosadiynoic acid (PCDA), in aqueous solution. The blue-to-red color transition of the DMPC/polymerized PCDA vesicles is related to the interaction of the positively charged head groups of CTAB with the negatively charged carboxylate groups on the surface of the vesicles. Whereas, the alkyl chain of CTAB molecule inserts into the hydrophobic domain of the vesicles, which disturbs the polymer backbone and leads to color change of the mixed vesicles. The colorimetric responses of the mixed vesicles induced by the addition of CTAB correlated with the DMPC content in the vesicles; an increase of DMPC content enhanced the interaction of CTAB with the mixed vesicles as displayed in Figure 1.13.
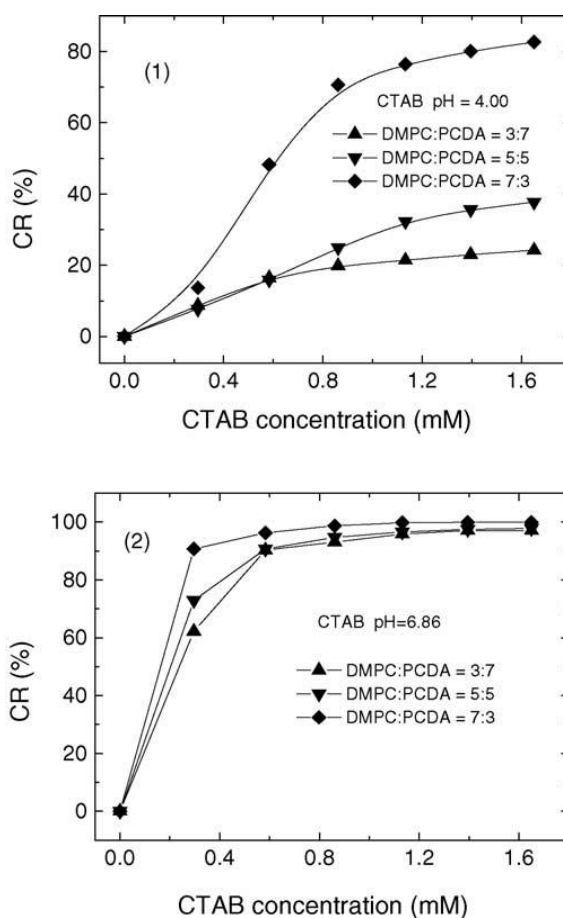
Figure 1 13 Colorimetric responses of the mixed DMPC/PCDA vesicles against CTAB at pH (1) 4.00 and (2) 6.88 [32].

In 2009, Chen *et al*. [58] have modified the head group of PCDA with 3,5-dihydrxylmenzaldehyde PCDA-HBA1 for colorimetric detection of cationic surfactants. The formation of intermolecular hydrogen bonding between the hydroxyl groups and adjacent aldehyde carbonyl moieties on the sureface of polydiacetylene vesicles was proposed. Cetyltrimethylammonium chloride (CTAC), a cationic surfactant, which contains both cationic ammonium group and along alkyl chain can interact with PCDA-HBA1, resulted in the disruption of the hydrogen bonding as shown in the Figure 1.14a. The disruption of the hydrogen bonding of PCDA-HBA1 by CTAC released the strain energy imposed on the alkyl side chains of the vesicles which

cause partial distortion of the arrayed p-orbitals, leading to a decrease in the conjugation length of the polymer, thus the blue-to-red color transition was observed. The colorimetric transition of PCDA-HBA 1 increased with increase CTAC concentration as shown in the Figure 1.14b.
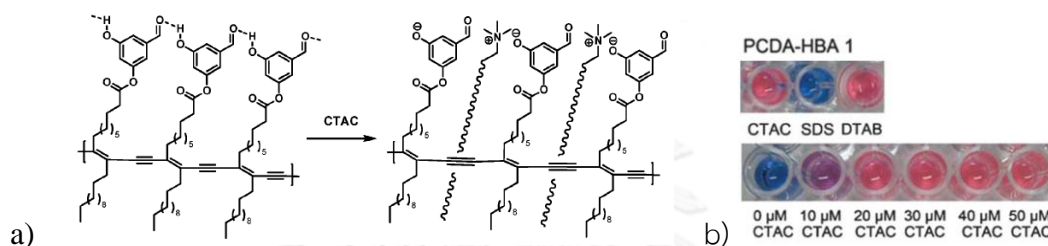
Figure 1.14 a) Proposed interaction between PDA derived from PCDA-HBA 1 and CTAC. b) Colorimetric transitions of PCDA-HBA 1 with various concentration of CTAC [58].

1.4.2 Utilization of acetylcholinesterase in sensing applications

In 2004, Jin *et al.* [1] synthesized a sensitive fluorescence probe, 2-butyl-6-(4-methyl-piperazin-1-yl)-benzo[de]isoquinoline-1,3-dione), and used as the pH indicator to determine the AChE enzyme inhibition activity of the organophosphate and carbamate pesticides. Normally, acetylcholine was hydrolyzed by AChE to acetic acid and choline. The fluorescence intensity of the probe was enhanced with increase acidity of the system. Therefore, the hydrolytic activity pf AChE leads to an increase of fluorescence intensity. When AChE activity is inhibited by the pesticides, the acidity decreases and so the fluorescence intensity. The inhibition percentage of the enzyme activity is correlated to the pesticide concentration. The detection limits for carbofuran, carbaryl, paraoxon and dichlorvos in water were 3.5, 50, 12 and 25 g/L, respectively.

In 2011, Xue *et al.* [59] presented the colorimetric detection of glucose and acetylcholinesterase (AChE) activity using amine-terminated polydiacetylene (PDA) vesicles as pH indicator. Generally, glucose can be oxidized to gluconic acid in the presence of glucose oxidase and acetylcholine can be hydrolyzed by AChE to acetic acid. The blue-to-red color transition of the vesicles correlated with the pH of the solution. Enzymatically, glucose and AChE activity can be detectermined with good selectivity and acceptable sensitivity. The detection limit of glucose and AChE activity were 2.5 μmol/L and 10.0 mU/mL, respectively.
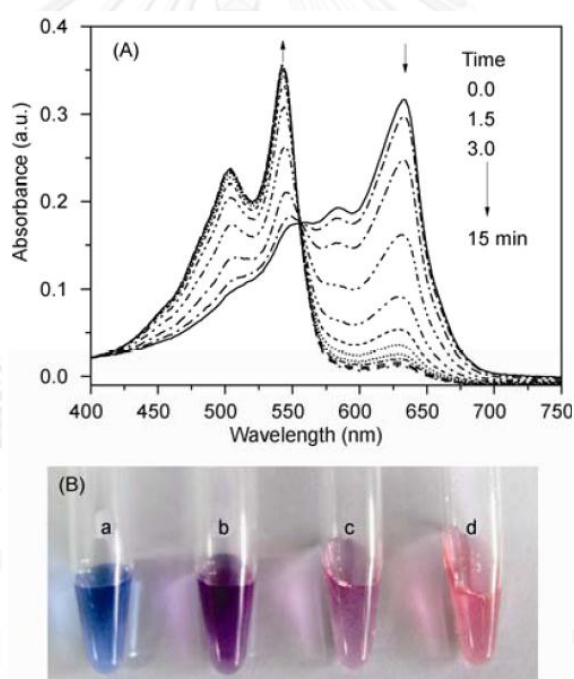
Figure 1.15 a) Absorption spectra of PDA vesicle solutions in the presence of ACh and AChE incubated for different times at room temperature.b) Photograph of the PDA vesicle solutions after the addition of acetylcholine with different amounts of AChE: a = 0; b = 20; c = 40; d = 80 mU/mL; each solution was incubated for 15 min at 25 °C [59].

1.4.3 Combination of cationic surfactants and acetylcholinesterase in sensing applications

In 2009, Wang *et al*. [15] established a fluorometric detection of AChE and its inhibitor based on the aggregation-induced emission (AIE) of a TPE (tetraphenylethylene) with two sulfonate ($-SO_3^{3-}$) units and myristoylcholine, an amphiphilic compound, as a substrate for AChE). The heteroaggregates formation of TPE and myristoylcholine led to the fluorescence enhancement of TPE. In the presence of AChE, the myristoylcholine was hydrolized into myristic acid and choline resulting in disassembly of the heteroaggregates of TPE, leading to the decrease of fluorescence intensity (Figure 1.16). Therefore, the fluorescence intensity is correlated to the AChE concentration. The hydrolysis with AChE can be monitored continuously, and AChE with concentration as low as 500 mU/mL can be determined.
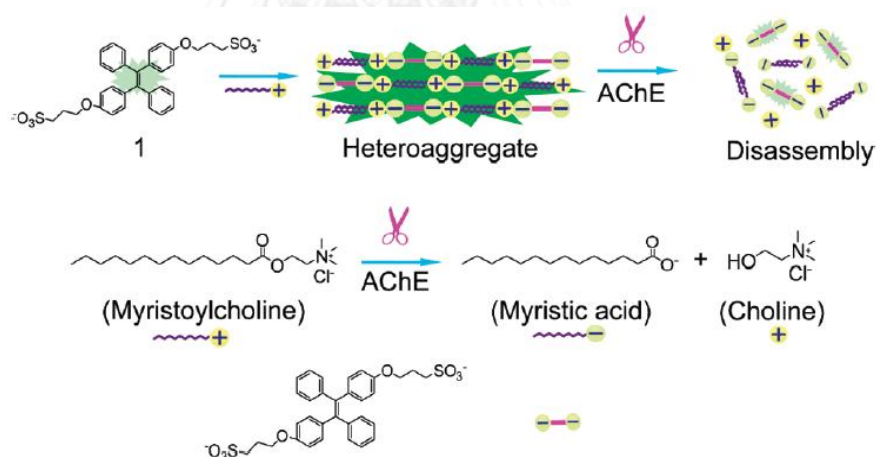
Figure 1.16 Schematic illustration of the formation of heteroaggregate between myristoylcholine and TPE and the disassembly of the myristoylcholine and Tetraphenylethylene aggregate in the presence of AChE [15].

1.4.4 Analysis and detection of dichlovos and other related organophosphates

In 2002, Andreou and Clonis [60] developed a fiber-optic biosensor for the pesticides carbaryl and dichlorvos detection based on cholinesterase inhibition. The sensing system comprised a three-layer sandwich. The outer layer was hydrophilic modified polyvinylidenefluoride membrane which immobilized with enzyme cholinesterase. The membrane was connected to the sol–gel layer which entrapped with bromocresol purple as a color indicator which deposited on an inner glass disk. In the presence of carbaryl or dichlovos, the enzyme is inhibited that results in pH alterations. Therefore, the signal transduction was related to the degree of enzyme inhibition, which measured by sol–gel entrapped pH indicator. Calibration curves were obtained for carbaryl and dichlorvos, with useful concentration ranges of 0.11–8.0 mg/L for carbaryl and 5.0–30 μg/L for dichlorvos. The detection limits were 108 μg/L and 5.2 μg/L.

In 2007, Vamvakaki and Chaniotakis [61] evaluated the organophosphorus pesticides dichlorvos and paraoxon levels using the AChE-based inhibitor liposome biosensor. AChE was encapsulated in the egg phosphatidylcholine liposomes which immobilized with the pH sensitive fluorescent indicator pyranine for the optical changing by the inhibiton of enzymatic activity. The increased concentration of pesticides causes the reduction of the enzymatic activity for the hydrolysis of the acetylcholine leading to a decrease in the fluorescent signal of the pH indicator. Figure 1.17 displayed that the fluorescence signal drastically decreases with increased pesticide concentrations. The dichlorvos and paraoxon concentration down to 10^{-10} M levels can be detected.
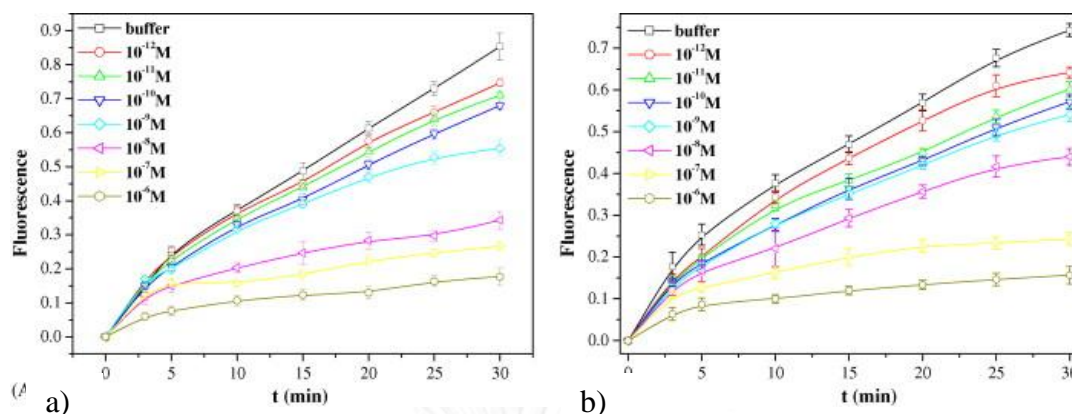
Figure 1.17 Fluorescence intensity of the AChE/liposome against time, 10 mM acetylcholine and different concentrations of a) dichlorvos and b) paraoxon. [61].

1.4.5 Development of paper-based sensors

Recently, analytical devices using paper as a sensing platform became very appealing for adaptable sensing system of clinical diagnosis, food quality control and environmental monitoring because of its versatility, high abundance and low cost [62][1,3–6]. The advantages of paper-based sensors are the aqueous media, chemicals, and biochemicals compatibility. Paper-based devices can be integrated in an approach that is flexible, portable, disposable and easy to operate are highly desirable.

In 2010, Pohanka *et al*. [63] developed a colorimetric dipstick for assay of nerve agents and organophosphate pesticides represented by sarin, VX and paraoxon based on enzymatic hydrolysis of acetylcholine. A disposable pH indicator strip was used as detectors. AChE was deposited on the dipstick which hydrolyzed acetylcholine into acetic acid and choline leading to accumulation of acetic acid. The dark red to yellow color transition was observed after pH shift. In the presence of an organophosphate pesticide or a nerve agent, the enzymatic hydrolysis was inhibited that the pH of the reaction was less acidic. The limit of detection of paraoxon-ethyl,

sarin and VX assay were 5×10^{-8} M for paraoxon-ethyl and 5×10^{-9} M for sarin and VX. Dipsticks were stable for at least one month.
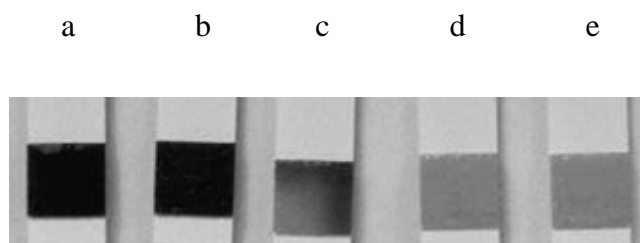
Figure 1.18 Photograph of dipsticks for assay of OPs; a) deionized water, b) paraoxon-ethyl concentration lower than the limit of detection (5×10^{-9} M), c) paraoxon-ethyl concentration equal to the limit of detection (5×10^{-8} M) and d,e) Paraoxon-ethyl concentration above the limit of detection (5×10^{-7} and 5×10^{-6} M). The light grey color relates to yellow, while the black relates to bright red [63].

In 2010, Luckham and Brennan [64] reported a bioactive paper-based colorimetric "dipstick" bioassay based on acetylcholinesterase (AChE) catalyzed enlargement of gold nanoparticles (AuNP). A paper substrate is coated with the co-entrapped AChE enzyme and AuNP in a sol–gel based silica as the bioactive test strips. The bioactive solutions which contained acetylthiocholine (ATCh) and a Au(III) salt are spotted on the sensing zone of the bioactive test strips. Generally, AChE hydrolyzed ATCh into thiocholine, which in turn reduces the Au(III), causing particle growth and a related increase in color intensity that correlated to the amount of substrate or inhibitor. The entrapped AuNP can be utilized for visual detection of paraoxon over the conentration range of 500 nM to 1 mM by naked eye or using a digital camera and image analysis, developing the assay suitable for remote analysis.
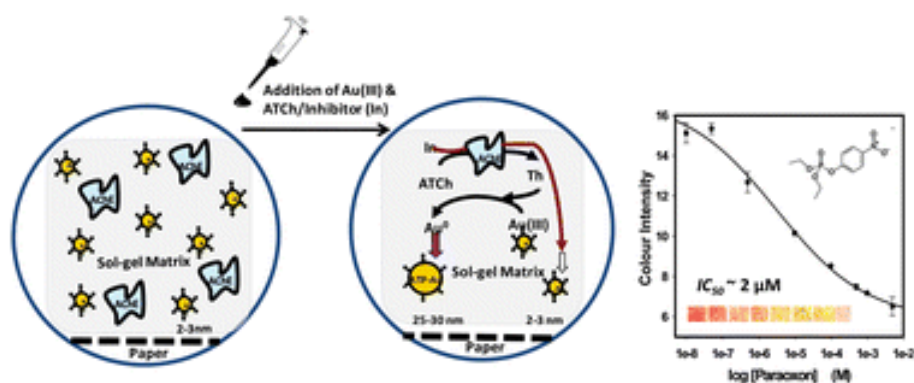
Figure 1.19 Schematic illustration of the co-entrapped AChE enzyme and gold nanoparticles (AuNP) in a sol–gel coated on paper substrate as paraoxon test strips [64].

In 2011, Pumtang *et al.* [65] reported the synthesis of a novel series of diacetylene acids from the condensation of pentacosa-10,12-diynylamine (PCDAmine) and dicarboxylic acid or its anhydrides. One of these diacetylene lipids, 4-(pentacosa-10,12-diynylamino)-4-oxobutanoic acid (PCDAS), is used in combination with pentacosa-10,12-diynoic acid (PCDA) for drop casting on pieces of filter paper which are consequently irradiated by UV light to generate a paper based sensor array for solvent detection and identification. Upon the exposure to various types of organic solvents, the blue colored sensors colorimetrically respond to give different shades of colors between blue to red (Figure 1.20). The color patterns of the sensor array are recorded as RedGreenBlue (RGB) values and statistically analyzed by principal component analysis (PCA). The PCA score plot reveals that the array is capable of identifying eleven common organic solvents.
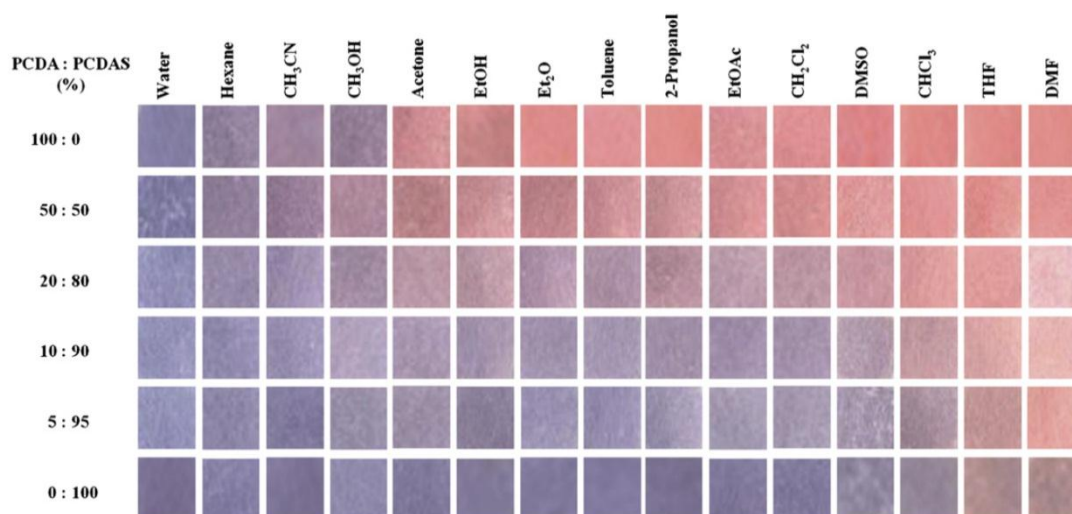
Figure 1.20 Array of cropped photographic images of PDAs on filter paper fabricated from PCDA and PCDAS responding to various organic solvents [65] .

In 2012, Eaidkong *et al.* [66] reported detection and identification of VOCs by paper-based polydiacetylene (PDA) colorimetric sensor array. They were prepared from eight diacetylene monomers, six of which are amphiphilic and the other two are bolaamphiphilic. To fabricate the sensors, monomers are coated onto a filter paper surface using the drop-casting technique and converted to PDAs by UV irradiation. The PDA sensors show solvent induced irreversible color transition upon exposure to VOC vapors as shown in Figure 1.21. When combined into a sensing array, the color change pattern as measured by RGB values and statistically analyzed by principal component analysis (PCA) is capable of distinguishing 18 distinct VOCs in the vapor phase. The PCA score and loading plots also allow the reduction of the sensing elements in the array from eight to three PDAs that are capable of classifying 18 VOCs.

a)

b)
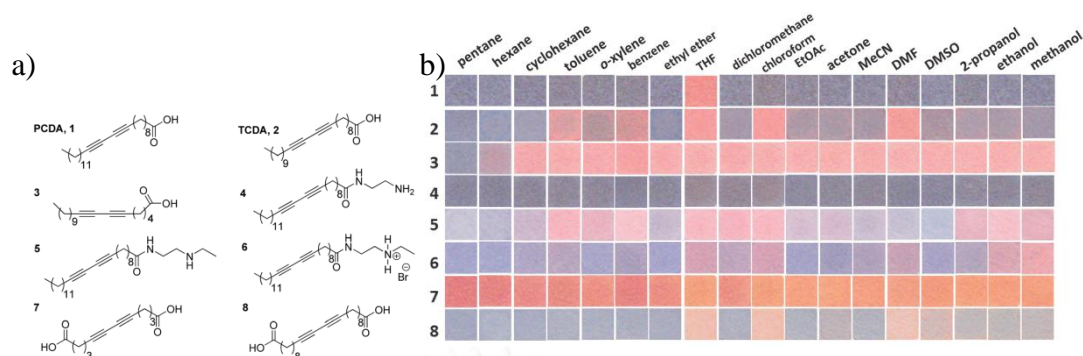
Figure 1.21 a) Structure of diacetylene monomers b)Scanned images of the paper-based PDA sensor array prepared from 1–8 exposed to various saturated vapors of volatile organic solvents [66].

1.5 Objectives and scope of the research

The objectives of this thesis are the investigation of OPs sensor based on colorimetric transition of polydiacetylene (PDAs) to the cationic surfactants and the AChE enzyme inhibition consequence by OPs. To achieve the objectives, the work scopes are shown as following;

1) To study the colorimetric response of poly(PCDA) to choline esters

2) To study the colorimetric response to mixture of choline esters and AChE

3) To study the colorimetric response to choline esters in the presence of AChE and OPs

4) To study the enhancement of OPs sensor using fatty acid (i.e. lauric acid, myristic acid, palmitic acid and stearic acid) or a phospholipid, dimyristoylphosphatidycholine (DMPC)

5) To study the preparation of paper-based PDAs for OPs indicators

CHAPTER II

EXPERIMENTAL

2.1 General Information

2.1.1 Chemicals and materials

1. 10,12-Pentacosadynoic acid (PCDA), GFS, USA

2. Acetylcholinesterase (EC 3.1.1.7, V-S type from electric eel, 2000 units mg^{-1} protein), Sigma Aldrich, Germany

3. Dimyristoylphosphatidycholine (DMPC), Sigma Aldrich, Germany

4. 2,2-Dichoroethenyl dimethyl phosphate (Dichlorvos), Fluka, Switzerland

5. O,O-diethyl O-3,5,6-trichloropyridin-2-yl phosphorothioate (Chlopyrifos), Fluka, Switzerland

6. Detail 2-[(dimethoxyphosphorothioyl) sulfanyl] butanedioate (Malathion), Fluka, Switzerland

7. 6-chloro-3-(diethoxyphosphinothioylsulfanylmethyl)-1,3-benzoxazol-2-one (Phosalone), Fluka, Switzerland

8. Chloroform ($CHCl_3$), AR grade, Lab-Scan, Ireland

9. Dichloromethane (CH_2Cl_2), commercial grade, Lab-Scan, Ireland

10. Potassium chloride (KCl), Merck, Germany

11. Sodium hydrogen phosphate (Na_2HPO_4), Merck, Germany

12. Potassium dihydrogen phosphate (KH_2PO_4), Merck, Germany

13. Sodium hydroxide (NaOH), Merck, Germany

14. Hydrochloric acid (HCl), Merck, Germany

15. Magnesium sulfate ($MgSO_4$) anhydrous, Riedel-deHan[®], Germany

16. Silica gel 60, Merck, Germany

2.1.2 Apparatus and equipments

1. Rotary evaporator, R200, Buchi, Switzerland

2. Ultrasonicator, Elma, Germany

3. Magnetic stirrer, Fisher Scientific, USA

4. Hot plated magnetic stirrer, IKA, Germany

5. Pipette man (P20, P200 and P5000), Gilson, France

6. Pipette man (Le100 and Le1000), Nichiryo, Japan

7. Nuclear Magnetic resonance spectrometer (NMR) 400 MHz, Mercury 400, Varian, USA

8. Confocal Laser Scanning Microscope (CLSM)

9. UV Lamp, TUV 15W/G15 T18 lamp, Philips, Holland

2.2 Preparation of choline ester

Lauroylcholine
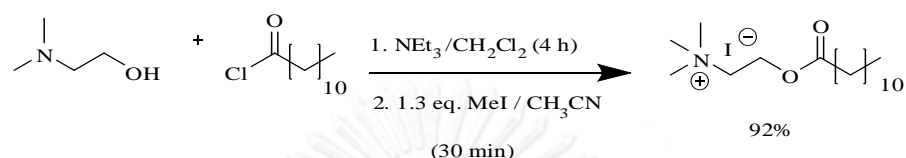
Lauroyl chloride (2.00 g, 9.14 mmol) was dissolved in dichloromethane (10 mL) and trimethylamine (2 mL) by stirring with a magnetic bar in a round-bottom flask. Then, dimethyl ethanol amine (2 mL) was added to the solution. The reaction mixture was stirred at room temperature for 4 h and then was added with distilled water (20 mL). The organic layer was separated and the aqueous phase was extracted with dichloromethane (2 × 20 mL). The combined organic liquid was dried over anhydrous $MgSO_4$. The solvent was removed by a rotary evaporator followed by a vacuum dry to afford 2-(dimethylamino)ethyl laureate in 93% yield (2.31 g, 8.50 mmol).

For the methylation, 2-(dimethylamino)ethyl lauroate was dissolved with acetronitrile (10 mL) in a round-bottom flask and methyl iodide (1.57 g, 11.1 mmol) was added under stirring with a magnetic bar. The reaction mixture was stirred at room temperature for 30 min. The solution was evaporated to dryness to afford lauroyl choline as white powder (3.48 g, 92 % yield). ^{1}H-NMR (CD$_3$OD, 400 MHz): δ (ppm) 4.54 (b, Hz, 2H), 3.75 (m, 2H), 3.25 (m, 9H), 2.40 (t, J = 7.6 Hz, 2H), 1.62 (t, J = 7.2 Hz, 2H), 1.28 (m, 16H), 0.89 (t, J = 6.6 Hz, 3H).

Myristoylcholine
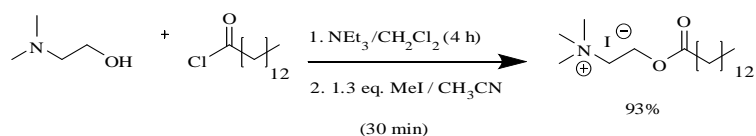
Myristoyl chloride (2.00 g, 8.10 mmol) was dissolved in dichloromethane (10 mL) and trimethylamine (2 mL) by stirring with a magnetic bar in a round-bottom flask. Then, dimethyl ethanol amine (2 mL) was added to the solution. The reaction mixture was stirred at room temperature for 4 h and then was added with distilled water (20 mL). The organic layer was separated and the aqueous phase was extracted with dichloromethane (2 × 20 mL). The combined organic liquid was dried over anhydrous $MgSO_4$. The solvent was removed by a rotary evaporator followed by a vacuum dry to afford 2-(dimethylamino)ethyl myristoate in 95% yield (2.26 g, 7.70 mmol).

For the methylation, 2-(dimethylamino)ethyl myristoate was dissolved with acetronitrile (10 mL) in a round-bottom flask and methyl iodide (1.39 g, 9.80 mmol) was added under stirring with a magnetic bar. The reaction mixture was stirred at room temperature for 30 min. The solution was evaporated to dryness to afford myristoyl choline as white powder (3.29 g, 93% yield).). ^{1}H-NMR (CD$_3$OD, 400 MHz): **δ** (ppm) 4.56 (m, 2H), 3.78 (m, 2H), 3.27 (s, 9H), 2.42 (t, J = 7.6 Hz, 2H), 1.64 (t, J = 7.2 Hz, 2H), 1.30 (m, 20H), 0.91 (t, J = 6.6 Hz, 3H).

Palmitoylcholine

Palmitoyl chloride (2.00 g, 7.28 mmol) was dissolved in dichloromethane (10 mL) and trimethylamine (2 mL) by stirring with a magnetic bar in a round-bottom flask. Then, dimethyl ethanol amine (2 mL) was added to the solution. The reaction mixture was stirred at room temperature for 4 h and then was added with distilled water (20 mL). The organic layer was separated and the aqueous phase was extracted with dichloromethane (2 × 20 mL). The combined organic liquid was dried over anhydrous $MgSO_4$. The solvent was removed by a rotary evaporator followed by a vacuum dry to afford 2-(dimethylamino)ethyl palmitoate in 96% yield (2.29 g, 6.99 mmol).

For the methylation, 2-(dimethylamino)ethyl palmitoate was dissolved with acetronitrile (10 mL) in a round-bottom flask and methyl iodide (1.29 g, 9.08 mmol) was added under stirring with a magnetic bar. The reaction mixture was stirred at room temperature for 30 min. The solution was evaporated to dryness to afford Palmitoyl choline as white powder (3.25 g, 95 % yield). ^{1}H-NMR (CD₃OD, 400 MHz): δ (ppm) 4.52 (m, 2H), 3.71 (m, 2H), 3.21 (s, 9H), 2.38 (t, J = 7.6 Hz, 2H), 1.61 (t, J = 7.2 Hz, 2H), 1.27 (m, 24H), 0.89 (t, J = 6.8 Hz, 3H).

Stearoylcholine

Stearoyl chloride (2.00 g, 6.60 mmol) was dissolved in dichloromethane (10 mL) and trimethylamine (2 mL) by stirring with a magnetic bar in a round-bottom flask. Then, dimethyl ethanol amine (2 mL) was added to the solution. The reaction mixture was stirred at room temperature for 4 h and then was added with distilled water (20 mL). The organic layer was separated and the aqueous phase was extracted with dichloromethane (2 × 20 mL). The combined organic liquid was dried over anhydrous $MgSO_4$. The solvent was removed by a rotary evaporator followed by a vacuum dry to afford 2-(dimethylamino)ethyl stearoate in 95% yield (2.23 g, 6.27 mmol).

For the methylation, 2-(dimethylamino)ethyl lauroate was dissolved with acetronitrile (10 mL) in a round-bottom flask and methyl iodide (1.16 g, 8.15 mmol) was added under stirring with a magnetic bar. The reaction mixture was stirred at room temperature for 30 min. The solution was evaporated to dryness to afford stearoyl choline as white powder (3.09 g, 94 % yield). ^{1}H-NMR (CD_3OD, 400 MHz): δ (ppm) 4.52 (m, 2H), 3.7 (m, 2H), 3.20 (s, 9H), 2.38 (t, J = 7.6 Hz, 2H), 1.61 (t, J = 7.0 Hz, 2H), 1.26 (m, 28H), 0.87 (t, J = 6.8 Hz, 3H).

2.3 Preparation of polydiacetylene vesicles

Poly(PCDA) vesicles:

PCDA (0.01 mmol) was dissolved in chloroform (2.5 mL) in a 50 mL test tube, and the solution was purged with N_2 gas to dryness. Water (10 mL) was added to the dry film of PCDA and the resulting PCDA suspension (1 mM) was sonicated in a 230 W sonicator bath at 80 $^{\circ}$C for 30 min. The suspension became translucent indicating the formation of a vesicle colloidal sol. The PCDA sol was kept at 4 $^{\circ}$C overnight before it was irradiated with 254 nm UV light for 5 min at room temperature to generate a blue poly(PCDA) sol. The poly(PCDA) sol was filtered through No.1 Whatman filter paper to remove any undesired aggregates.

Mixed lipid vesicle:

For the preparation of mixed lipid vesicle sols, a saturated fatty acids (i.e. lauric acid, myristic acid, palmitic acid and stearic acid) or a phospholipid, dimyristoylphosphatidycholine (DMPC) was dissolved in chloroform. Each lipid was mixed with PCDA, at designated PCDA/lipid mole ratios, in the preparation step of $CHCl_3$ solution, and the solution was purged with N_2 gas to dryness. Water (10 mL) was added to the dry film of mixed lipid and the resulting mixed lipid suspension (1 mM) was sonicated in a 230 W sonicator bath at 80 $^{\circ}$C for 30 min. The suspension became translucent indicating the formation of a vesicle colloidal sol. The mixed lipid sol was kept at 4 $^{\circ}$C overnight before it was irradiated with 254 nm UV light for

5 min at room temperature to generate a blue PCDA/lipid sol. The PCDA/lipid sol was filtered through No.1 Whatman filter paper to remove any undesired aggregates. For PCDA/DMPC mixed lipid, the sonication was performed at 60 $^{\circ}$C for 10 min to avoid a premature blue-to-red color transition.

2.4 Colorimetric measurements

The blue-to-red color transition of the polymerized sols was observed by naked eye and photographed by a digital camera. Moreover, the absorption spectra of the sols were recorded by UV-visible spectrophotometer. Quantitative values for the blue-to-red color transition were evaluated as percent colorimetric response (%CR) calculated from the following equation.

$$\%CR = \frac{100 \times (PB_0 - PB)}{PB_0}$$

where PB is the percent blue calculated from Ablue/(Ablue + Ared). The Ablue and Ared refer to the absorbance at the peak wavelength (λ_{max}) of the blue phase and red phase, respectively, of poly (PCDA). The λ_{max} of the blue phase and red phase were approximately 630 and 500 nm, respectively. The initial percent blue (PB_0) of the samples was determined before exposure to the external stimulus.

2.5 Colorimetric response of poly(PCDA) to choline esters

The poly(PCDA) (0.3 mM) was mixed with each choline ester, i.e. lauroylcholine, myristoylcholine, palmistoylcholine and sterylcholine in PBS (10 mM)

buffer solution pH 6.0, at various concentrations (0-50 μM). The solution was incubated at 30 $^\circ$C for 10 min. Then, the absorption spectrum of the solution was measured by UV-vis spectrophotometer at 800-400 nm with the absorbance at 800 nm set to zero.

2.6 Colorimetric response of poly(PCDA) to mixture of MC and AChE

Myristoylcholine (MC; 40 μM) was mixed with AChE at various activities (30-400 mU/mL) in PBS buffer solution pH 6.0 (10 mM). The solution was incubated at 30 $^\circ$C for 30 min. The incubated solution was then added with poly(PCDA) (0.3 mM) and incubated for additional 10 min. The absorption spectrum of the solution was recorded under the same condition described above.

2.7 Colorimetric response of poly(PCDA) to MC in the presence of AChE and dichlorvos

AChE (0.40 U/mL) was mixed with dichlorvos at various concentrations (0-1.0 ppm) in PBS buffer solution pH 6.0 (10 mM) and the mixture was incubated at 30 $^\circ$C for 10 min. Then, myristoyl choline (40 μM) was added and the incubation was continued for 30 min more. After that poly(PCDA) (0.3 mM) was added into the solution and incubated at 30 $^\circ$C for 10 min. The absorption spectrum of the solution was recorded under the same condition described above.

2.8 Preparation of paper-based PDA for dichlorvos indicators

A solution of PCDA and PCDA/DMPC monomer with designated concentration (10 mM) in $CHCl_3$ was dropped onto a piece of filter paper (Whatman No.1) (1 $\times$ 5 cm^2) and dried in the air for 1 h. Then, it was irradiated with UV 254 nm to obtain the blue indicator. The mixed solution of MC (300μM)/AChE (3U/mL)/dichlorvos, AChE was incubated with dichlorvos for 10 min before adding to MC and followed by 30 min incubation at 30 min, was dropped into a paper-based indicator at room temperature (~ 30 °C) for 5 min. The indicator pieces were dried in the air. The different concentration of dichlorvos was tested and deionized water was used for the blank test. The colors of the indicators were recorded by an office scanner (Epson V33) in 5 pieces for each concentration.

2.9 %RGB measurements

The color image of the blue zone was cropped into a 2x2 cm^2 (resolution 72 pixel/$inch^2$) and the RGB values were read by an image processing software (Adobe Photoshop CS6). The percentages of red (%R), green (%G) and blue (%B) colors were calculated from the following equations.

$$\%R= R/(R+G+B)\times100 \quad (1)$$

$$\%G= G/(R+G+B)\times100 \quad (2)$$

$$\%B= B/(R+G+B)\times100 \quad (3)$$

At each concentration, the %B and %R were plotted as a function of time. The time required for the intersection between the %B and %R curves was assigned as a color transition time that used to evaluate the sensor sensitivity.

2.10 Fluorescence microscopy

Fluorescence microscopy analysis was performed for evaluating the effect of the mixed solution of MC (300μM)/AChE (3U/mL)/dichlorvos on the paper-based polydiacetylene indicators. Samples were prepared according to the procedure described above (colorimetric analysis) with optimal conditions for the sensitive paper-based polydiacetylene indicators. Fluorescence images of the paper indicator were acquired on a laser-scanning confocal microscope Laica (Laica, Germany) with a Plan-Neofluar 100×/1.3 oil objective. Excitation was 488 nm using an argon laser source. The emitted light was collected through a band-pass 625–655 nm filter.

CHAPTER III

RESULTS AND DISCUSSION

This dissertation involved the study of the new colorimetric sensor for organophosphate pesticide based on PDA and enzymatic action. There are four successive steps in our development sensor for organophosphate pesticide detection. First, cationic choline esters of four fatty acids were synthesized and tested as the stimulants for poly(PCDA) vesicle sol to identified the best choline ester that give the highest blue-to-red color transition of poly(PCDA). Second, the colorimetric response of poly(PCDA) vesicle sol to the best stimulant in the presence of AChE was investigated to determine the minimum activity of the enzyme required to prevent the blue-to-red color transition. Third, the colorimetric response of poly(PCDA) vesicle sol to the best stimulant in the presence of AChE and organophosphate was studied to determine the relationship between the colorimetric response and the organophosphate concentration. In the final step, the sensitivity enhancement was performed. Moreover, the development of PDA on filter paper for dichlorvos indicator was investigated which should be more practical for onsite application. The results of these investigations are reported and discussed below.

3.1. Synthesis of cationic choline esters

In this contribution, we investigated cationic choline (lauroylcholine, myristoylcholine, palmitoylcholine and stearoylcholine) containing the choline unit with different number of methylene chains (Figure 3.1).
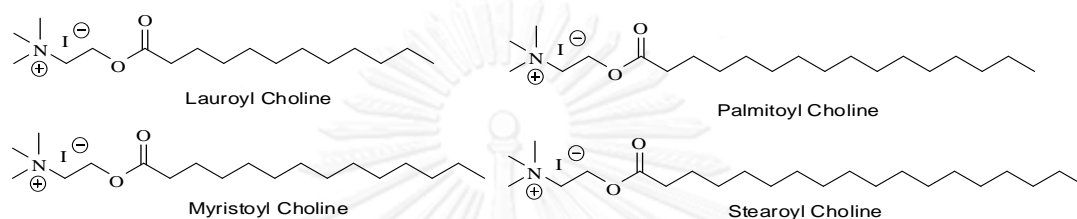
Figure 3.1 Cationic choline (lauroylcholine, myristoylcholine, palmitoylcholine and stearoylcholine).

3.1.1. Synthesis and characterization of cationic choline.

All cationic choline were synthesized according to Scheme 3.1 using esterification and methylation reaction as the key reaction. The synthesis was started with the esterification reaction of acid chlorine with trimethylamine using trimethylamine in dichloromethane followed by methylation to afford cationic choline (lauroylcholine, myristoylcholine, palmitoylcholine and stearoylcholine).
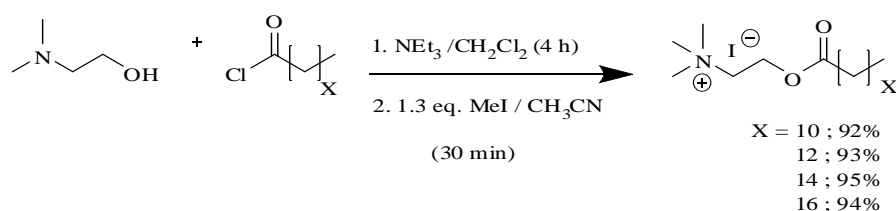
Scheme 3.1 Synthetic route of cationic choline.

The ^{1}H-NMR spectra of lauric acid and lauroylcholine are shown in Figure 3.2 All signals can be assigned to all protons in each corresponding structure. Initially, we compare with lauric acid that showed two triplet signals at 0.89, 1.59 and 2.27 ppm and multiplet at 1.28 ppm corresponding to its alkyl chains protons. Then, lauric acid chlorine react with trimethylamine and methylation using methyliodine product showed signals of the methyl ammonium protons as a multiplet at 3.25 ppm and broad and multiplet signals at 4.58 and 3.78 as an ethylene ester from lauroylcholine.
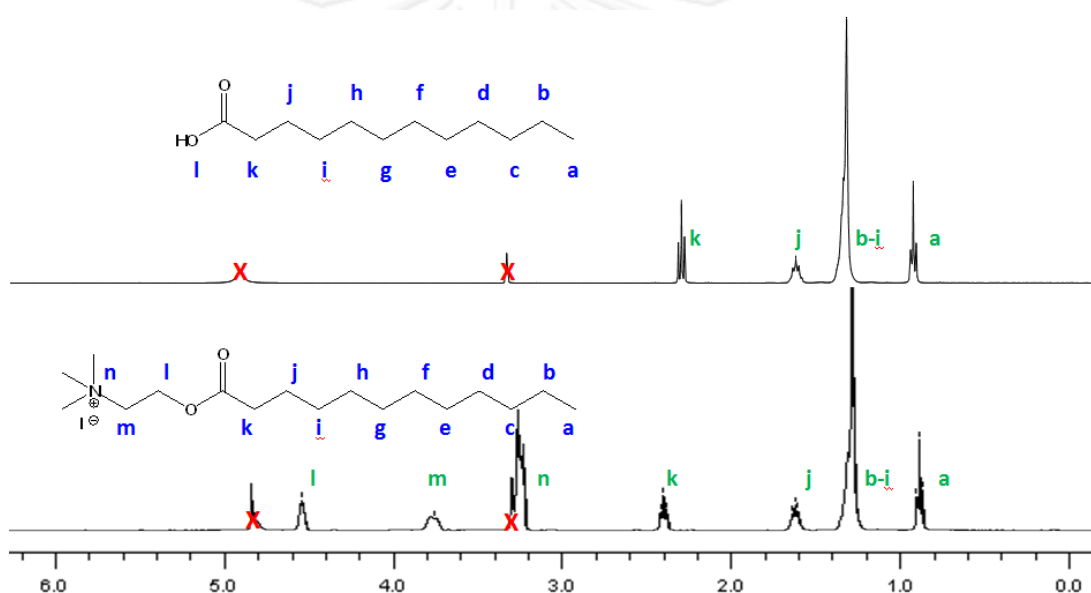
Figure 3.2 ^{1}H-NMR (400 MHz) spectra of lauric acid and lauroylcholine.

For myristoylcholine, palmitoylcholine and stearoylcholine showed signals of ammonium protons at 3.27, 3.21 and 3.20 and ethylene ester proton signal from choline unit that are shown in Figure 3.3, 3.4 and 3.5.
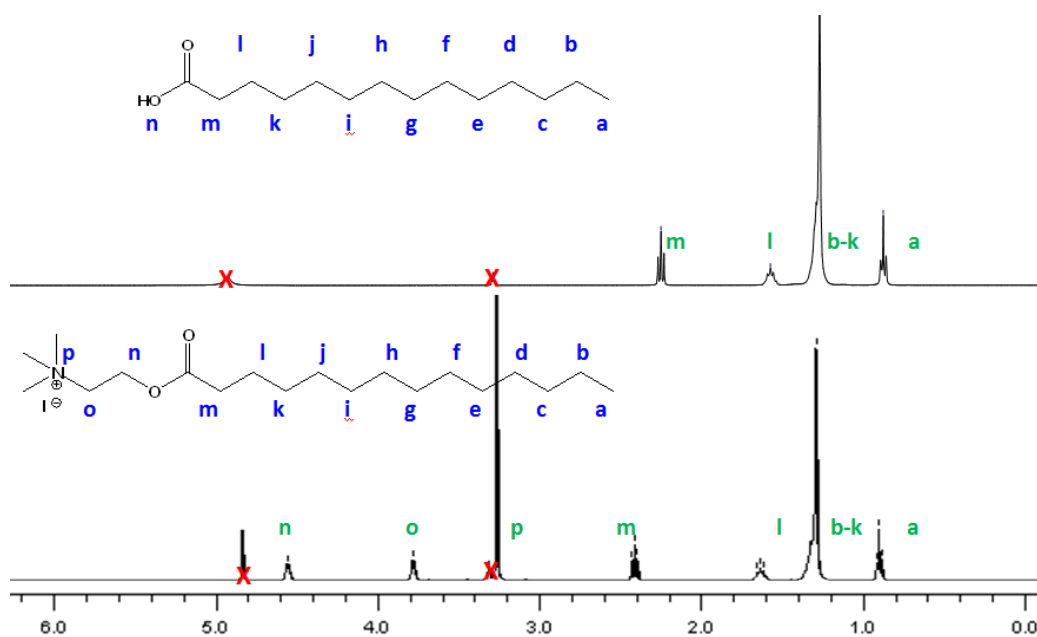
Figure 3.3 ^{1}H-NMR (400 MHz) spectra of Myristic acid and Myristoylcholine.
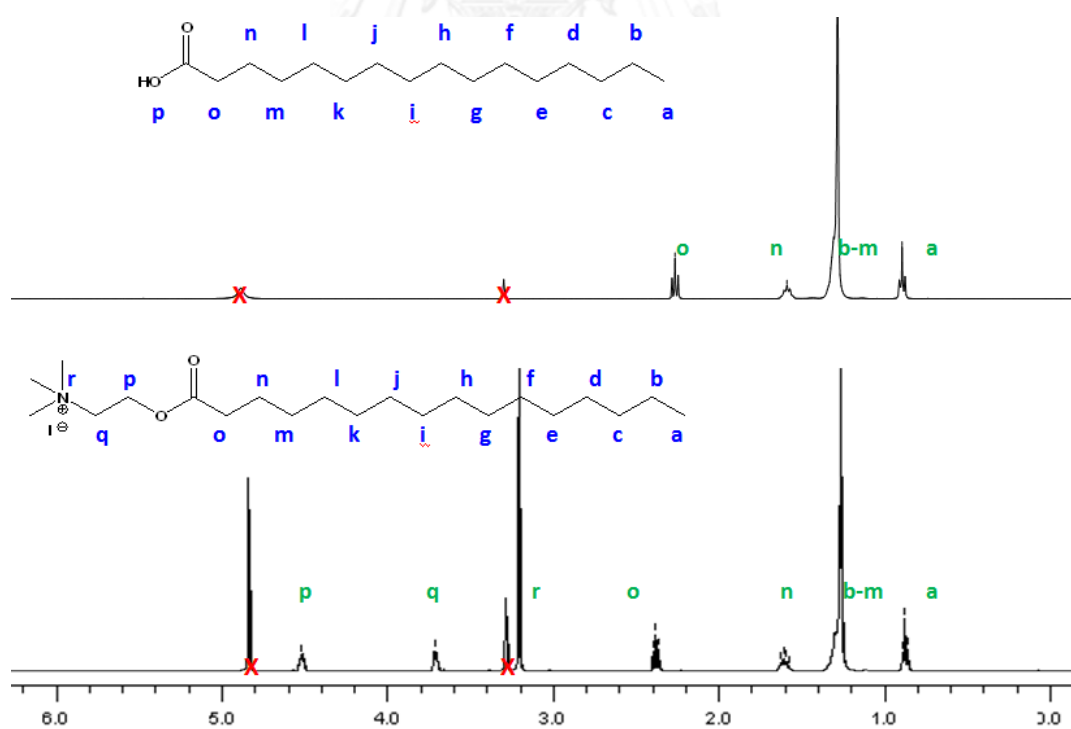
Figure 3.4 ^{1}H-NMR (400 MHz) spectra of Palmitic acid and Palmitoylcholine.

3.2. Colorimetric response of poly(PCDA) to choline esters

Colorimetric response of poly(PCDA) vesicle sol to cationic surfactants was studied with four choline esters i.e. lauroylcholine (LC), myristoylcholine (MC), palmitoylcholine (PC) and sterylcholine (SC). At 40 µM, MC gave the highest blue-to-red colorimetric response percentage (% CR) of poly(PCDA) (Figure 3.5). The critical micelle concentration (cmc) of myristoylcholine was determined to be 2.5 mM [15] which is significantly higher than the concentration used in this experiment. It has been proposed that the positively charged ammonium unit of the choline ester interacted with negatively charged carboxylate groups of poly(PCDA) resulting in the interruption of hydrogen bonding on the surface of poly(PCDA) vesicles. In addition, the hydrophobic alkyl chain of choline ester can insert into the hydrophobic layer of poly(PCDA) vesicles, leading to the change of eyn-yne conjugation in the back bone of poly(PCDA) and its colorimetric response [67]. The cmc values of the choline esters with longer alkyl chains (PC and SC) are hypothetically expected to be lower than that of MC and their stronger self-aggregation may reduce the probability of their alkyl chain insertion into the vesicle layer. This attributed to the lower colorimetric transition induction ability of PC and SC. For LC, its lower lipophilicity is probably responsible for its slightly lower colorimetric transition induction ability than that of MC. Our finding here is consistent with reports utilizing mostly MC and DMPC (dimyristoylphosphatidycholine) for inducing deaggregation of other lipids in various sensing applications [15, 67–69].
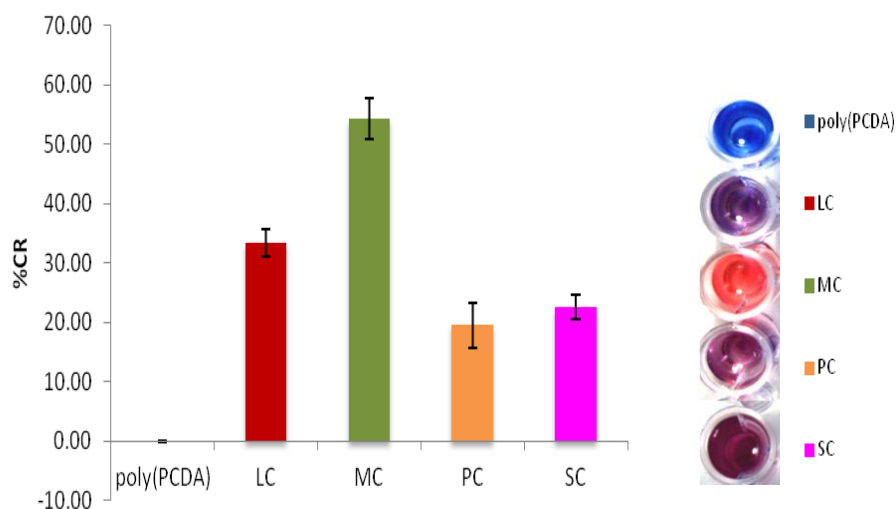
Figure 3.5 Colorimetric response percentage of poly(PCDA) sol (0.3 mM in 10 mM PBS buffer pH = 6.0) to different types of choline esters (40 μM): ■poly(PCDA), ■LC, ■MC, ■PC, ■SC after 10 min of incubation at 30 °C. Inset photograph shows color of poly(PCDA) sol containing different types of choline esters.

3.3. Colorimetric response of poly(PCDA) to pH

The absorption spectra of the poly(PCDA) and poly(PCDA)/MC mixtures were measured in PBS buffer solutions of different pH values. As depicted in Figure 3.6a, MC induced the absorption changes from the band around 640 nm to a new band around 540 nm when the study was conducted at the pH > 5.5. The color of the PDA vesicles also changed from blue to red as the pH~6.0 (Figure 3.6b). Previous studies suggest that this spectral and color switches are associated with the structural changes during the transformation of the blue- to red-phase of PDA [27–30]. Here, the structural changes is probably induced by first the electronic interaction between the carboxylate groups of PDA and ammonium groups of MC and later in collaboration with the hydrophobic interaction among their aliphatic chains leading to the alteration of the PDA backbone conformations and strains [59].

In the pH range of 5.0-5.5, the blue color of the PDA vesicles was relatively stable that MC was incapable of inducing the blue-to-red color transition. At this lower pH range, the carboxylic head groups of poly(PCDA) side chains are less likely to deprotonate to form the anionic carboxylate groups. Consequently, the ammonium groups of MC molecules cannot interact with the side chains of poly(PCDA). Whereas at higher pH range of 7.0-7.5, poly(PCDA) displayed the peak at 540 nm of the red-phase PDA even in the absence of MC inducer. Therefore, further investigation was conducted at pH~6.0 as the blue phase of poly(PCDA) sol was stable without the inducer while it also gave a sharp colorimetric response to MC.
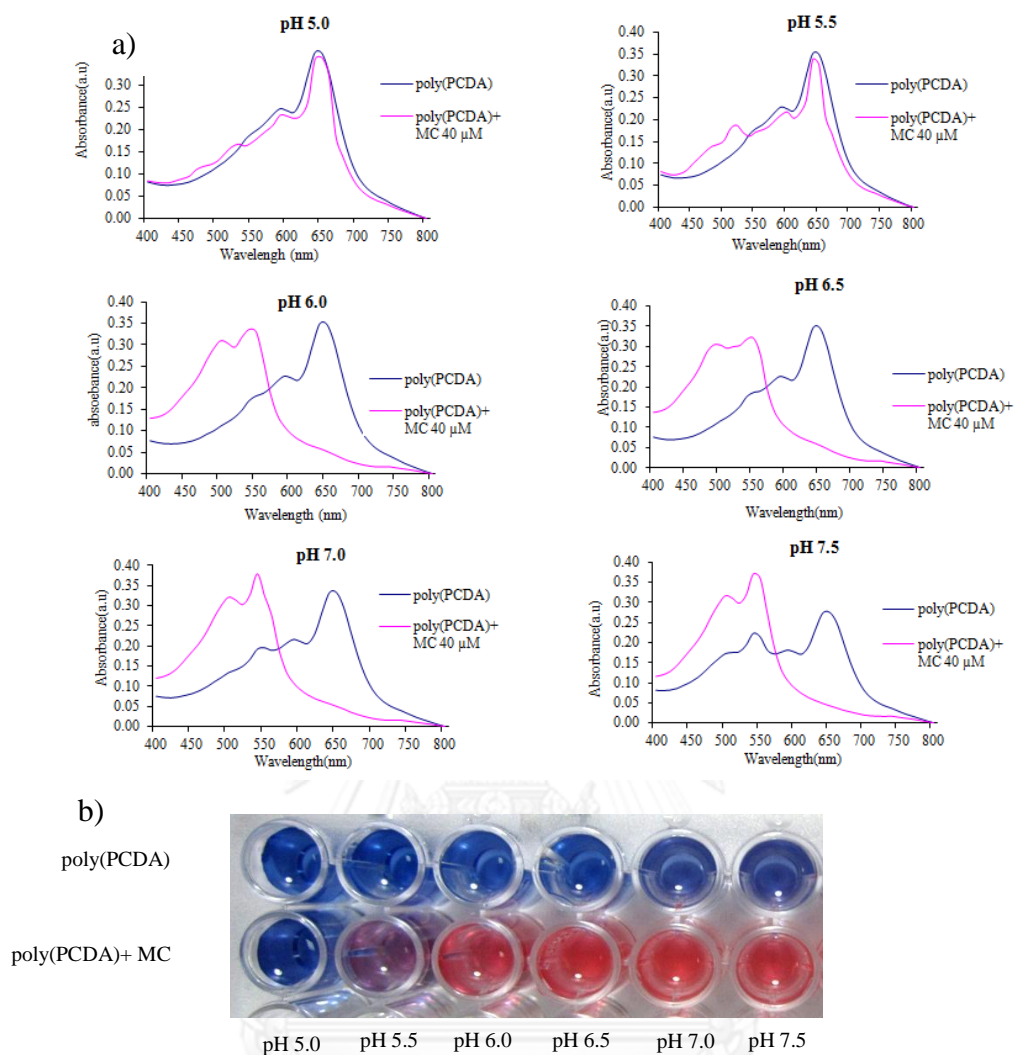
Figure 3.6 a) Absorption spectra of poly(PCDA) sol (0.3 mM in different pH of 10 mM PBS buffer solution) added to MC (40µM). Measurements were performed 10 min of incubation at 30 °C after mixing of poly(PCDA) with MC mixture. b) Photograph shows color of poly(PCDA)/MC sol in different pH of 10 mM PBS buffer solution.

In the next step, the concentration of MC required for clear blue-to-red colorimetric response of poly(PCDA) was determined. The MC concentration induced blue-to-red transition of poly(PCDA) was monitored by its absorption spectra. Figure 3.7a shows that the addition of MC from 0 to 50 µM affected a gradual decrease in

absorption at around 640 nm with a contemporary increase at around 530 nm. From Figure 3.7b, the clear red color of poly(PCDA) was observed at the MC concentration of at least 40 µM, which produced %CR around 60%. The %CR increased almost linearly with the MC concentration in the range of 0-50 µM. For visual detection, the concentration of MC was thus fixed at 40 µM in further experiments.
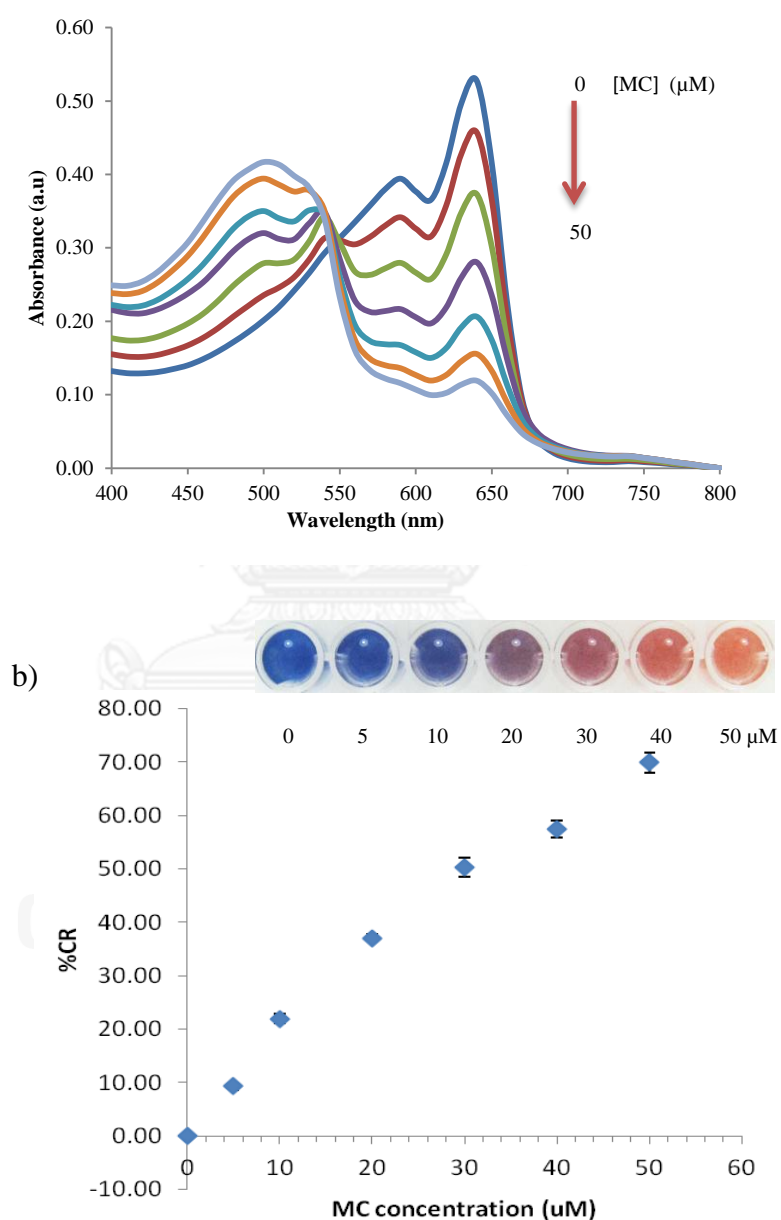
Figure 3.7 a) Absorption spectra of poly(PCDA) sol (0.3 mM in 10 mM PBS buffer pH = 6.0) to different concentrations of MC after 10 min of incubation at 30 °C. b)

Colorimetric response of poly(PCDA) sol (0.3 mM in 10 mM PBS buffer pH = 6.0) to different concentrations of MC. Inset photograph in b shows color of poly(PCDA) sol containing different concentrations of MC.

3.4. Colorimetric response of poly(PCDA) to mixture of MC and AChE

According to the detection scheme shown in Figure 1.1, the product from the enzymatic hydrolysis of MC by AChE should not affect the blue color of poly(PCDA). After various AChE activity pretreatment of the MC (40µM) containing solution, it was added to the poly(PCDA) sol. The resulting absorption spectra of poly(PCDA) sol was found to depend on the AChE activity. At 400 mU/mL of AChE, the absorption at around 640 nm of the poly(PCDA) sol added with the reaction mixture of MC and AChE increased to nearly that of the poly(PCDA) sol without added MC. On the other hand, the absorption at around 530 nm of the poly(PCDA) sol decreased with increased AChE concentration (Figure 3.8a). Figure 3.9b displayed the decrease of %CR of poly(PCDA) with the increase of AChE activity. The visual observation showed that the blue-to-red color transition of poly(PCDA) was completely inhibited in the presence of 400 mU/mL AChE (Figure 3.8b inset). The results confirmed that AChE hydrolyzed MC to myristic acid and choline [15] which cannot induce the blue-to-red color transition of poly(PCDA) [67]. Again, for the visual detection purpose, the 400 mU/mL activity of AChE was used with 40µM MC in the optimization of the subsequent step of dichlorvos detection.
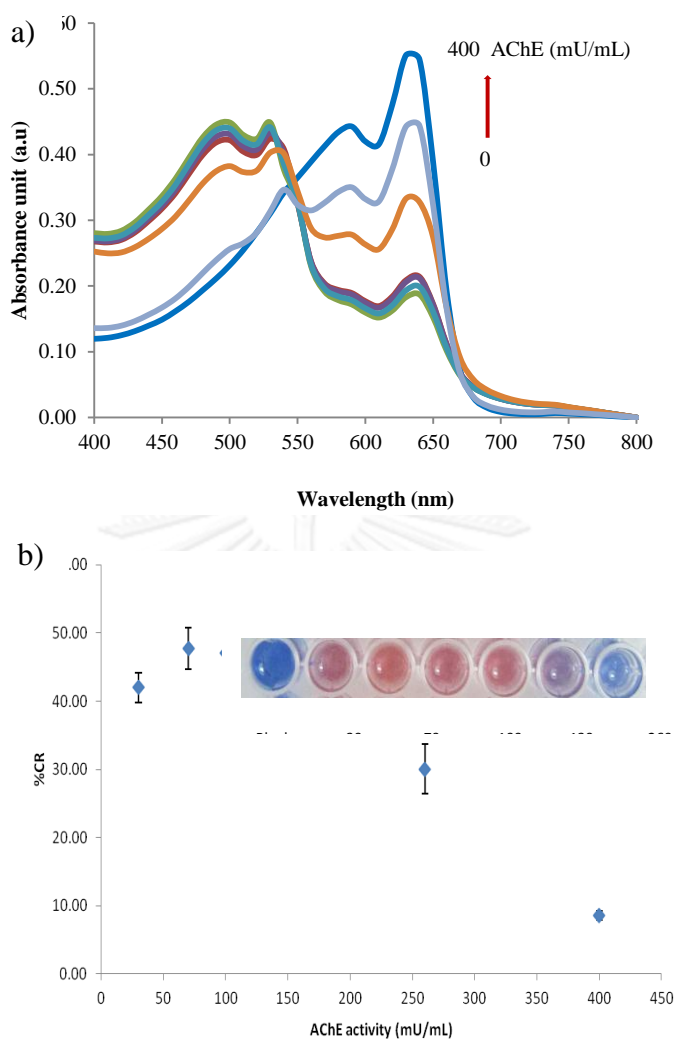
Figure 3.8 a) Absorption spectra of poly(PCDA) sol (0.3 mM in 10 mM PBS buffer pH = 6.0) to MC (40µM) preincubated at 30 °C for 30 min with varied activities of AChE. Measurements were performed 10 min after mixing of poly(PCDA) with MC/AChE at 30 °C. b) Colorimetric response of poly(PCDA) sol (0.3 mM in 10 mM PBS buffer pH = 6.0) to MC (40µM) preincubated at 30 °C for 30 min with varied activities of AChE. Inset photograph in b shows the color appearance of poly(PCDA) sol at various activities of AChE used.

3.5. Colorimetric response of poly(PCDA) to choline esters in the presence of AChE and OPs

As a potent AChE inhibitor [3, 9, 70–72] [15, 73] and highly toxic organophosphate pesticide [1], [3], [9], [11], [41], [44], [45], [46], [47], dichlorvos was selected as a representative analyst in this study. According to the detection scheme in Figure 1.1, the binding of dichlorvos to AChE should inhibit the hydrolytic activity of the enzyme which in turn restore the MC induced color transition of poly(PCDA). Figure 3.9a showed the absorption spectra of poly(PCDA) sol mixed with the incubated mixture of MC/AChE/dichlorvos. As anticipated, the blue-to-red color transition of poly(PCDA) and its %CR increased with the dichlorvos concentration. The plot of %CR against the dichlorvos concentration showed a linear dynamic range of 0-0.20 ppm dichlorvos with R^2 = 0.9752. Limit of detection (LOD at 3 × noise) for this calibration line was 6.7 ppb. The LOD of this method is well below the EPA maximum residue limit (MRL) for dichlorvos in drinking water of 10 ppb [60].
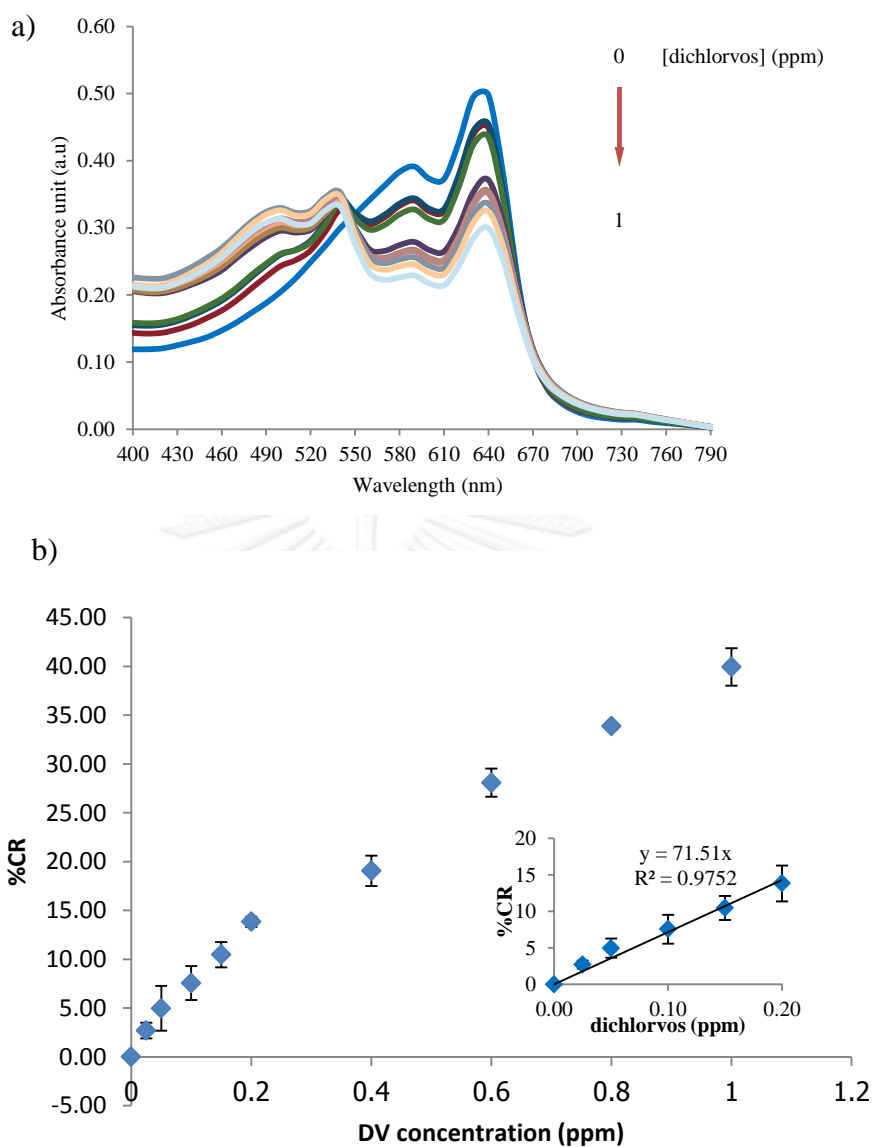
Figure 3.9 a) Absorption spectra of poly(PCDA) sol (0.3 mM in 10 mM PBS buffer pH = 6.0) added to mixture of MC (40μM)/AChE (400 mU/mL)/dichlorvos (varied concentration). AChE was incubated with dichlorvos for 10 min before adding to MC and followed by 30 min incubation. Measurements were performed 10 min after mixing of poly(PCDA) with MC/AChE/dichlorvos mixture. b) Colorimetric response of poly(PCDA) sol (0.3 mM in 10 mM PBS buffer pH = 6.0) added to mixture of MC (40μM)/AChE (400 mU/mL)/dichlorvos (varied concentration). Inset graph in b shows linear dynamic range of %CR against dichlorvos concentration.

Besides dichlorvos, other organophosphate pesticides i.e. paraoxon and malathion are also known as AChE inhibitors [1] of which the oxo forms are generally stronger inhibitor than the thio forms [77]. It is thus of our interest to investigate if our enzymatic PDA based sensing system can give higher selectivity toward dichlorvos over others thio organophosphates i.e. dichlovos, malathion, triazophos. Figure 3.10 shows that only dichlorvos (~ 150 ppb) can induce the blue-to-red color transition of poly(PCDA) sol. The other organophosphates which are the thio forms did not induce the color change of the poly(PCDA) sol even at 1.00 ppm. Therefore, this method is selective to dichlovos.
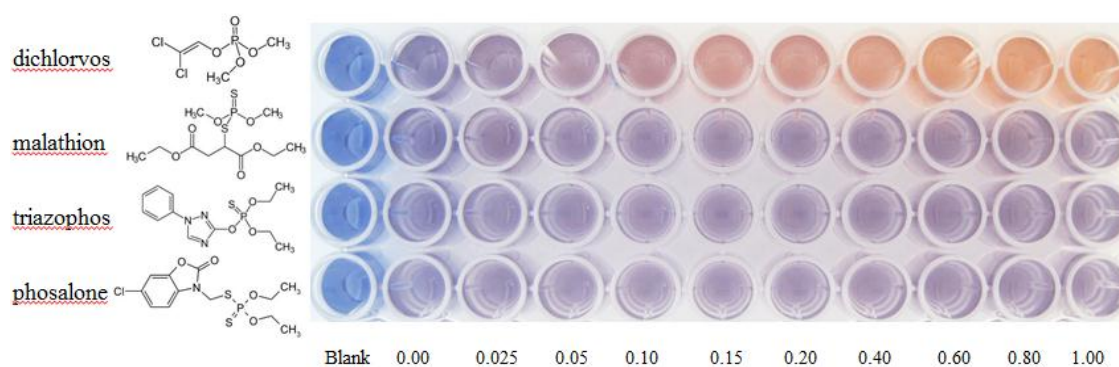
Figure 3.10 Comparison of colorimetric selectivity of poly(PCDA) sensing system in detection of different types of organophosphates.

3.6. Sensitivity enhancement of dichlorvos detection by poly(PCDA)/lipid mixed vesicles

In visual detection of dichlorvos, the blue-to-red color transition of poly(PCDA) was clearly observed only when the concentration of dichlorvos was at least 150 ppb which is significantly higher than the EPA maximum residue limit (MRL = 10 ppb). Therefore, the sensitivity for the naked eye detection of dichlovos by this method should be improved. It has been reported that the insertion of lipids to

poly(PCDA) vesicles can reduce the rigidity of the vesicles structure that lead to greater colorimetric sensitivity [32, 68, 69, 77]. We therefore investigated the utilization of lipid mixing to enhance the colorimetric sensitivity of our method for dichlorvos detection. A lipid i.e. lauric acid (LA), myristic acid (MA), palmitic acid (PA), stearic acid (SA) and dimiristoylphosphatidylcholine (DMPC) was mixed with PCDA to prepare a poly(PCDA)/lipid sol. With 10% lipid, the poly(PCDA)/DMPC sol exhibited the highest blue-to-red color transition sensitivity induced by MC (Figure 3.11).
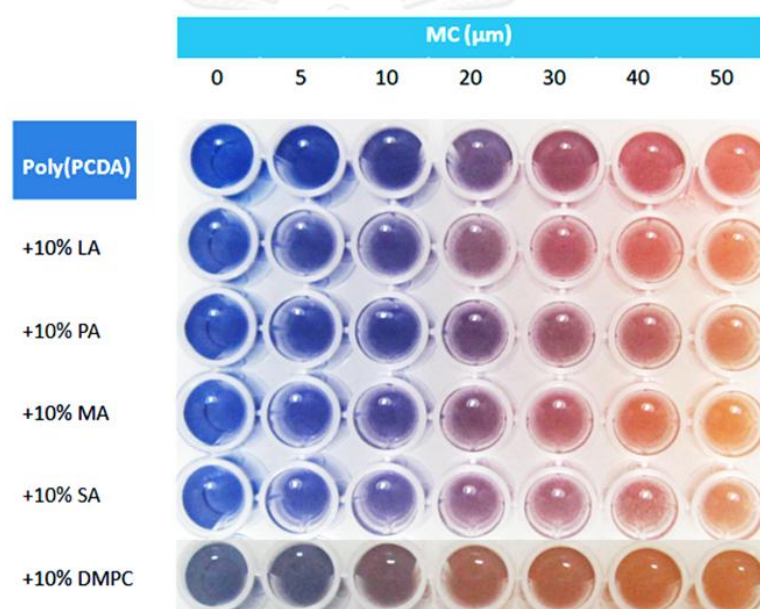
Figure 3.11 Color of poly(PCDA)/lipid sols (0.3 mM in 10 mM PBS buffer pH 6.0).

Further optimization of DMPC mixing content revealed that the higher content of DMPC gave the higher colorimetric sensitivity (Figure 3.12). However, the higher content of DMPC also led to lower thermal stability of the vesicle sols that their color change was observed upon standing even without MC. The amount of DMPC at 15% gave the poly(PCDA)/DMPC sol with satisfactory thermal stability and colorimetric sensitivity which required 20 µM MC to induce a clear blue-to-red color transition.
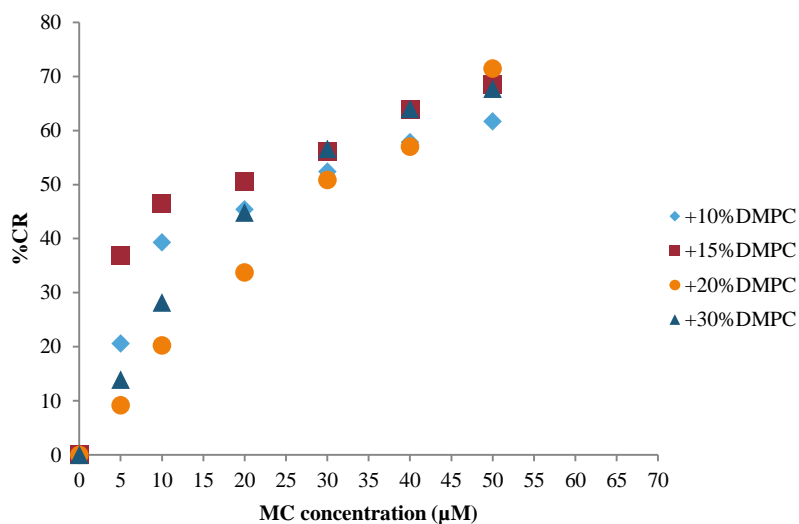
Figure 3.12 The plot of %CR of poly(PCDA)/ DMPC sol (0.3 mM in 10 mM PBS buffer pH = 6.0) to different concentration of MC.

As the poly(PCDA)/DMPC sol required lower MC concentration for induction of the blue-to-red color transition, the AChE activity required for MC hydrolysis should be less than 400 mU/mL needed for the pure poly(PCDA) sensing system. Figure 3.13 indeed shows that the color transition was completely inhibited by 260 mU/mL of AChE
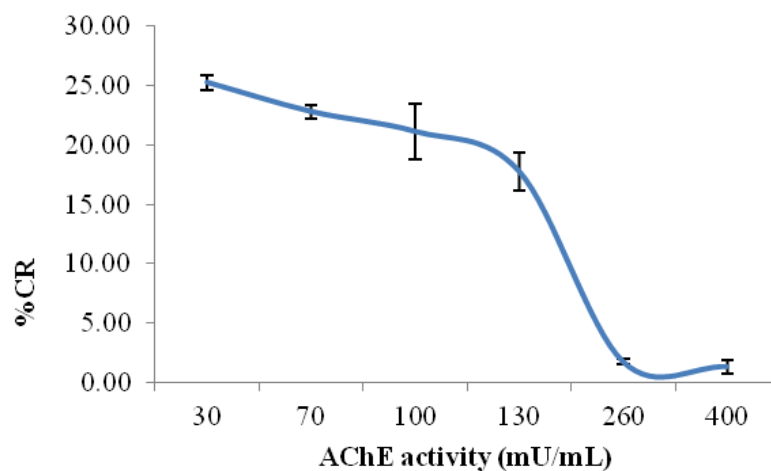
Figure 3.13 The plot of %CR of poly(PCDA)/15% DMPC sol (0.3 mM in 10 mM PBS buffer pH = 6.0) to MC (20µM) preincubated at 30 $^{\circ}$C for 30 min with varied activities of AChE.

The particle size of poly(PCDA) and poly(PCDA)/15%DMPC vesicles were determined by dynamic light scattering (DLS). The DLS results showed the average particle size of poly(PCDA) vesicles of 90 nm and that of poly(PCDA)/15%DMPC vesicles of 120 nm (Figure 3.14). With the phospholipid insertion, the particle size increased with the increasing DMPC content due to the interruption of PCDA molecular packing that altered the curvature of the mixed lipid bilayer [32, 68, 69].

a

b
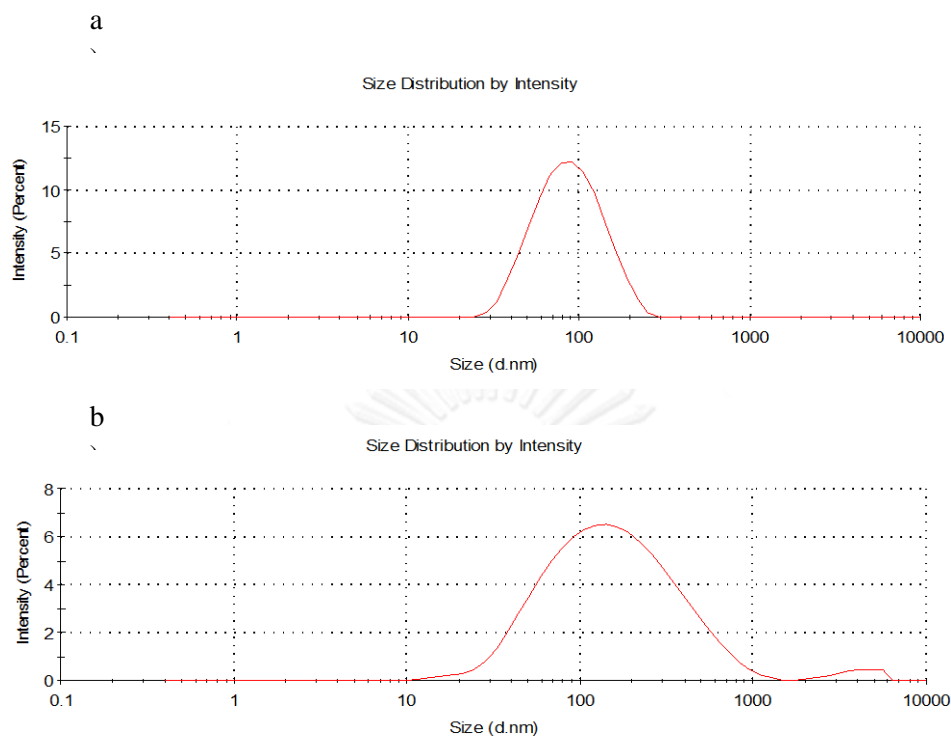
Figure 3.14 Particle size distribution derived from dynamic light scattering of a) poly(PCDA) and b) poly(PCDA)/15%DMPC before addition of the mixture of MC/AChE/dichlorvos.

For the detection of dichlorvos, MC (20µM) was incubated with a mixture of AChE (260 mU/mL) and dichlorvos before testing with either pure poly(PCDA) or poly(PCDA) mixed 15%DMPC sol. The %CR plot clearly showed a greater sensitivity of poly(PCDA)/15%DMPC sol (Figure 3.15). In a linear range of 0-0.20 ppm dichlorvos, poly(PCDA)/15%DMPC sol gave the higher slope than that of poly(PCDA) sol. In the naked eye detection, the blue-to-red color transition of poly(PCDA)/15%DMPC sol was observed with the minimum dichlorvos concentration of 50 ppb, whereas that of poly(PCDA) sol was observed at three times higher concentration, 150 ppb (Figure 3.15 inset). As a result, a 3 time sensitivity improvement of dichlovos detection was achieved by mixing 15%DMPC with PCDA in the preparation of the vesicle sol. The

detection limit of 50 ppb dichlorvos for this naked eye detection is among the best comparing with previous reports on the determination of dichlovos and other related organophosphate compounds (Table. A4; [16, 60, 61, 67, 71, 78, 79].
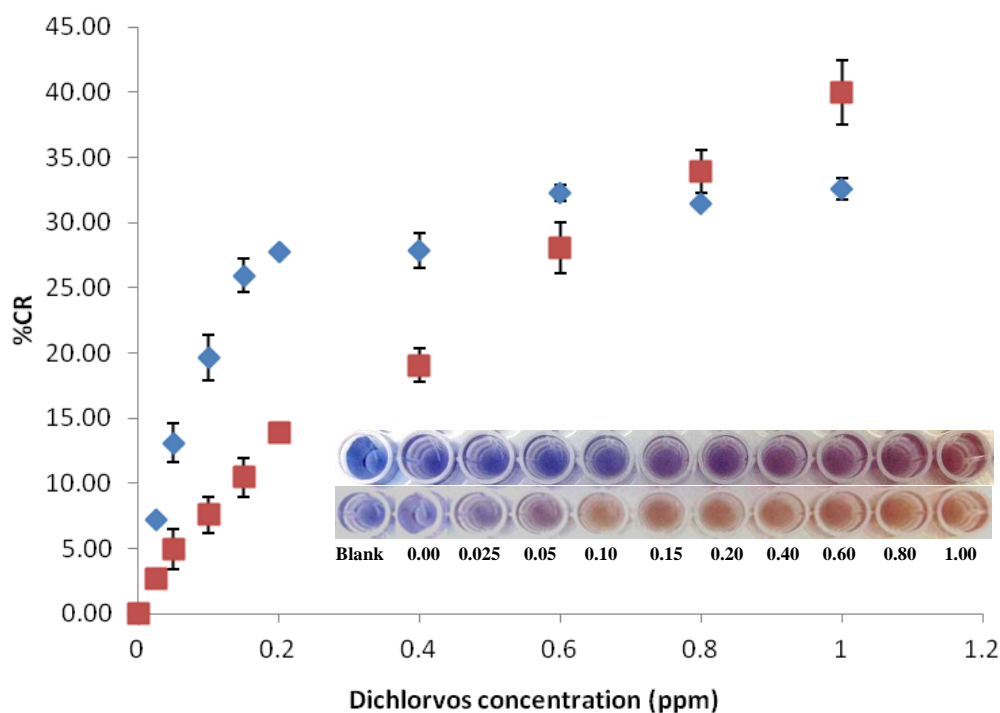
Figure 3.15 Colorimetric response plots of ■ poly(PCDA)and ◆ poly(PCDA)/15%DMPC sols in dichlorvos detection. Inset photograph shows corresponding color changes of poly(PCDA) (above) and poly(PCDA)/15%DMPC (below) at various dichlorvos concentrations.

3.7. Development of paper-based sensor for dichlorvos detection

The subsequent study is to develop paper-based indicator type sensor from PCDA that should be more convenient for portability and onsite analysis. Filter paper was selected as the substrate because of its low-cost, environmentally friendly and available in consistent quality. There are also four steps in the development of the

paper-based sensors i.e. (1) preparation of PDA coated paper, (2) optimization of the amount of MC required for clear blue-to-red color transition, (3) determination of minimum activity of AChE required to prevent the blue-to-red color transition and (4) evaluation of the paper-based indicator for determination of dichlovos. The results of these studies are reported and discussed below.

First, a solution (10 mM, 1 µL) of PCDA or PCDA/15%DMPC monomer in chloroform was dropped on a peice of filter paper and followed by UV irradiation to afford blue dot on the paper indicating a successful polymerization. In the next step, colorimetric response of poly(PCDA) coated paper to MC was studied with different volumes and concentrations of MC. Figure 3.16 shows that the clear blue-to-red color transition was observed with at least 12 µL of 300 µM MC. The %CR plot also indicates that the clear blue-to-red color transition is observed when the %R and %B become saturated at ∼40% and 30%, respectively. The volume of 12 µL and concentration of 300 µM of MC were thus used for further study.
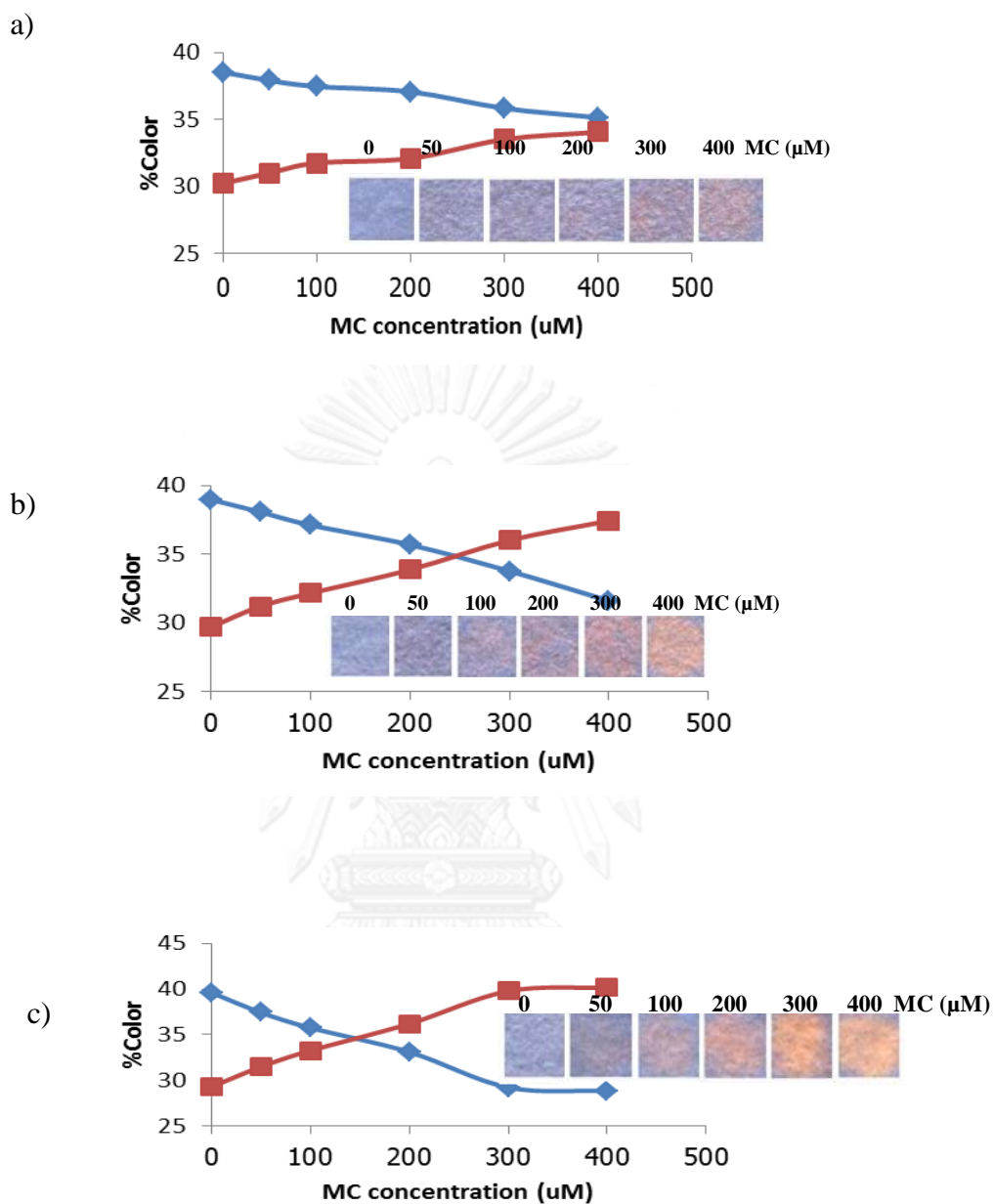
Figure 3.16 Colorimetric responses, ■%R and ◆%B, of paper-based poly(PCDA) indicators obtained with different volumes and concentration of MC (a) 4 µL, (b) 8 µL and (c) 12 µL. Insets show the corresponding color appearance.

In the present of AChE, AChE hydrolyzed MC to myristic acid and choline which should not affect the blue color of poly(PCDA). Therefore, minimum activity of AChE required to paper-based poly(PCDA) indicators was investigated. After a 300µM MC containing solution incubated with AChE at different AChE activity. The mixture of 300µM MC/AChE was dropped on the paper-based poly(PCDA) indicators. Figure 3.17 shows that the clear blue-to-red color transition was observed with at least 3U/mL of AChE. The %CR plot also indicates that the clear blue-to-red color transition is observed when the %R and %B become saturated at ∼30% and 40%, respectively. The AChE activity of 3U/mL AChE was used in the next step.
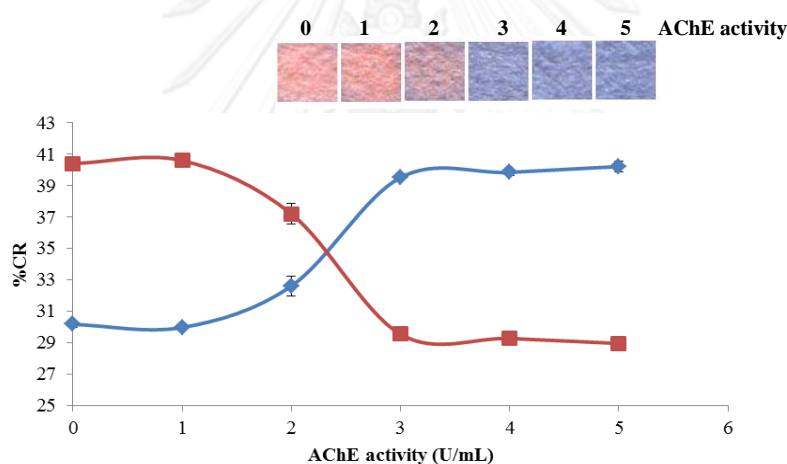
Figure 3.17 Colorimetric responses, ■%R and ◆%B, of paper-based poly(PCDA) indicators obtained with different AChE activity. Insets show the corresponding color appearance.

According to the dichlorvos detection proposed scheme (scheme 1.1), dichlorvos should inhibit the hydrolytic activity of AChE which in turn restore the MC induced color transition of poly(PCDA). Dichlorvos determination on paper-based poly(PCDA) indicator was also investigated. The mixture 12 µL of 300 mM MC/3U/mL AChE/dichlorvos was dropped on the paper-based poly(PCDA) indicators. Figure 3.18

shows that the clear blue-to-red color transition was observed with at least 0.50 ppm of dichlorvos. The %CR plot displayed that the clear blue-to-red color transition is observed which gave the %R and %B at around 37% and 31%, respectively.
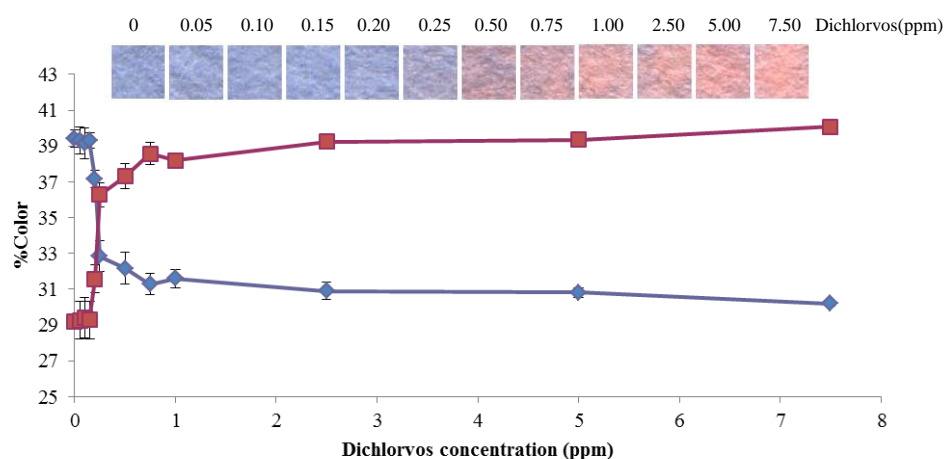
Figure 3.18 Colorimetric responses, ■%R and ◆%B, of paper-based poly(PCDA) indicators obtained with different dichlorvos concentration. Insets show the corresponding color appearance.

As a result of the solution sensing, the mixing of 15%DMPC to PCDA can reduce the rigidity of the vesicles structure that lead to enhance the colorimetric sensitivity. We therefore investigated the sensitivity enhancement by using paper-based poly(PCDA)/15%DMPC indicator for dichlorvos detection with similar optimization step of paper-based poly(PCDA) indicator. Figure 3.19 shows that the clear blue-to-red color transition was observed with at least 12 μL of 300 μM MC. The %CR plot also indicates that the clear blue-to-red color transition is observed when the %R and %B become saturated at ∼39% and 31%, respectively. The volume of 12 μL and concentration of 300 μM of MC were thus used for further study.
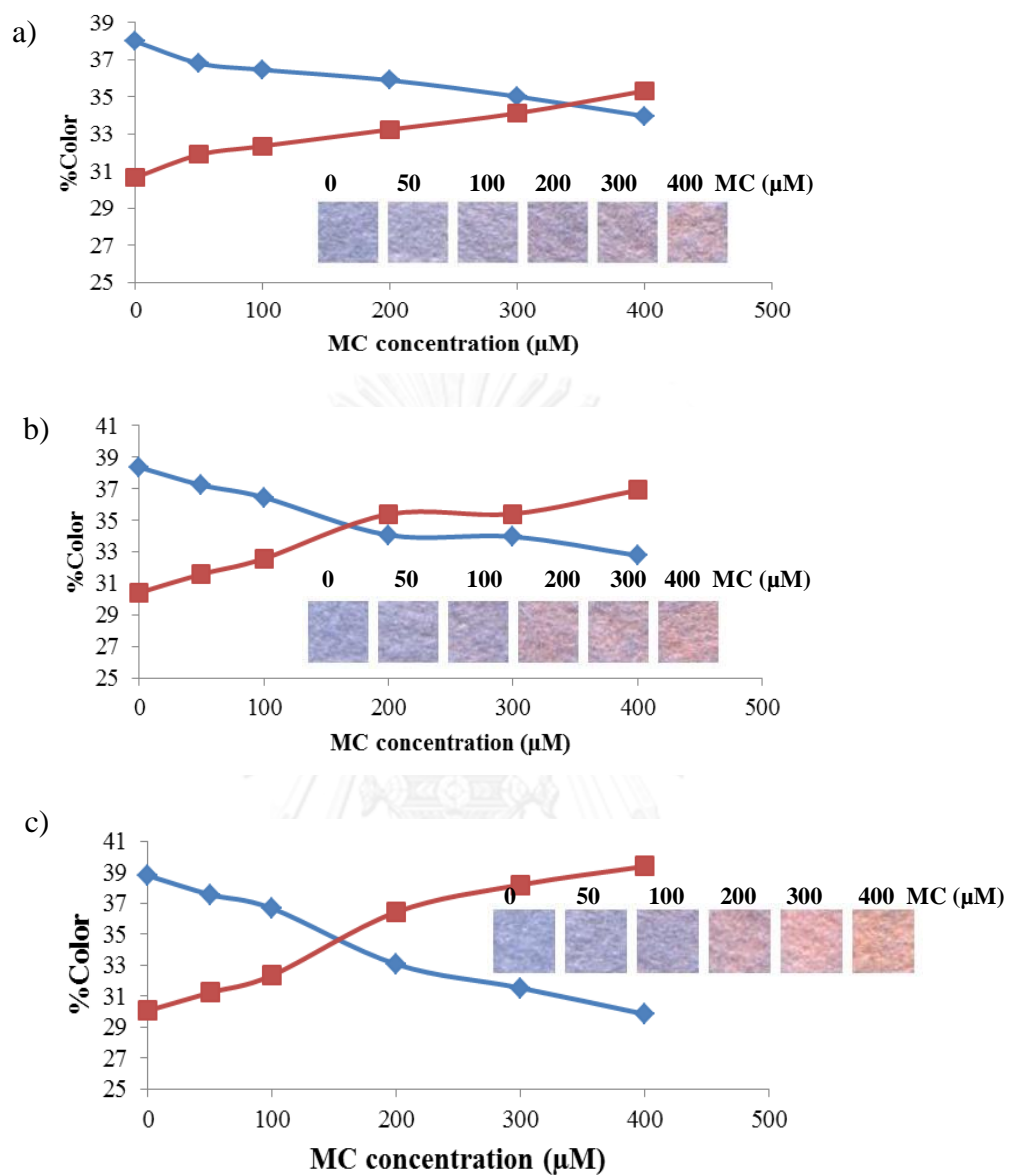
Figure 3.19 Colorimetric responses, ■%R and ◆%B, of paper-based poly(PCDA)/15%DMPC indicators obtained with different volumes and concentration of MC (a) 4 μL, (b) 8 μL and (c) 12 μL. Insets show the corresponding color appearance.

Consequently, color transition of paper-based poly(PCDA)/15%DMPC indicators to mixture of MC and AChE were investigated. After 300μM MC was incubated with difference AChE activity, it was dropped onto the paper-based poly(PCDA) indicators. Figure 3.20 shows that 3U/mL of AChE activity completely inhibited the blue-to-red color transition of paper-based poly(PCDA)/15%DMPC indicators. The clear blue-to-red color transition is detected when the %R and %B become saturated at ∼29% and 41%, respectively. The AChE activity of 3U/mL AChE was used in the next step.
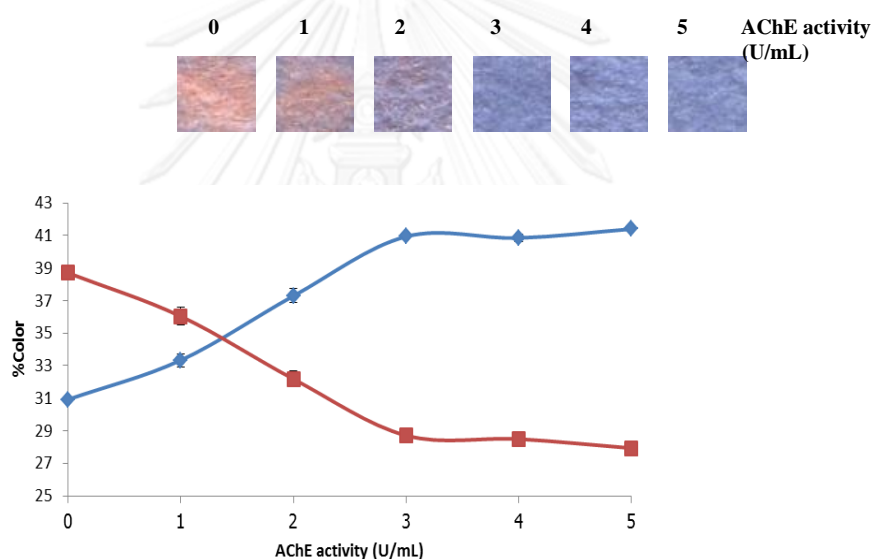
Figure 3.20 Colorimetric responses, ■%R and ◆%B, of paper-based poly(PCDA)/ DMPC indicators obtained with different AChE activity. Insets show the corresponding color appearance.

The dichlorvos detection on paper-based PDA indicators was evaluated, 300μM MC was incubated with a mixture of 3U/mL AChE and dichlorvos before dropped on paper-based poly(PCDA)/15%DMPC indicators. Figure 3.21 shows that the blue-to-red color transition was observed with at least 0.15 ppm of dichlorvos. The %CR plot displayed that the blue-to-red color transition is observed which gave the

%R and %B at around 35% and 34%, respectively. However, using paper-based poly(PCDA)/15%DMPC indicators ambiguously enhanced the sensitivity of dichlorvos detection. We presumed that the insertion of DMPC to PCDA on paper-based indicator ineffectively interrupted the PCDA molecular packing comparing with PDA vesicle.
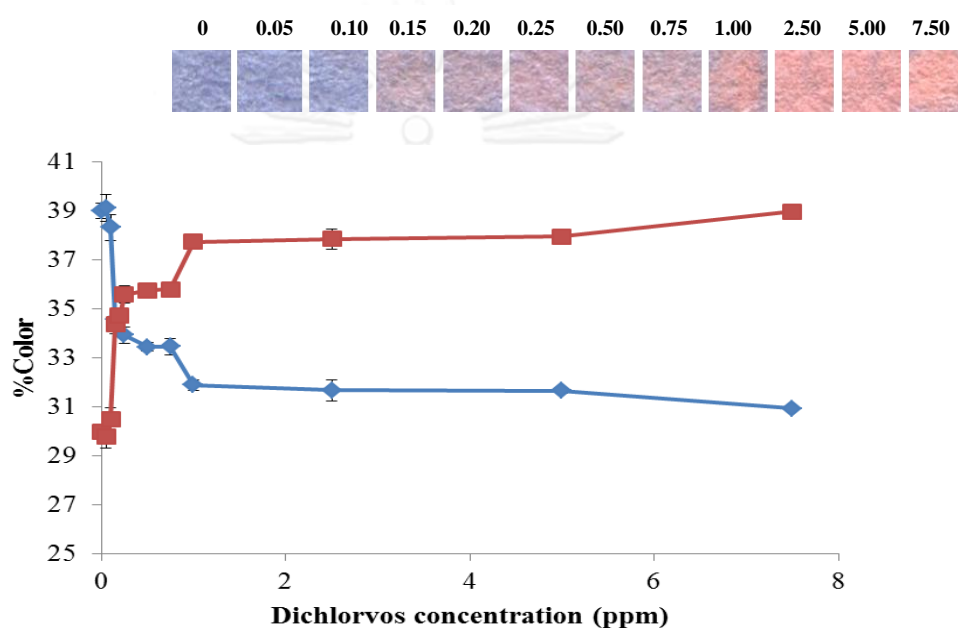
Figure 3.21 Colorimetric responses, ■%R and ◆%B, of paper-based poly(PCDA)/15%DMPC indicators obtained with different dichlorvos concentration. Insets show the corresponding color appearance.

Although, a typical blue-to-red color transition of PDAs have relied on UV-visible spectroscopy. It has been known that the blue-to-red color transition of the PDAs was found to generate red fluorescent upon external stimulation [67, 80]. Therefore, we have investigated the paper-based poly(PCDA) indicator for dichlorvos detection using fluorescent microscope image. Figure 3.22 shows the red color transition of paper-based poly(PCDA) indicators was observed with the minimum dichlorvos concentration of 0.15 ppm. As a result, the fluorescent image method can

enhance sensitivity of dichlorvos detection by using paper-based poly(PCDA) indicator, when compared with naked eye detection.

0.00　　0.05　　0.10　　0.15　　0.20　　0.25 dichlovos (ppm)
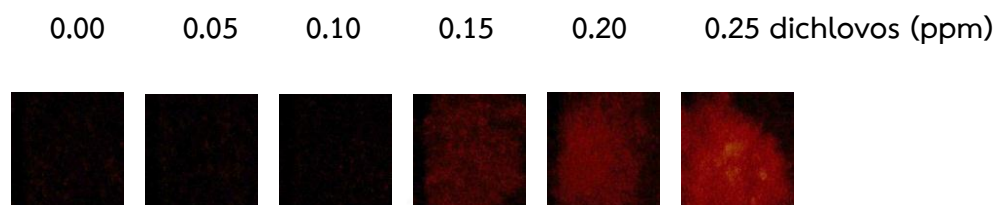
Figure 3.22 Fluorescent microscope images of paper-based PDA indicator of poly(PCDA) at difference dichlorvos concentration.

CHAPTER IV

CONCLUSION

A new colorimetric method for the detection of dichlorvos pesticide based on the blue-to-red color transition of poly(pentacosadiynoic acid) (poly(PCDA)) and inhibition of enzymatic activity of acetylcholinesterase (AChE) was successfully developed. To induce the blue-to-red color transition of poly(PCDA) vesicle sol, myristoyl choline (MC) was more effective comparing with the choline esters of other fatty acids i.e. lauric acid, palmitic acid and stearic acid. The color transition induced by MC could be completely suppressed by the effect of enzymatic hydrolysis of AChE. In the presence of dichlorvos, the activity of AChE was inhibited and the color transition induced by MC was restored. The dichlorvos concentration could thus be determined from the colorimetric response of poly(PCDA) sol in the presence of MC, AChE and dichlorvos sample. The detection limit of this method was 6.7 ppb for the colorimetric measurement using UV-vis absorption spectrometer. With naked eye observation, a detection of 150 ppb of dichlorvos was possible. The method exhibited good selectivity toward dichlorvos (oxo-forms) over thio organophosphate pesticides. The sensitivity of the naked eye detection of dichlorvos was enhanced by 3 times to the detectable level of 50 ppb by mixing diacetylene/DMPC in the preparation of vesicle sol. The blue-to-red color transition of the mixed lipid polydiacetylene sol was clearly observed at 50 ppb dichlorvos. Moreover, the paper-based PDAs indicator for dichlorvos naked eye detection was developed but the sensitivity was significantly dropped to the detectable level of 500 ppb.

REFERENCES

[1]   Jin, S.; Xu, Z.; Chen, J.; Liang, X.; Wu, Y.; Qian, X. Determination of organophosphate and carbamate pesticides based on enzyme inhibition using a pH-sensitive fluorescence probe. *Anal. Chim. Acta.* 523 (2004): 117–123.

[2]   Crew, A; Lonsdale, D.; Byrd, N.; Pittson, R.; Hart, J. P. A screen-printed, amperometric biosensor array incorporated into a novel automated system for the simultaneous determination of organophosphate pesticides. *Biosens. Bioelectron.* 26 (2011): 2847–2851.

[3]   Singh, a K.; Flounders, a W.; Volponi, J. V; Ashley, C. S.; Wally, K.; Schoeniger, J. S. Development of sensors for direct detection of organophosphates. Part I: Immobilization, characterization and stabilization of acetylcholinesterase and organophosphate hydrolase on silica supports. *Biosens. Bioelectron.* 14 (1999): 703–713.

[4]   Mishra, R. K.; Dominguez, R. B.; Bhand, S.; Muñoz, R.; Marty, J.-L. A novel automated flow-based biosensor for the determination of organophosphate pesticides in milk. *Biosens. Bioelectron.* 32 (2012): 56–61.

[5]   Galán-Cano, F.; Lucena, R.; Cárdenas, S.; Valcárcel, M. Dispersive micro-solid phase extraction with ionic liquid-modified silica for the determination of organophosphate pesticides in water by ultra performance liquid chromatography. *Microchem. J.* 106 (2013): 311–317.

[6]   Gao, Z.; Deng, Y.; Hu, X.; Yang, S.; Sun, C.; He, H. Determination of organophosphate esters in water samples using an ionic liquid-based sol-gel fiber for headspace solid-phase microextraction coupled to gas

chromatography-flame photometric detector. *J. Chromatogr. A.* 1300 (2013): 141–150.

[7]   Celano, R.; Rodríguez, I.; Cela, R.; Rastrelli, L.; Piccinelli, A. L. Liquid chromatography quadrupole time-of- fl ight mass spectrometry quanti fi cation and screening of organophosphate compounds in sludge *Talanta.* 118 (2014): 312–320.

[8]   Xu, Z.; Fang, G.; Wang, S. Molecularly imprinted solid phase extraction coupled to high-performance liquid chromatography for determination of trace dichlorvos residues in vegetables. *Food Chem.* 119 (2010): 845–850.

[9]   Kumaran, S.; Tran-Minh, C. Determination of organophosphorous and carbamate insecticides by flow injection analysis. *Anal. Biochem.* 200 (1992): 187–194.

[10]   Roger, K. R.; Cao, C. J.; Valdes, J. J.; Eldefrawi, A. T.; Eldefrawi, M. E. Acetylcholinesterase Fiber-Optic Biosensor for Detection of Anticholinesterases. *Toxicol. Sci.* 16 (1991): 810–820.

[11]   Skládal, P. Detection of organophosphate and carbamate pesticides using disposable biosensors based on chemically modified electrodes and immobilized cholinesterase. *Anal. Chim. Acta.* 269 (1992): 281–287.

[12]   Liu, S.; Yuan, L.; Yue, X.; Zheng, Z.; Tang, Z. Recent Advances in Nanosensors for Organophosphate Pesticide Detection. *Adv. Powder Technol.* 19 (2008): 419–441.

[13]   Liu, W.; Kou, J.; Xing, H.; Li, B. Biosensors and Bioelectronics Paper-based chromatographic chemiluminescence chip for the detection of dichlorvos in vegetables. *Biosens. Bioelectron.* 52 (2014): 76–81.

[14]   Thakur, S.; Venkateswar Reddy, M.; Siddavattam, D.; Paul, a. K. A fluorescence based assay with pyranine labeled hexa-histidine tagged

organophosphorus hydrolase (OPH) for determination of organophosphates. *Sensors Actuators B Chem.* 163 (2012): 153–158.

[15]   Wang, M.; Gu, X.; Zhang, G.; Zhang, D.; Zhu, D. Convenient and continuous fluorometric assay method for acetylcholinesterase and inhibitor screening based on the aggregation-induced emission. *Anal. Chem.* 81 (2009): 4444–4449.

[16]   Lee, J.; Seo, S.; Kim, J. Colorimetric Detection of Warfare Gases by Polydiacetylenes Toward Equipment-Free Detection. *Adv. Funct. Mater.* 22 (2012): 1632–1638.

[17]   Carpick, R. W.; Mayer, T. M.; Sasaki, D. Y.; Burns, A. R. Spectroscopic Ellipsometry and Fluorescence Study of Thermochromism in an Ultrathin Poly (diacetylene) Film : Reversibility and Transition Kinetics. *Langmuir.* 16 (2000): 4639–4647.

[18]   Chen, X.; Yoon, J. A thermally reversible temperature sensor based on polydiacetylene: Synthesis and thermochromic properties. *Dye. Pigment.* 89 (2011): 194–198.

[19]   Gou, M.; Guo, G.; Zhang, J.; Men, K.; Song, J.; Luo, F.; Zhao, X.; Qian, Z.; Wei, Y. Time–temperature chromatic sensor based on polydiacetylene (PDA) vesicle and amphiphilic copolymer. *Sensors Actuators B Chem.* 150 (2010): 406–411.

[20]   Jung, Y. K.; Park, H. G.; Kim, J.-M. Polydiacetylene (PDA)-based colorimetric detection of biotin-streptavidin interactions. *Biosens. Bioelectron.* 21 (2006): 1536–44.

[21]   Lee, D.; Sahoo, S. K.; Cholli, A. L.; Sandman, D. J. Structural Aspects of the Thermochromic Transition in Urethane-substituted Polydiacetylenes. *Macromolecules.* 35 (2002): 4347–4355.

[22]   Rubner, M. F.; Rubner, M. F.; Sandman, D. J.; Velazquez, C. On the structural origin of the thermochromic behavior of urethane-substituted poly(diacetylenes). *Macromolecules.* 20 (1987): 1296 – 1300.

[23]   Wang, X.; Whitten, J. E.; Sandman, D. J. Ultraviolet photoelectron spectroscopy study of the thermochromic phase transition in urethane-substituted polydiacetylenes. *J. Chem. Phys.* 126 (2007): 184905.

[24]   Ye, Q.; Zou, G.; You, X.; Yu, X.; Zhang, Q. Tunable morphologies, structure and unusual responsive thermochromism of polydiacetylene supramolelular assemblies. *Mater. Lett.* 62 (2008): 4025–4027.

[25]   Kwon, I. K.; Kim, J. P.; Sim, S. J. Enhancement of sensitivity using hybrid stimulus for the diagnosis of prostate cancer based on polydiacetylene (PDA) supramolecules. *Biosens. Bioelectron.* 26 (2010): 1548–1553.

[26]   Miyano, K.; Hasegawa, T. Pressure anisotropy and orientational order of a polydiacetylene monolayer and its use as a template for vacuum deposition. *Thin Solid Films.* 205 (1991): 117–123.

[27]   Charoenthai, N.; Pattanatornchai, T.; Wacharasindhu, S.; Sukwattanasinitt, M.; Traiphol, R. Roles of head group architecture and side chain length on colorimetric response of polydiacetylene vesicles to temperature, ethanol and pH. *J. Colloid Interface Sci.* 360 (2011): 565–573.

[28]   Li, J.; Yu, Z.; Jiang, H.; Zou, G.; Zhang, Q. Photo and pH dual-responsive polydiacetylene smart nanocontainer. *Mater. Chem. Phys.* 136 (2012): 219–224.

[29]   Seo, S.; Kim, D.; Jang, G.; Kim, D.-M.; Kim, D. W.; Seo, B.-K.; Lee, K.-W.; Lee, T. S. Fluorescence resonance energy transfer between polydiacetylene

vesicles and embedded benzoxazole molecules for pH sensing. *React. Funct. Polym.* 73 (2013): 451–456.

[30] Potisatityuenyong, A.; Tumcharern, G.; Dubas, S. T.; Sukwattanasinitt, M. Layer-by-layer assembly of intact polydiacetylene vesicles with retained chromic properties. *J. Colloid Interface Sci.* 304 (2006): 45–51.

[31] Sabatani, E.; Kalisky, Y.; Berman, A.; Golan, Y.; Gutman, N.; Urbach, B.; Sa'ar, A. Photoluminescence of polydiacetylene membranes on porous silicon utilized for chemical sensors. *Opt. Mater. (Amst).* 30 (2008): 1766–1774.

[32] Su, Y.-L.; Li, J.-R.; Jiang, L. A study on the interactions of surfactants with phospholipid/polydiacetylene vesicles in aqueous solutions. *Colloids Surfaces A Physicochem. Eng. Asp.* 257-258 (2005): 25–30.

[33] Takami, K.; Kuwahara, Y.; Ishii, T.; Akai-Kasaya, M.; Saito, A.; Aono, M. Significant increase in conductivity of polydiacetylene thin film induced by iodine doping. *Surf. Sci.* 591 (2005): L273–L279.

[34] Xia, Y.; Deng, J.; Jiang, L. Simple and highly sensitive detection of hepatotoxin microcystin-LR via colorimetric variation based on polydiacetylene vesicles. *Sensors Actuators B Chem.* 145 (2010): 713–719.

[35] Vinod, T. P.; Chang, J. H.; Kim, J.; Rhee, S. W. Self-Assembly and Photopolymerization of Diacetylene Molecules on Surface of Magnetite Nanoparticles. *Bulletin-Korean Chem. Soc.* 29 (2008): 799–804.

[36] Okada, S.; Peng, S.; Spevak, W.; Charych, D. Color and Chromism of Polydiacetylene Vesicles. *Acc. Chem. Res.* 31 (1998): 229-239

[37] Schott, M. The colors of polydiacetylenes: a commentary. *J. Phys. Chem. B.* 110 (2006): 15864–15868.

[38] Dobrosavljevic, V.; Stratt, R. Role of conformational disorder in the electronic structure of conjugated polymers: Substituted polydiacetylenes. *Phys. Rev. B. Condens. Matter.* 35 (1987): 2781–2794.

[39] Carpick, R. W.; Sasaki, D. Y.; Marcus, M. S.; Eriksson, M. a; Burns, A. R. Polydiacetylene films: a review of recent investigations into chromogenic transitions and nanomechanical properties. *J. Phys. Condens. Matter.* 16 (2004): R679–R697.

[40] Shibata, M.; Kaneko, F.; Aketagawa, M.; Kobayashi, S. Reversible colour phase transitions and annealing properties of Langmuir-Blodgett polydiacetylene films. *Thin Solid Films.* 179 (1989): 433–437.

[41] Yoon, J.; Chae, S. K.; Kim, J.-M. Colorimetric sensors for volatile organic compounds (VOCs) based on conjugated polymer-embedded electrospun fibers. *J. Am. Chem. Soc.* 129 (2007): 3038–3039.

[42] Yoon, J.; Jung, Y.-S.; Kim, J.-M. A Combinatorial Approach for Colorimetric Differentiation of Organic Solvents Based on Conjugated Polymer-Embedded Electrospun Fibers. *Adv. Funct. Mater.* 19 (2009): 209–214.

[43] Kew, S. J.; Hall, E. a H. pH response of carboxy-terminated colorimetric polydiacetylene vesicles. *Anal. Chem.* 78 (2006): 2231–2238.

[44] Müller, H.; Eckhardt, C. J. Stress Induced Change of Electronic Structure in a Polydiacetylene Crystal. *Mol. Cryst. Liq. Cryst.* 45 (1978): 313–318.

[45] Nallicheri, R. a.; Rubner, M. F. Investigations of the mechanochromic behavior of poly(urethane-diacetylene) segmented copolymers. *Macromolecules.* 24 (1991): 517–525.

[46] Kim, J.; Lee, J.; Choi, H.; Sohn, D.; Ahn, D. J. Rational Design and in-Situ FTIR Analyses of Colorimetrically Reversibe Polydiacetylene Supramolecules. *Macromolecules.* 38 (2005): 9366–9376.

[47] Lee J, Jeong Jeong E, K. J. Selective and sensitive detection of melamine by intra/inter liposomal interaction of polydiacetylene liposomes. *Chem Commun.* 47 (2011): 358–360.

[48] Su, Y.-L.; Li, J.-R.; Jiang, L. Chromatic immunoassay based on polydiacetylene vesicles. *Colloids Surf. B. Biointerfaces.* 38 (2004): 29–33.

[49] Wikipedia Foundation Inc. RGB color model. *Wikipedia,* 2014.

[50] Mogda K. Mansour, Afaf A.I. El-Kashoury, M. A. R. and K. M. K. Oxidative and biochemical alterations induced by profenofos insecticide in rats. *Nat. Sci.* 7 (2009): 1–15.

[51] Vijaya, S.; Sudhakar, Y.; Venkateswarlu, B. Current review on organophosphorus poisoning. *Arch. Appl. Sci. Res.* 2 (2010): 199–215.

[52] Bolognesi, C. Genotoxicity of pesticides: a review of human biomonitoring studies. *Mutat. Res. Mutat. Res.* 543 (2003): 251–272.

[53] Pesticide Information Profiles - Parathion. Oregon State University: Extension Toxicology Network, 1993.

[54] Jurewicz, J.; Hanke, W. Prenatal and childhood exposure to pesticides and neurobehavioral development: review of epidemiological studies. *Int. J. Occup. Med. Environ. Health.* 21 (2008): 121–32.

[55] Hayden, K. M.; Norton, M. C.; Darcey, D.; Ostbye, T.; Zandi, P. P.; Breitner, J. C. S.; Welsh-Bohmer, K. a. Occupational exposure to pesticides increases the risk of incident AD: the Cache County study. *Neurology.* 74 (2010): 1524–30.

[56] Parathion. U. S. Environmental Protection Agency: Integrated Risk Information System, 2007.

[57] Woods, H. F. Organophosphates. Committee on Toxicity of Chemicals in Food, Consumer Products and the Environment, 1999.

[58] Chen, X.; Lee, J.; Jou, M. J.; Kim, J.-M.; Yoon, J. Colorimetric and fluorometric detection of cationic surfactants based on conjugated polydiacetylene supramolecules. *Chem. Commun. (Camb).* (2009): 3434–3436.

[59] Xue, W.; Zhang, D.; Zhang, G.; Zhu, D. Colorimetric detection of glucose and an assay for acetylcholinesterase with amine-terminated polydiacetylene vesicles. *Chinese Sci. Bull.* 56 (2011): 1877–1883.

[60] Andreou, V. G.; Clonis, Y. D. A portable fiber-optic pesticide biosensor based on immobilized cholinesterase and sol – gel entrapped bromcresol purple for in-field use. *Biosens. Bioelectron.* 17 (2002): 61–69.

[61] Vamvakaki, V.; Chaniotakis, N. Pesticide detection with a liposome-based nano-biosensor. *Biosens. Bioelectron.* 22 (2007): 2848–2853.

[62] Martinez, A. W.; Phillips, S. T.; Whitesides, G. M.; Carrilho, E. Diagnostics for the Developing World: Microfluidic Paper-Based Analytical Devices. *Anal. Chem.* 82 (2010): 3–10.

[63] Pohanka, M.; Karasova, JZ.; Kuca, K.; et al. Colorimetric dipstick for assay of organophosphate pesticides and nerve agents represented by paraoxon, sarin and VX. *Talanta* 81 (2010): 621-624.

[64] Luckham, R. E.; Brennan, J. D. Bioactive paper dipstick sensors for acetylcholinesterase inhibitors based on sol–gel/enzyme/gold nanoparticle composites. *Analyst.* 135 (2010): 2028–2035.

[65] Pumtang, S.; Siripornnoppakhun, W.; Sukwattanasinitt, M.; Ajavakom, A. Solvent colorimetric paper-based polydiacetylene sensors from diacetylene lipids. *J. Colloid Interface Sci.* 364 (2010): 366–372.

[66] Eaidkong, T.; Mungkarndee, R.; Phollookin, C.; Tumcharern, G.; Sukwattanasinitt, M.; Wacharasindhu, S. Polydiacetylene paper-based colorimetric sensor array for vapor phase detection and identification of volatile organic compounds. *J. Mater. Chem.* 22 (2012): 5970.

[67] Zhou, G.; Wang, F.; Wang, H.; Kambam, S.; Chen, X.; Yoon, J. Colorimetric and Fluorometric Assays Based on Conjugated Polydiacetylene Supramolecules for Screening Acetylcholinesterase and Its Inhibitors. *ACS Appl. Mater. Interfaces.* 5 (2013): 3275–3280.

[68] Kim, K.-W.; Choi, H.; Lee, G. S.; Ahn, D. J.; Oh, M.-K. Effect of phospholipid insertion on arrayed polydiacetylene biosensors. *Colloids Surf. B. Biointerfaces.* 66 (2008): 213–217.

[69] Kang, D. H.; Jung, H.-S.; Lee, J.; Seo, S.; Kim, J.; Kim, K.; Suh, K.-Y. Design of polydiacetylene-phospholipid supramolecules for enhanced stability and sensitivity. *Langmuir.* 28 (2012): 7551–7556.

[70] Nagatani, N.; Takeuchi, A.; Anwar Hossain, M.; Yuhi, T.; Endo, T.; Kerman, K.; Takamura, Y.; Tamiya, E. Rapid and sensitive visual detection of residual pesticides in food using acetylcholinesterase-based disposable membrane chips. *Food Control.* 18 (2007): 914–920.

[71] No, H.-Y.; Kim, Y. A.; Lee, Y. T.; Lee, H.-S. Cholinesterase-based dipstick assay for the detection of organophosphate and carbamate pesticides. *Anal. Chim. Acta.* 594 (2007): 37–43.

[72] Tran-Minh, C.; Pandey, P. C.; Kumaran, S. Studies on acetylcholine sensor and its analytical application based on the inhibition of cholinesterase. *Biosens. Bioelectron.* 5 (1990): 461–471.

[73] Xu, S.; Wu, A.; Chen, H.; Xie, Y.; Xu, Y.; Zhang, L.; Li, J.; Zhang, D. Production of a novel recombinant Drosophila melanogaster acetylcholinesterase for

detection of organophosphate and carbamate insecticide residues. *Biomol. Eng.* 24 (2007): 253–261.

[74] Flounders, a W.; Singh, a K.; Volponi, J. V; Carichner, S. C.; Wally, K. Development of sensors for direct detection of organophosphates . Part II : sol – gel modified field effect transistor with immobilized organophosphate hydrolase. *Wild.* 14 (1999): 715–722.

[75] Namera, a; Utsumi, Y.; Yashiki, M.; Ohtani, M.; Imamura, T.; Kojima, T. Direct colorimetric method for determination of organophosphates in human urine. *Clin. Chim. Acta Int. J. Clin. Chem.* 291 (2000): 9–18.

[76] Pogacnik, L.; Franko, M. Detection of organophosphate and carbamate pesticides in vegetable samples by a photothermal biosensor. *Biosens. Bioelectron.* 18 (2003): 1–9.

[77] Chen, X.; Lee, K.-M.; Yoon, J.-Y. A Polydiacetylenes-Based Sensor for Discriminating Oleic Acid from Stearic acid and Elaidic Acid. *Bull. Korean Chem. Soc.* 32 (2011): 3775–3778.

[78] Fu, G.; Chen, W.; Yue, X.; Jiang, X. Highly sensitive colorimetric detection of organophosphate pesticides using copper catalyzed click chemistry. *Talanta.* 103 (2013): 110–115.

[79] Li, Z.; Wang, Y.; Ni, Y.; Kokot, S. Unmodified silver nanoparticles for rapid analysis of the organophosphorus pesticide, dipterex, often found in different waters. *Sensors Actuators B Chem.* 193 (2014): 205–211.

[80] Lee, C. H.; Oh, E-H.; Kim, J-M.; Ahn, D. J. Immobilization of polydiacetylene vesicles on cellulose acetate butyrate (CAB)-coated substrates for self-assembled supramolecular sensor arrays. *Colloids Surfaces A Physicochem Eng Asp.* 313 (2008): 500–503.

APPENDIX

APPENDIX A

UV-VIS ABSORPTION SPECTRA AND COLORIMETRIC RESPONSE DATA
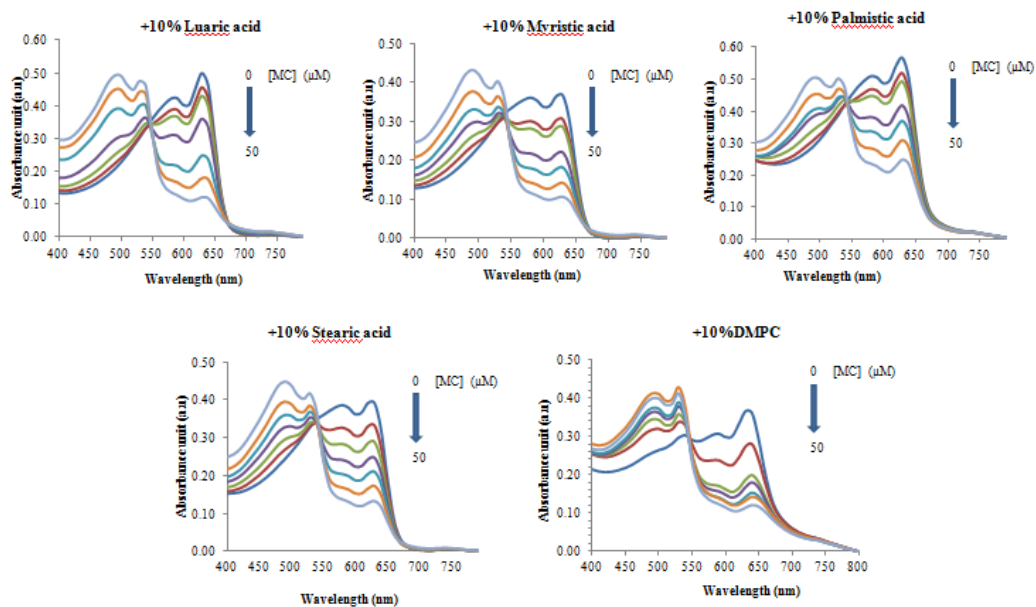
Figure A1 UV-vis absorption spectra of poly(PCDA)/lipids sol (0.3 mM in 10 mM PBS buffer pH = 6.0) tested against MC.
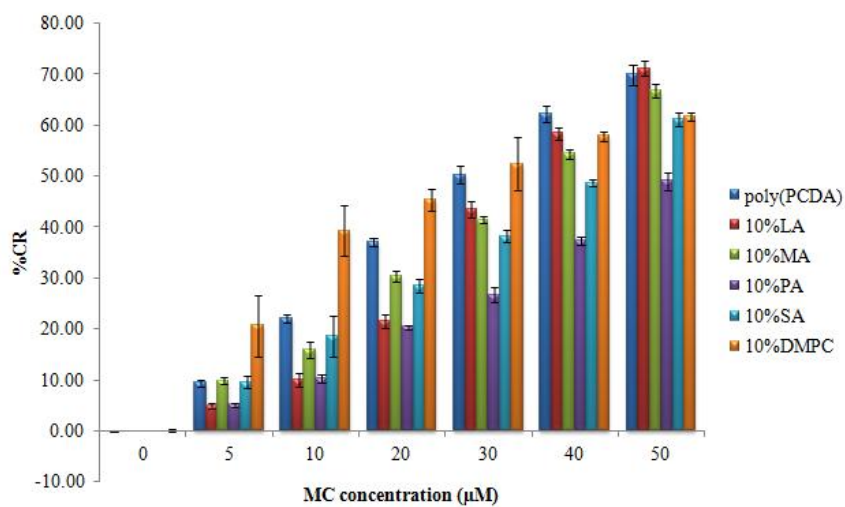
Figure A2 Colorimetric responses of poly(PCDA)/lipids sol (0.3 mM in 10 mM PBS buffer pH = 6.0) tested against MC.
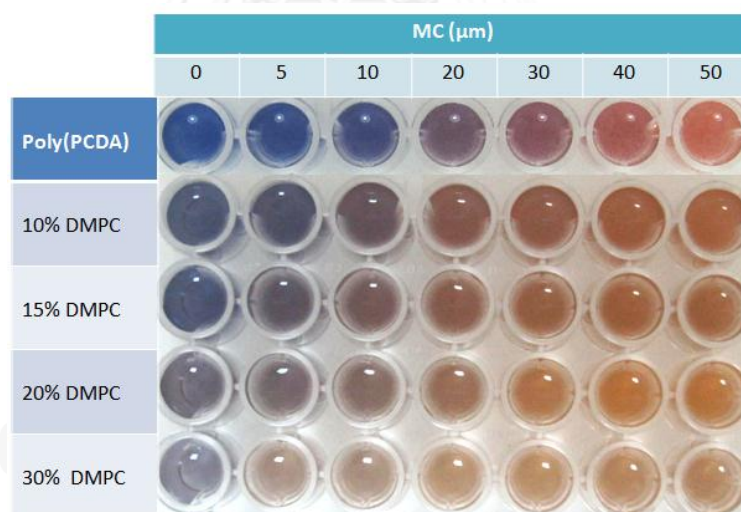
Figure A3 Photograph of poly(PCDA)/DMPC sol tested against different concentration of MC.
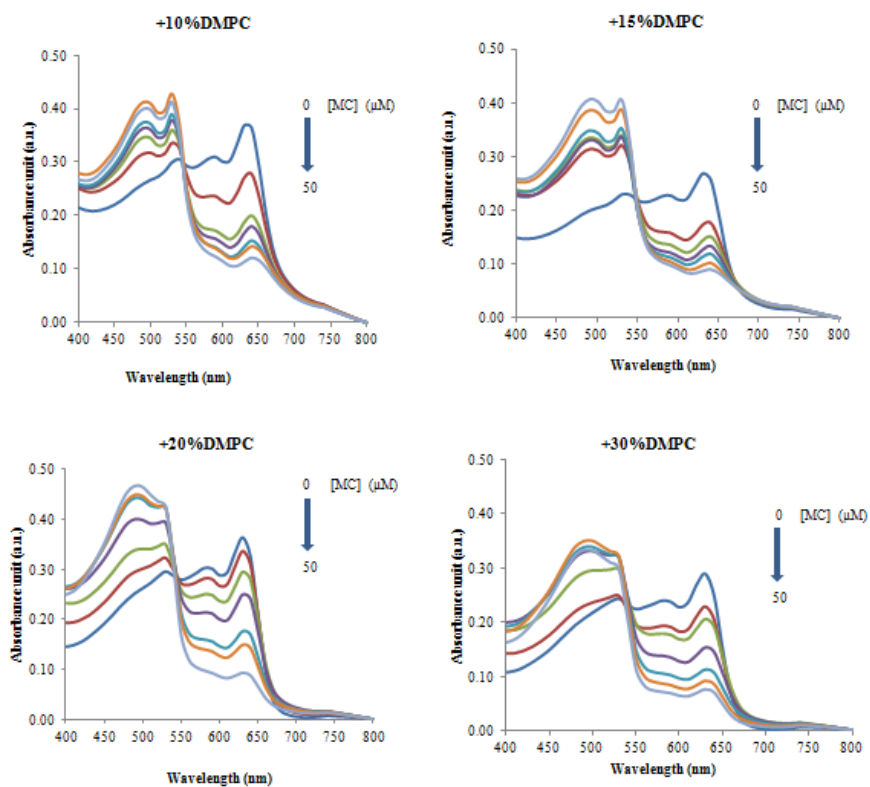
Figure A4 Absorption spectra of poly(PCDA)/DMPC sol (0.3 mM in 10 mM PBS buffer

pH = 6.0) tested against different concentration of MC.
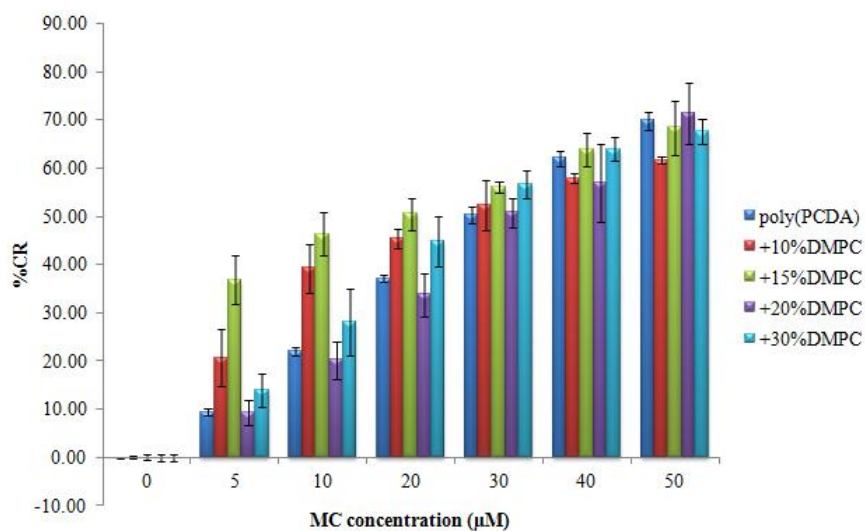
Figure A5 Colorimetric responses of poly(PCDA)/DMPC sol (0.3 mM in 10 mM PBS buffer pH = 6.0) tested against different concentration of MC.
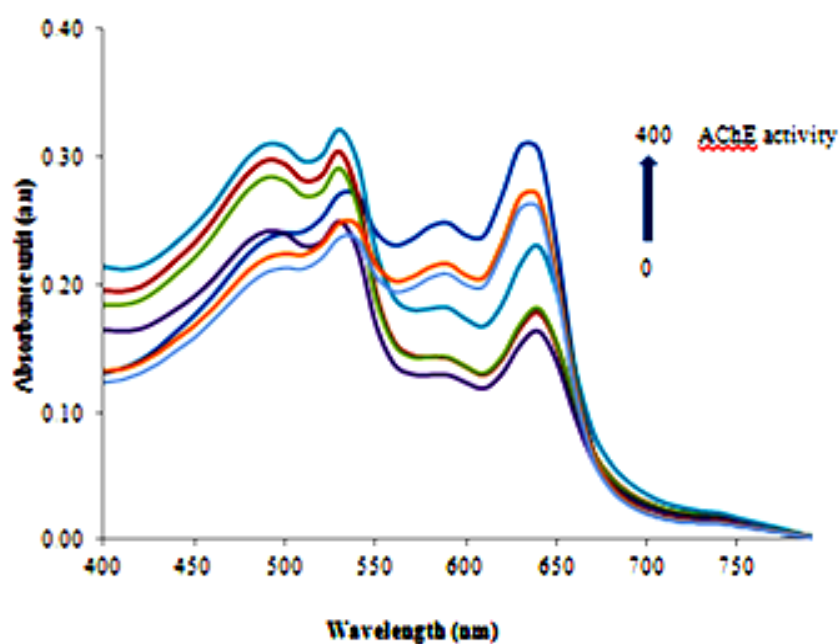
Figure A6 Absorption spectra of poly(PCDA)/15% DMPC sol (0.3 mM in 10 mM PBS buffer pH = 6.0) added to MC (40µM) preincubated at 30 $^\circ$C for 30 min with varied activities of AChE.
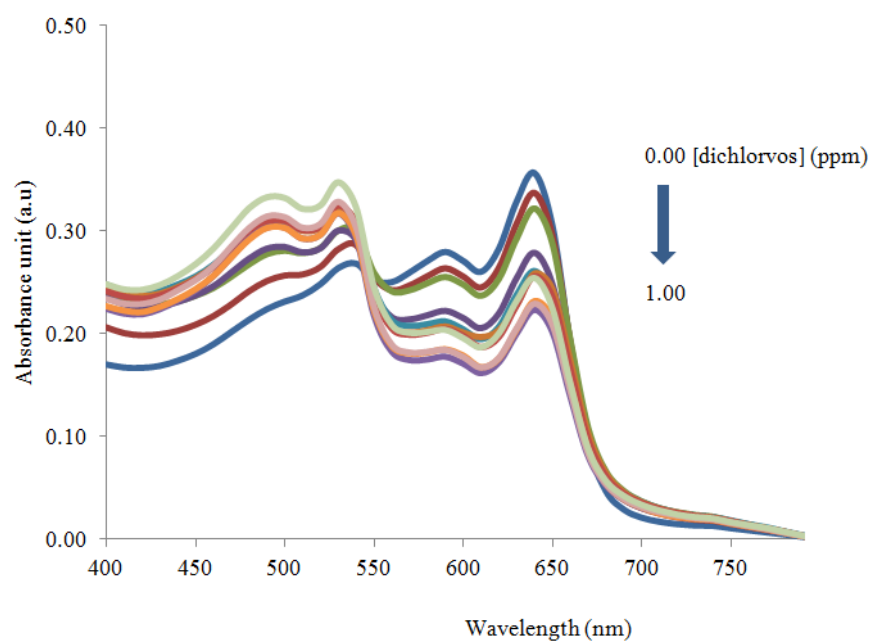
Figure A7 Absorption spectra of poly(PCDA)/15% DMPC sol (0.3 mM in 10 mM PBS buffer pH = 6.0) added to mixture of MC (40μM)/AChE (400 mU/mL)/dichlorvos (varied concentration). AChE was incubated with dichlorvos for 10 min before adding to MC and followed by 30 min incubation. Measurements were performed 10 min after mixing of poly(PCDA))/15% DMPC with MC/AChE/dichlorvos mixture.

APPENDIX B

COLOR RESPONSE DATA OF PAPER-BASED poly(PCDA) INDICATORS

Table B1 RGB values of paper-based poly(PCDA) indicators at difference MC volumes and concentrations (5 independent experiments)

MC Volume (uL) (uL)	MC Concentration (uM)	1				2				3				4				5			
		B	R	G	Sum	B	R	G	Sum	B	R	G	Sum	B	R	G	Sum	B	R	G	Sum
4	0	203	159	164	526	203	159	165	527	203	159	165	527	203	159	164	526	202	159	164	525
	50	190	156	156	502	190	156	156	502	191	156	156	503	191	156	156	503	191	156	156	503
	100	187	159	154	500	187	159	154	501	187	159	154	501	187	159	154	500	187	159	154	500
	200	189	164	157	510	189	164	157	510	189	164	157	510	189	164	157	509	189	163	157	509
	300	179	167	153	500	179	167	153	499	179	168	153	500	179	168	153	500	179	168	153	500
	400	180	174	158	512	180	174	158	513	180	175	158	513	180	175	158	513	180	175	158	513
8	0	204	156	164	524	204	156	165	525	204	155	164	522	204	155	164	523	204	155	164	522
	50	185	151	149	485	185	151	149	486	185	151	149	486	185	151	149	485	184	152	149	485
	100	189	164	157	510	190	164	157	511	190	164	157	511	189	164	157	510	189	164	157	510
	200	178	169	152	499	178	169	152	499	178	169	152	499	178	169	152	499	178	169	152	499
	300	171	182	153	507	171	183	153	507	171	183	153	508	171	182	153	507	171	182	153	506
	400	171	203	168	542	171	203	168	542	171	203	168	542	171	203	168	542	171	202	168	541
12	0	202	149	158	509	202	149	159	511	202	149	159	510	202	149	158	509	201	148	158	507
	50	177	149	147	474	178	149	147	474	178	149	147	474	177	149	147	474	177	149	147	473
	100	186	173	161	520	186	173	161	520	186	173	161	520	186	173	161	519	186	173	161	519
	200	173	189	160	522	173	189	160	522	173	189	160	522	173	189	160	523	173	189	161	523
	300	154	209	163	525	153	209	163	525	153	209	163	525	153	209	163	525	154	209	163	526
	400	164	219	176	559	164	218	176	558	164	218	176	558	164	218	176	558	164	218	176	557

Table B2 %RGB values of paper-based poly(PCDA) indicators at difference MC volumes and concentrations (5 independent experiments)

MC Volume (uL)	MC Concentration (uM)	1			2			3			4			5		
		%B	%R	%G	%B	%R	%G	%B	%R	%G	%B	%R	%G	%B	%R	%G
4	0	38.5	30.3	31.2	38.5	30.3	31.2	38.5	30.2	31.2	38.6	30.2	31.2	38.6	30.2	31.2
	50	37.9	31.0	31.1	37.9	31.0	31.1	37.9	31.0	31.1	37.9	31.0	31.1	37.9	31.0	31.1
	100	37.5	31.7	30.8	37.4	31.8	30.8	37.4	31.8	30.8	37.5	31.7	30.8	37.5	31.7	30.8
	200	37.1	32.1	30.8	37.1	32.1	30.8	37.1	32.1	30.8	37.1	32.1	30.8	37.1	32.1	30.8
	300	35.9	33.5	30.6	35.9	33.5	30.6	35.8	33.5	30.6	35.8	33.5	30.6	35.8	33.5	30.7
	400	35.2	34.0	30.8	35.2	34.0	30.8	35.2	34.0	30.8	35.1	34.1	30.8	35.1	34.1	30.8
8	0	38.9	29.7	31.4	39.0	29.7	31.4	39.0	29.6	31.4	39.0	29.6	31.4	39.0	29.6	31.4
	50	38.1	31.2	30.7	38.1	31.2	30.7	38.1	31.2	30.7	38.1	31.2	30.7	38.0	31.2	30.7
	100	37.1	32.1	30.7	37.1	32.1	30.8	37.1	32.1	30.8	37.1	32.1	30.7	37.1	32.2	30.7
	200	35.7	33.8	30.5	35.7	33.8	30.5	35.7	33.9	30.5	35.7	33.9	30.5	35.7	33.9	30.5
	300	33.8	36.0	30.2	33.8	36.0	30.2	33.7	36.0	30.2	33.8	36.0	30.2	33.8	36.0	30.2
	400	31.6	37.5	31.0	31.6	37.4	31.0	31.6	37.4	31.0	31.6	37.4	31.0	31.6	37.4	31.0
12	0	39.6	29.3	31.1	39.6	29.3	31.1	39.6	29.3	31.1	39.6	29.3	31.1	39.7	29.3	31.1
	50	37.4	31.5	31.1	37.4	31.5	31.1	37.5	31.5	31.1	37.4	31.5	31.1	37.4	31.5	31.1
	100	35.8	33.3	31.0	35.8	33.3	31.0	35.8	33.3	31.0	35.8	33.3	31.0	35.8	33.3	31.0
	200	33.1	36.2	30.7	33.1	36.2	30.7	33.1	36.2	30.7	33.1	36.2	30.7	33.1	36.2	30.7
	300	29.2	39.8	31.0	29.2	39.8	31.0	29.2	39.8	31.0	29.2	39.8	31.0	29.2	39.8	31.0
	400	29.3	39.1	31.5	29.4	39.1	31.5	29.4	39.1	31.5	29.4	39.1	31.5	29.4	39.1	31.5

Table B3 RGB values of paper-based poly(PCDA) indicators at difference MC concentrations and drops (5 independent experiments)

Number of drop	MC Concentration (µM)	1				2				3				4				5			
		B	R	G	Sum	B	R	G	Sum	B	R	G	Sum	B	R	G	Sum	B	R	G	Sum
1	0	203	145	159	507	203	145	159	507	203	145	159	507	202	144	158	504	204	146	159	509
	50	194	156	159	510	194	156	159	510	194	156	159	509	194	156	159	509	194	156	159	508
	100	188	157	154	499	188	157	154	499	188	157	154	498	188	157	154	498	187	157	154	498
	200	176	184	158	517	176	184	158	518	176	184	158	519	177	184	158	519	176	184	158	518
	300	172	194	158	524	172	195	158	524	172	195	158	525	172	195	158	525	173	195	158	526
	400	164	223	161	548	164	223	161	548	164	223	161	547	164	222	161	546	164	223	161	547
2	0	202	144	157	504	202	144	157	503	201	144	157	502	202	143	156	501	201	143	156	500
	50	195	161	161	517	195	161	161	517	195	160	161	516	195	160	161	517	195	161	161	517
	100	178	163	151	492	178	162	151	491	179	163	151	493	179	163	152	493	178	162	150	490
	200	167	186	150	504	168	187	151	505	167	184	150	501	167	186	150	504	167	186	150	503
	300	169	200	158	526	168	200	157	525	168	198	157	523	169	199	157	525	167	198	156	521
	400	170	222	165	557	169	223	165	558	169	223	165	557	169	222	164	555	170	221	164	555
4	0	199	141	153	492	199	140	153	492	199	140	152	491	199	141	153	493	199	140	153	492
	50	190	155	156	501	191	155	156	502	190	155	156	501	190	155	156	501	191	155	156	502
	100	181	168	154	503	180	168	154	502	181	168	154	503	180	168	153	501	181	167	154	502
	200	168	184	151	502	168	183	151	502	167	183	150	501	168	184	151	502	168	184	151	504
	300	167	208	158	533	166	208	158	532	167	207	157	531	166	208	157	532	166	210	158	534
	400	167	225	162	554	167	225	163	554	167	226	163	557	168	227	164	559	168	226	164	557
6	0	197	141	154	492	197	141	153	490	196	141	153	490	196	140	153	489	196	140	152	488
	50	197	159	161	517	197	160	162	518	197	160	162	520	198	161	162	521	198	161	162	521
	100	177	166	151	494	177	165	151	493	177	165	150	491	176	165	151	493	177	164	150	491
	200	168	186	152	506	168	186	152	506	168	187	152	507	169	187	153	508	169	187	152	508
	300	172	224	168	564	172	225	168	565	172	224	168	564	172	226	168	566	172	225	168	566
	400	164	234	165	564	163	234	165	562	163	234	164	561	162	234	164	560	163	233	164	559

Table B4 %RGB values of paper-based poly(PCDA) indicators at difference MC concentrations and drops (5 independent experiments)

Number of drop	MC Concentration (uM)	1			2			3			4			5		
		%B	%R	%G	%B	%R	%G	%B	%R	%G	%B	%R	%G	%B	%R	%G
1	0	40.1	28.6	31.3	40.1	28.6	31.3	40.1	28.6	31.3	40.1	28.6	31.3	40.1	28.6	31.3
	50	38.1	30.7	31.2	38.1	30.7	31.2	38.1	30.7	31.2	38.1	30.7	31.2	38.1	30.7	31.2
	100	37.7	31.4	30.9	37.6	31.5	30.9	37.6	31.5	30.9	37.7	31.5	30.9	37.6	31.5	30.9
	200	34.0	35.5	30.5	34.0	35.5	30.5	34.0	35.5	30.5	34.0	35.5	30.5	34.0	35.5	30.5
	300	32.9	37.1	30.1	32.9	37.1	30.0	32.8	37.2	30.0	32.8	37.1	30.0	32.9	37.1	30.0
	400	29.9	40.7	29.4	29.9	40.7	29.4	29.9	40.7	29.4	29.9	40.7	29.4	29.9	40.7	29.4
2	0	40.1	28.6	31.2	40.1	28.6	31.2	40.2	28.6	31.2	40.3	28.6	31.2	40.2	28.6	31.2
	50	37.7	31.0	31.2	37.7	31.1	31.2	37.8	31.0	31.2	37.8	31.0	31.2	37.7	31.0	31.2
	100	36.3	33.1	30.7	36.3	33.1	30.7	36.3	33.0	30.7	36.3	33.0	30.7	36.3	33.0	30.7
	200	33.2	37.0	29.8	33.2	37.0	29.8	33.5	36.7	29.9	33.3	36.9	29.8	33.2	37.0	29.8
	300	32.0	38.0	30.0	32.0	38.0	29.9	32.1	37.9	30.0	32.1	37.9	30.0	32.0	38.1	29.9
	400	30.5	39.9	29.6	30.4	40.0	29.6	30.4	40.1	29.6	30.5	39.9	29.6	30.5	39.9	29.6
4	0	40.4	28.5	31.0	40.4	28.5	31.0	40.5	28.5	31.0	40.4	28.5	31.0	40.4	28.5	31.0
	50	38.0	30.9	31.1	38.0	30.9	31.1	38.0	30.9	31.1	38.0	30.9	31.1	38.1	30.8	31.1
	100	36.0	33.4	30.6	36.0	33.4	30.6	36.0	33.4	30.6	36.0	33.4	30.6	36.0	33.4	30.6
	200	33.4	36.6	30.0	33.4	36.5	30.0	33.4	36.5	30.0	33.4	36.6	30.0	33.5	36.5	30.0
	300	31.3	39.1	29.6	31.2	39.2	29.6	31.4	39.0	29.6	31.3	39.1	29.6	31.1	39.3	29.6
	400	30.1	40.6	29.3	30.1	40.5	29.3	30.1	40.6	29.3	30.0	40.7	29.3	30.1	40.5	29.4
6	0	40.1	28.7	31.2	40.1	28.7	31.2	40.1	28.7	31.2	40.1	28.7	31.2	40.1	28.7	31.2
	50	38.0	30.8	31.2	38.0	30.8	31.2	38.0	30.8	31.2	38.0	30.9	31.2	38.0	30.9	31.2
	100	35.8	33.6	30.6	35.9	33.5	30.6	35.9	33.5	30.6	35.8	33.6	30.6	36.0	33.4	30.6
	200	33.2	36.7	30.1	33.2	36.8	30.0	33.2	36.8	30.0	33.3	36.7	30.0	33.3	36.7	30.0
	300	30.5	39.7	29.7	30.5	39.8	29.7	30.5	39.7	29.7	30.4	39.9	29.7	30.4	39.8	29.7
	400	29.1	41.6	29.3	29.0	41.7	29.3	29.1	41.7	29.3	29.0	41.7	29.2	29.1	41.6	29.3

Table B5 RGB values of paper-based poly(PCDA) indicators in the present of 300 uM of MC (12 uL) with various AChE activities (5 independent experiments)

AChE	1				2				3				4				5			
(U/mL)	B	R	G	Sum	B	R	G	Sum	B	R	G	Sum	B	R	G	Sum	B	R	G	Sum
Blank	202	154	160	517	202	154	160	516	199	148	157	504	200	154	158	511	199	152	157	508
0	178	236	172	586	178	237	173	589	168	224	163	554	175	237	173	585	175	237	173	585
1	166	223	162	551	165	227	163	556	169	227	166	561	166	227	164	557	166	223	162	550
2	173	195	159	527	173	190	158	521	174	207	164	544	174	205	163	542	174	194	159	526
3	198	149	156	502	199	149	156	504	200	148	156	504	196	146	153	494	198	148	154	500
4	198	147	154	500	199	146	153	498	203	146	157	507	201	147	155	502	200	148	155	503
5	208	154	162	524	199	141	152	491	201	142	154	497	198	144	151	493	198	142	151	490

Table B6 %RGB values of paper-based poly(PCDA) indicators in the present of 300 uM of MC (12 uL) with various AChE activities

(5 independent experiments)

AChE (U/mL)	1			2			3			4			5		
	%B	%R	%G	%B	%R	%G	%B	%R	%G	%B	%R	%G	%B	%R	%G
Blank	39.1	29.8	31.0	39.1	29.8	31.0	39.5	29.5	31.1	39.0	30.0	30.9	39.1	29.9	30.9
0	30.4	40.3	29.3	30.3	40.3	29.4	30.3	40.4	29.3	29.9	40.5	29.5	30.0	40.5	29.5
1	30.1	40.5	29.4	29.7	40.9	29.4	30.1	40.4	29.5	29.9	40.7	29.4	30.1	40.5	29.4
2	32.9	36.9	30.2	33.3	36.4	30.3	31.9	38.0	30.1	32.0	37.8	30.1	33.0	36.8	30.2
3	39.4	29.6	31.0	39.4	29.6	31.0	39.7	29.4	31.0	39.6	29.5	30.9	39.6	29.6	30.9
4	39.6	29.5	30.9	39.8	29.4	30.8	40.1	28.9	31.0	39.9	29.2	30.9	39.8	29.4	30.9
5	39.7	29.4	31.0	40.5	28.7	30.9	40.5	28.6	30.9	40.3	29.1	30.6	40.3	28.9	30.8

Table B7 RGB values of paper-based poly(PCDA) indicators in the present of the mixture of MC/AChE with various dichlorvos concentrations

(5 independent experiments)

DV Concentration (ppm)	1				2				3				4				5			
	B	R	G	Sum	B	R	G	Sum	B	R	G	Sum	B	R	G	Sum	B	R	G	Sum
0.00	207	151	164	523	208	152	164	524	206	159	168	534	206	151	163	521	203	149	160	513
0.05	206	154	165	525	165	153	165	484	209	157	168	534	208	157	168	533	210	155	167	532
0.10	206	155	165	527	169	158	169	496	205	151	163	520	209	155	166	530	207	159	168	534
0.15	211	158	169	538	165	153	165	484	212	159	170	541	214	157	170	541	209	160	169	538
0.20	197	169	167	534	163	163	163	489	196	166	165	528	198	170	167	535	200	168	166	535
0.25	193	176	166	535	170	180	170	519	195	182	169	547	195	174	166	536	197	181	170	548
0.00	199	159	162	520	164	162	164	491	202	162	165	529	201	158	163	521	200	161	164	525
0.25	179	209	170	559	171	212	171	554	172	188	157	517	175	203	164	543	175	202	164	540
0.50	178	207	166	552	165	205	165	535	178	209	167	554	186	203	169	558	180	207	167	553
0.75	175	221	170	567	169	218	169	555	171	208	162	541	179	212	171	562	176	222	172	570
1.00	173	213	167	553	168	211	168	547	177	208	167	552	176	211	168	556	177	219	171	567
2.50	169	217	163	549	166	219	166	550	170	209	162	541	172	222	168	562	173	219	168	560
5.00	173	226	168	567	166	215	166	547	175	224	171	570	176	225	171	572	174	221	167	562
7.50	170	229	168	566	174	227	174	575	172	228	168	567	178	239	176	593	177	239	176	591
10.00	177	237	174	588	167	221	167	556	176	203	165	544	175	221	167	562	183	217	173	572

Table B8 %RGB values of paper-based poly(PCDA) indicators in the present of the mixture of MC/AChE with various dichlorvos concentrations

(5 independent experiments)

DV Concentration	1			2			3			4			5		
(ppm)	%B	%R	%G	%B	%R	%G	%B	%R	%G	%B	%R	%G	%B	%R	%G
0.00	39.7	29.0	31.4	39.7	29.0	31.3	38.6	29.9	31.5	39.6	29.0	31.3	39.7	29.1	31.3
0.05	39.3	29.3	31.4	34.2	31.6	34.2	39.2	29.3	31.5	39.1	29.5	31.5	39.5	29.1	31.4
0.10	39.2	29.4	31.4	34.1	31.9	34.1	39.5	29.1	31.4	39.3	29.3	31.3	38.9	29.7	31.4
0.15	39.2	29.3	31.5	34.2	31.7	34.2	39.2	29.4	31.4	39.5	29.1	31.4	38.9	29.7	31.4
0.20	37.0	31.7	31.3	33.3	33.3	33.3	37.1	31.5	31.3	36.9	31.8	31.3	37.4	31.4	31.1
0.25	36.1	32.9	31.0	32.7	34.7	32.7	35.7	33.3	31.0	36.5	32.5	31.0	36.0	33.0	31.1
0.00	38.3	30.5	31.2	33.4	33.1	33.4	38.2	30.6	31.2	38.5	30.3	31.2	38.2	30.7	31.2
0.25	32.1	37.5	30.4	30.9	38.2	30.9	33.2	36.4	30.4	32.3	37.4	30.3	32.4	37.3	30.3
0.50	32.3	37.6	30.1	30.8	38.3	30.8	32.1	37.7	30.2	33.3	36.4	30.3	32.5	37.4	30.2
0.75	31.0	39.0	30.1	30.4	39.2	30.4	31.5	38.5	30.0	31.9	37.7	30.4	30.8	39.0	30.1
1.00	31.3	38.6	30.1	30.7	38.6	30.7	32.0	37.7	30.2	31.8	38.0	30.2	31.1	38.7	30.2
2.50	30.7	39.5	29.7	30.1	39.8	30.1	31.5	38.7	29.9	30.7	39.4	29.9	30.9	39.2	29.9
5.00	30.5	39.9	29.7	30.3	39.4	30.3	30.7	39.3	30.0	30.8	39.3	29.8	31.0	39.3	29.8
7.50	30.0	40.4	29.6	30.3	39.5	30.3	30.2	40.1	29.7	29.9	40.4	29.7	30.0	40.4	29.7
10.00	30.1	40.3	29.5	30.1	39.8	30.1	32.4	37.3	30.3	31.0	39.3	29.7	31.9	37.9	30.2

APPENDIX C

COLORIMETRIC RESPONSE OF PAPER-BASED poly(PCDA)/15%DMPC INDICATORS

Table C1 RGB values of paper-based poly(PCDA)/15%DMPC indicators at difference MC volumes and concentrations (5 independent experiments)

MC Volume (uL)	MC Concentration (uM)	1				2				3				4				5			
		B	R	G	Sum	B	R	G	Sum	B	R	G	Sum	B	R	G	Sum	B	R	G	Sum
4	0	200	161	164	525	206	164	169	539	200	160	164	524	202	165	168	535	200	163	166	530
	50	203	176	173	553	205	176	173	555	204	178	174	556	202	175	172	549	203	175	172	550
	100	198	175	169	542	198	175	169	542	197	175	168	540	198	176	170	544	197	175	169	541
	200	187	173	160	520	187	173	160	520	187	173	161	521	187	174	161	522	187	173	161	521
	300	187	183	165	536	188	183	165	536	187	182	165	534	187	183	165	534	187	182	165	533
	400	188	195	170	553	188	196	170	555	187	195	169	552	187	195	169	551	188	195	170	553
8	0	205	163	166	534	205	162	167	533	203	161	165	529	205	164	168	537	204	161	166	531
	50	200	170	168	538	200	170	167	537	200	169	167	537	200	169	168	537	200	170	168	539
	100	193	173	164	531	192	171	163	527	193	173	164	531	193	172	163	527	194	174	165	533
	200	182	191	164	537	183	190	164	537	182	190	164	536	183	188	164	535	183	189	163	535
	300	185	193	167	545	185	193	167	545	186	193	167	546	185	192	167	544	185	194	167	546
	400	176	199	163	538	176	199	163	539	176	199	163	538	176	198	163	537	176	199	163	538
12	0	209	163	169	540	206	159	165	529	209	162	168	539	207	162	167	537	207	160	165	532
	50	203	169	169	540	203	170	169	542	203	169	168	540	204	169	169	542	203	168	168	539
	100	194	171	164	530	194	172	164	530	195	172	165	533	195	172	165	532	196	172	165	533
	200	182	201	168	551	182	201	168	550	182	199	167	548	182	200	168	550	183	202	169	553
	300	183	224	177	584	181	220	174	574	182	219	175	576	184	221	177	582	181	221	175	577
	400	164	220	171	556	165	219	171	555	168	221	173	562	166	217	170	553	168	221	173	562

Table C2 %RGB values of paper-based poly(PCDA)/15%DMPC indicators at difference MC volumes and concentrations (5 independent experiments)

MC Volume (uL)	MC Concentration (uM)	1			2			3			4			5		
		%B	%R	%G	%B	%R	%G	%B	%R	%G	%B	%R	%G	%B	%R	%G
4	0	38.1	30.6	31.3	38.2	30.5	31.4	38.1	30.6	31.3	37.8	30.8	31.4	37.8	30.8	31.4
	50	36.8	31.9	31.3	36.9	31.8	31.3	36.6	32.0	31.4	36.8	31.9	31.3	36.9	31.8	31.3
	100	36.5	32.4	31.2	36.5	32.4	31.2	36.5	32.3	31.2	36.5	32.3	31.2	36.5	32.4	31.2
	200	35.9	33.2	30.8	35.9	33.2	30.9	35.9	33.2	30.9	35.9	33.2	30.9	35.9	33.3	30.9
	300	35.0	34.2	30.9	35.1	34.1	30.9	35.0	34.1	30.9	35.0	34.2	30.8	35.0	34.1	30.9
	400	34.0	35.3	30.7	33.9	35.4	30.7	34.0	35.3	30.7	34.0	35.3	30.7	34.0	35.3	30.7
8	0	38.3	30.5	31.2	38.4	30.4	31.2	38.4	30.4	31.2	38.3	30.5	31.3	38.5	30.3	31.2
	50	37.2	31.6	31.2	37.2	31.6	31.2	37.3	31.5	31.2	37.3	31.5	31.2	37.2	31.6	31.2
	100	36.4	32.6	31.0	36.5	32.5	31.0	36.4	32.6	31.0	36.5	32.5	31.0	36.4	32.6	31.0
	200	34.0	35.5	30.5	34.1	35.4	30.5	34.0	35.5	30.5	34.2	35.2	30.6	34.1	35.3	30.5
	300	33.9	35.5	30.6	33.9	35.5	30.6	34.1	35.3	30.6	34.0	35.4	30.6	33.9	35.5	30.6
	400	32.8	36.9	30.3	32.7	37.0	30.3	32.7	36.9	30.3	32.9	36.8	30.3	32.8	36.9	30.3
12	0	38.7	30.1	31.2	38.9	30.0	31.1	38.8	30.0	31.1	38.6	30.2	31.2	38.9	30.0	31.1
	50	37.6	31.2	31.2	37.5	31.3	31.2	37.6	31.2	31.2	37.6	31.2	31.2	37.6	31.2	31.2
	100	36.7	32.3	31.0	36.6	32.4	31.0	36.6	32.4	31.0	36.7	32.3	31.0	36.7	32.3	31.0
	200	33.0	36.5	30.5	33.0	36.5	30.5	33.2	36.3	30.5	33.1	36.4	30.5	33.0	36.5	30.5
	300	31.4	38.3	30.3	31.5	38.3	30.2	31.7	38.1	30.3	31.7	38.0	30.3	31.4	38.3	30.3
	400	29.6	39.7	30.8	29.8	39.5	30.8	29.9	39.4	30.8	30.1	39.1	30.8	29.9	39.3	30.8

Table C3 RGB values of paper-based poly(PCDA)/15%DMPC indicators at difference MC concentrations and drops (5 independent experiments)

Number of drop	MC Concentration (uM)	1				2				3				4				5			
		B	R	G	Sum	B	R	G	Sum	B	R	G	Sum	B	R	G	Sum	B	R	G	Sum
1	0	160	166	202	528	161	166	203	529	160	164	202	526	161	165	202	528	162	166	202	530
	50	160	160	195	515	162	163	197	522	160	162	196	517	160	161	195	516	159	161	196	515
	100	187	165	185	537	187	164	185	536	187	164	184	535	185	165	187	536	187	164	184	535
	200	193	159	175	527	193	159	174	525	195	159	174	528	191	160	176	527	195	159	174	528
	300	237	174	174	584	236	173	173	583	236	174	174	585	236	173	173	583	237	174	174	586
	400	246	184	187	617	245	183	186	614	243	185	190	618	245	186	189	620	246	185	188	619
2	0	163	166	201	530	166	168	203	537	162	165	200	527	165	168	203	536	162	165	200	527
	50	159	162	198	519	154	158	196	508	163	166	202	530	154	157	195	506	161	164	200	525
	100	166	154	179	499	165	154	180	499	166	154	179	499	166	154	180	500	166	154	180	500
	200	204	167	180	552	201	166	181	548	204	167	181	552	203	167	181	551	198	166	181	544
	300	232	167	170	568	229	166	169	564	231	167	170	568	232	167	170	568	230	167	170	567
	400	234	171	174	579	234	171	173	578	232	169	171	572	232	170	171	573	231	169	171	572
4	0	162	168	207	536	163	169	207	539	163	168	207	539	164	170	208	541	164	168	205	537
	50	158	159	195	512	159	160	196	515	157	158	194	509	158	158	195	511	159	161	197	516
	100	181	168	192	541	179	168	193	540	179	167	192	539	178	167	192	537	177	166	193	536
	200	211	164	172	547	209	164	172	545	210	164	172	546	210	165	173	548	209	164	173	546
	300	234	169	171	575	233	168	171	573	233	169	172	574	233	169	172	573	234	169	171	574
	400	244	174	174	592	245	174	174	592	244	174	174	592	243	173	174	590	241	172	173	586
6	0	166	166	201	533	166	169	203	538	167	167	201	535	166	166	199	531	166	168	202	537
	50	164	164	197	525	162	163	196	521	164	164	197	525	161	163	196	520	162	164	197	524
	100	180	157	178	516	177	156	179	512	179	157	178	513	180	158	179	517	180	157	178	515
	200	213	168	176	557	210	167	177	554	213	169	178	559	214	169	177	560	213	169	178	560
	300	226	166	168	560	226	167	169	562	226	165	167	557	225	164	166	556	227	167	169	563
	400	242	172	169	583	242	172	169	583	242	171	169	582	242	172	169	582	241	172	169	583

Table C4 %RGB values of paper-based poly(PCDA)/15%DMPC indicators at difference MC concentrations and drops (5 independent experiments)

Number of drop	MC Concentration (uM)	1			2			3			4			5		
		%B	%R	%G	%B	%R	%G	%B	%R	%G	%B	%R	%G	%B	%R	%G
1	0	30.4	31.3	38.3	30.4	31.3	38.3	30.4	31.2	38.4	30.4	31.2	38.3	30.6	31.3	38.1
	50	31.0	31.1	37.9	31.0	31.2	37.8	30.9	31.2	37.9	31.0	31.1	37.9	30.8	31.2	38.0
	100	34.8	30.7	34.5	34.9	30.6	34.4	35.0	30.6	34.4	34.5	30.7	34.8	34.9	30.7	34.5
	200	36.5	30.2	33.2	36.7	30.2	33.1	36.9	30.2	32.9	36.3	30.4	33.3	36.9	30.2	32.9
	300	40.6	29.7	29.7	40.4	29.8	29.8	40.4	29.8	29.8	40.4	29.8	29.8	40.5	29.8	29.7
	400	39.9	29.9	30.3	39.9	29.9	30.2	39.3	30.0	30.7	39.6	30.0	30.5	39.8	29.9	30.3
2	0	30.7	31.3	37.9	30.9	31.3	37.7	30.7	31.3	38.0	30.8	31.4	37.8	30.7	31.3	38.0
	50	30.6	31.2	38.1	30.4	31.1	38.5	30.7	31.3	38.0	30.4	31.1	38.5	30.7	31.2	38.1
	100	33.3	30.8	35.9	33.1	30.8	36.1	33.3	30.8	35.9	33.3	30.8	35.9	33.3	30.8	35.9
	200	37.0	30.3	32.6	36.7	30.4	33.0	36.9	30.3	32.8	36.8	30.4	32.8	36.3	30.4	33.3
	300	40.7	29.4	29.8	40.6	29.5	30.0	40.7	29.4	29.9	40.8	29.4	29.8	40.6	29.4	30.0
	400	40.4	29.6	30.0	40.4	29.6	30.0	40.5	29.6	29.9	40.5	29.6	29.9	40.5	29.6	29.9
4	0	30.2	31.3	38.6	30.3	31.3	38.4	30.3	31.2	38.4	30.3	31.4	38.4	30.5	31.3	38.3
	50	30.9	31.1	38.0	30.9	31.1	38.0	30.8	31.0	38.2	30.9	31.0	38.1	30.8	31.1	38.1
	100	33.5	31.1	35.4	33.2	31.1	35.8	33.3	31.1	35.7	33.1	31.1	35.8	33.0	31.1	36.0
	200	38.5	30.1	31.4	38.3	30.1	31.6	38.5	30.1	31.4	38.4	30.1	31.5	38.2	30.1	31.7
	300	40.7	29.4	29.8	40.7	29.4	29.9	40.5	29.5	30.0	40.7	29.4	29.9	40.8	29.4	29.8
	400	41.2	29.3	29.4	41.4	29.3	29.3	41.3	29.3	29.4	41.1	29.4	29.5	41.2	29.3	29.5
6	0	31.2	31.2	37.6	30.9	31.4	37.7	31.2	31.2	37.6	31.3	31.2	37.5	30.9	31.4	37.7
	50	31.2	31.2	37.6	31.1	31.3	37.6	31.3	31.2	37.5	30.9	31.3	37.8	31.0	31.3	37.7
	100	35.0	30.5	34.5	34.6	30.5	34.9	34.8	30.5	34.7	34.8	30.5	34.7	34.9	30.5	34.5
	200	38.2	30.1	31.7	37.8	30.2	31.9	38.1	30.2	31.8	38.2	30.1	31.7	38.1	30.2	31.7
	300	40.4	29.6	30.0	40.3	29.7	30.0	40.5	29.6	29.9	40.5	29.6	29.9	40.3	29.6	30.1
	400	41.6	29.5	29.0	41.6	29.5	28.9	41.6	29.5	29.0	41.5	29.5	29.0	41.5	29.5	29.1

Table C5 RGB values of paper-based poly(PCDA)/15%DMPC indicators in the present of 300 uM of MC (12 uL) with various AChE activities (5 independent experiments)

AChE (U/mL)	1				2				3				4				5			
	B	R	G	Sum	B	R	G	Sum	B	R	G	Sum	B	R	G	Sum	B	R	G	Sum
0	167	209	164	540	167	209	164	540	168	209	165	542	167	210	164	541	167	208	163	538
20	172	183	158	513	164	173	149	486	162	180	150	491	164	173	149	486	162	180	150	491
40	175	147	143	466	176	148	142	466	177	156	146	479	176	154	145	475	177	156	146	479
60	189	134	140	463	188	132	140	460	180	128	134	442	189	131	140	460	188	130	139	457
80	186	128	138	452	195	135	146	476	196	138	147	481	192	133	145	470	195	138	147	480
100	208	139	153	501	208	140	154	502	203	138	151	493	201	135	148	484	203	137	151	490

Table C6 RGB values of paper-based poly(PCDA)/15%DMPC indicators in the present of 300 uM of MC (12 uL)

with various AChE activities (5 independent experiments)

AChE (U/mL)	1			2			3			4			5		
	%B	%R	%G	%B	%R	%G	%B	%R	%G	%B	%R	%G	%B	%R	%G
0	30.9	38.8	30.4	30.9	38.7	30.4	30.9	38.7	30.4	30.9	38.8	30.4	31.0	38.6	30.4
20	33.5	35.6	30.9	33.7	35.7	30.6	32.9	36.6	30.5	33.7	35.7	30.6	32.9	36.6	30.5
40	37.7	31.6	30.8	37.8	31.7	30.5	36.9	32.6	30.5	37.2	32.4	30.5	36.9	32.6	30.5
60	40.8	28.9	30.3	40.9	28.8	30.3	40.8	29.0	30.2	41.0	28.5	30.4	41.2	28.4	30.4
80	41.3	28.2	30.5	40.9	28.4	30.8	40.7	28.7	30.6	40.8	28.4	30.8	40.6	28.7	30.7
100	41.5	27.9	30.6	41.4	27.9	30.6	41.3	28.0	30.7	41.5	27.9	30.6	41.3	28.0	30.7

Table C7 RGB values of paper-based poly(PCDA)/15%DMPC indicators in the present of the mixture of MC/AChE with various dichlorvos concentrations (5 independent experiments)

DV Concentration (ppm)	1				2				3				4				5			
	B	R	G	Sum	B	R	G	Sum	B	R	G	Sum	B	R	G	Sum	B	R	G	Sum
0.00	199	154	159	511	203	158	164	525	200	151	157	508	201	153	159	513	202	157	162	521
0.05	203	157	163	522	199	156	161	517	204	150	159	513	206	153	162	521	206	159	165	529
0.10	202	165	167	534	203	162	166	531	200	155	161	516	202	155	161	519	208	170	172	550
0.15	185	189	169	543	181	179	162	523	186	189	169	544	184	179	163	527	185	180	165	531
0.20	185	188	166	538	180	180	160	520	185	187	166	538	180	178	159	517	186	188	166	540
0.25	191	201	172	563	186	189	165	540	186	199	169	553	191	200	171	563	188	198	169	555
0.50	183	198	170	551	184	195	168	547	184	198	170	552	186	196	170	552	184	197	170	551
0.75	186	201	172	558	183	197	169	548	186	199	171	556	185	191	167	543	186	201	172	558
1.00	172	195	160	526	174	195	161	531	175	191	160	525	175	195	162	531	174	195	161	531
2.50	180	208	170	558	183	209	172	564	180	206	170	555	185	202	169	556	185	204	170	559
5.00	174	197	162	532	178	199	166	544	178	201	166	545	178	203	168	549	178	201	167	547
7.50	170	213	165	547	169	213	165	547	169	213	164	546	168	213	164	546	168	213	164	545
10.00	177	227	173	577	177	227	173	577	176	227	172	576	176	225	171	572	175	225	171	572

Table C 8 % RGB values of paper-based poly(PCDA)/15%DMPC indicators in the present of the mixture of MC/AChE with various dichlorvos concentrations

(5 independent experiments)

DV Concentration	1			2			3			4			5		
(ppm)	%B	%R	%G	%B	%R	%G	%B	%R	%G	%B	%R	%G	%B	%R	%G
0.00	38.9	30.1	31.1	38.6	30.2	31.2	39.4	29.6	31.0	39.2	29.8	31.0	38.8	30.2	31.0
0.05	38.8	30.1	31.1	38.5	30.3	31.3	39.8	29.2	31.0	39.6	29.4	31.0	38.9	30.0	31.1
0.10	37.8	31.0	31.2	38.2	30.5	31.2	38.8	30.1	31.2	39.0	29.9	31.1	37.8	30.9	31.3
0.15	34.1	34.8	31.1	34.7	34.2	31.1	34.2	34.7	31.0	34.9	34.0	31.0	34.9	34.0	31.1
0.20	34.3	34.8	30.9	34.6	34.6	30.7	34.4	34.8	30.9	34.8	34.5	30.8	34.4	34.8	30.8
0.25	33.9	35.6	30.5	34.5	35.0	30.5	33.6	36.0	30.5	33.9	35.6	30.5	33.8	35.7	30.5
0.50	33.3	35.9	30.9	33.6	35.6	30.8	33.3	35.9	30.9	33.6	35.6	30.8	33.5	35.8	30.8
0.75	33.2	36.0	30.8	33.3	35.8	30.8	33.4	35.8	30.8	34.0	35.3	30.7	33.2	36.0	30.8
1.00	32.6	37.0	30.3	32.8	36.8	30.4	33.2	36.3	30.5	32.9	36.7	30.4	32.8	36.8	30.4
2.50	32.2	37.3	30.5	32.4	37.0	30.5	32.4	37.1	30.5	33.2	36.3	30.5	33.0	36.5	30.5
5.00	32.7	36.9	30.4	32.8	36.7	30.6	32.6	36.8	30.5	32.5	37.0	30.5	32.6	36.8	30.5
7.50	31.0	38.8	30.1	30.9	38.9	30.1	30.9	39.0	30.1	30.9	39.0	30.1	30.9	39.0	30.1
10.00	30.7	39.4	29.9	30.6	39.4	29.9	30.7	39.4	29.9	30.7	39.4	29.9	30.7	39.4	30.0

SENSITIVITY COMPARISON WITH OTHER ORGANOPHOSPHATE DETECTION

METHOD

Table D 1 Comparison of sensitivity of the organophosphate detection with methods previously

reported for detection of related organophosphates

Reagents	Analysts	LOD	Mode of detection or instruments	References
AChE/phosphatidylcholine/iposomes/ porin/acetylthiocholine chloride	dichlorvos paraoxon	0.15 ppb (6.7×10^{-10} M) 0.06 ppb (2.0×10^{-10} M)	Fluorometer	(Vamvakaki and Chaniotakis, 2007)
AChE/, Hybond N^{+} membrane / indophenyl acetate	parathion chlorpyrifos malathion	10^{-6}–10^{2} ppm (3.43×10^{-6} - 3.43 10^{-4} M)	Reflectometer	(No et al., 2007)
AChE/polyvinylidenefluoride membrane/bromcresol purple	carbaryl dichlorvos	108 ppb (0.54×10^{-6} M) 5.2 ppb (0.024×10^{-6} M)	Absorption using optical fiber	(Andreou and Clonis, 2002)
PCDA- p BO/PCDA- p BA liposome	DCP DFP	DCP = 17,255 ppm (0.10 M) DFP = 5,530 ppm (0.03M) DFP = 0.16 ppm (0.87×10^{-6} M)	UV-vis absorption spectrometer Naked eye detection on paper substrate	(Lee et al., 2012)
PDAs /AChE/MC	neostigmine tacrine dimethyl methylphosphonate	IC_{50} = 4.2 nM (0.94 ppb) IC_{50} = 6.9 nM (1.37 ppb) IC_{50} = 201 μM (24.94 ppm)	Fluorometer	(Zhou et al., 2013)
Au: gold nanoparticles/AChE/ATCl/ / CuO nanoparticles	paroxon	10 ppb (0.04×10^{-6} M)	Naked eye detection	(Fu et al., 2013)
citrate-capped AgNPs/ ATCh	dipterex	0.18 ppb (7×10^{-10} M)	UV-vis absorption spectrometer	(Li et al., 2014)
Poly(PCDA) /AChE/MC,	dichlorvos	6.7 ppb (30×10^{-9} M) 150 ppb (0.68×10^{-6} M)	UV-vis absorption spectrometer Naked eye detection in solution	This work
Poly(PCDA)/15%DMPC /AChE/MC		6.4 ppb (29×10^{-9} M) 50 ppb (0.23×10^{-6} M)	UV-vis absorption spectrometer Naked eye detection in solution	

Remarks: AgNPs = silver nanoparticles, ATCh= Acetylthio-choline, DCP =

diethylchlorophosphate, DFP = diisopropylfl uorophosphate

VITA

Mrs. Rungnapha Pimsen was born on January 19th, 1972 in Ranong, Thailand. She received a Bachelor's Degree of Science, majoring in Chemistry from Faculty of Science, Ramkhumhang University in 1993. She graduated with a master degree in petrochemistry and polymer science at Chulalongkorn University in 2006. After graduated in Master degree, she have been worked at Nakhon Si Thammarat Rajabhat University as a lecturer and then she continued his study in a Ph.D degree in program of Petrochemistry at Chulalongkorn University in academic year and completed in 2013. Her current address is 168/1 moo 5, Srakeaw, Thasala, Nakhon Si Thammarat, 80160.